FINITE ELEMENT ANALYSIS OF DYNAMIC PLANTAR PRESSURE DISTRIBUTION TO ENHANCE THE DESIGN OF DIABETIC INSOLE

LEUNG SIN HANG MATTHEW

MPhil

The Hong Kong Polytechnic University

2023

The Hong Kong Polytechnic University

School of Fashion and Textiles

Finite Element Analysis of Dynamic Plantar Pressure Distribution to enhance the Design of Diabetic Insole

Leung Sin Hang Matthew

A thesis submitted in partial fulfilment of the requirements for the degree of Master of Philosophy

December 2022

CERTIFICATE OF ORIGINALITY

I hereby declare that this thesis is my own work and that, to the best of my knowledge and belief, it reproduces no material previously published or written, nor material that has been accepted for the award of any other degree or diploma, except where due acknowledgement has been made in the text.

_____ (Signed)

Leung Sin Hang Matthew (Name of student)

Abstract

Diabetes mellitus (DM) is one of the most concerning diseases worldwide because the ailment has such a large economic burden on health systems. In 2021, more than 422 million people globally suffered from diabetes and the number is increasing every year. Due to the loss of the protective sensation that is associated with neuropathy, diabetic patients have difficulties in responding to pressure, wounds and/or injuries, especially on their feet. Wounds could quickly become infected with a long recovery duration, thus leading to foot ulceration and even foot amputation which greatly deteriorate their quality of life.

Diabetic insoles are frequently used to provide optimal fit and reduce the magnitude of plantar pressure. It is anticipated that the three-dimensional (3D) design of diabetic footwear and insoles and the type of footwear material have a major impact on fit and wear comfort, which lead to increased compliance with treatment to prevent neuropathic diabetic foot ulcers. Diabetic insoles can also protect the plantar of the foot thus reducing the risk of such ulcers because they have the most contact with the plantar of the foot and can evenly distribute the pressure throughout the entire plantar. Diabetic insoles are generally made of soft materials, such as polypropylene (PP), ethylene vinyl acetate (EVA), polyethylene (PE), microcellular rubber (MCR), etc. As the pressure offloaded between the insole and plantar of the foot as well as the geometry of the foot during walking differ greatly from those of standing, a more in-depth understanding of the effects of changes in the geometry of the foot and insole material properties on diabetic insoles is therefore important to provide better protection for the diabetic foot.

This study began with a discussion on the pressure distribution under different insole conditions during walking. The properties of 3 different traditional insole materials: EVA foam - Lunalastik®, a PE material - PeLite®, and a PU material - Poron®, were outlined. Also, the mean peak pressure of the plantar with the insole and barefoot condition were systematically evaluated. The result showed that the PU material had the best performance which could readily absorb energy and reduce the plantar pressure. The findings of this study provided very useful guidelines to enhance the anatomical design of diabetic insoles to optimize the pressure distribution throughout the plantar of the foot.

After that, the geometry of the foot during an entire walking cycle was captured by using a four-dimensional (4D) foot scanning system. Different parts of the foot measured at 3 different walking speeds (slow, normal, and fast) and 5 different stances during walking (first heel contact, first metatarsal head contact, first toe contact, heel take off and metatarsal head take off) were systematically evaluated. The results showed that the foot measurements had no statistical difference with regard to walking speed, while 12 of the 13 foot measurements had a statistical difference with regard to the stances during walking. The deformation ratio could be used to provide a better understanding of the foot deformation which advanced the design and development of diabetic insoles.

In addition, considering the very high contact pressure in the rearfoot and forefoot regions, insoles with a braced frame structure that used traditional insole materials were proposed to further reduce the shear stress and contact pressure at the interface between the plantar-insole surface to reduce the risk of foot injury. Finite element models (FEMs) were developed to evaluate the structural changes of the developed braced frame structure upon exertion of

compressive forces. Also, the effect of different braced frame structures on the shear stress, contact area as well as the maximum contact force on the plantar were analysed through a finite element analysis (FEA). The validated FEMs showed that the proposed braced frame structure provided a reduction in the shear stress (~21%) and maximum contact force (~55%) in comparison to traditional diabetic insoles.

To evaluate the planter pressure during heel strike posture, an auxetic heel pad was examined and a wear trial with the heel pad was subsequently conducted. This was a novel pressure relieving heel pad based on a circular auxetic re-entrant honeycomb structure which was constructed by using 3D printing technology to minimize the pressure on the heel, thus reducing the occurrence of foot ulcers. FEMs were developed to evaluate the structural changes of the developed circular auxetic structure upon exertion of compressive forces. Moreover, the effects of the internal angle of the re-entrant structure on the peak contact force and the mean pressure acting on the heel as well as the contact area between the heel and the pads were investigated through an FEA. Based on the result from the validated FEMs, the proposed heel pad facilitated a distinct reduction in the peak contact force (~ 10%) and the mean pressure (~14%) in comparison to the structure of a conventional diabetic insole (made of PU foam). The wear trial result confirmed that the proposed heel pad offered a better pressure relief performance than the traditional heel pad, hence reducing the risk of heel ulcers. The characterized result of the designed circular auxetic structure not only provided new insights into diabetic foot protection, but also the design and advancement of other impact resistance products. The outputs of this project therefore added a new dimension to diabetic insole design and diabetic foot treatment. More importantly, it could be used to protect the feet and reduce the risk of foot ulcers, and thus preserve the mobility of diabetic patients.

Publications arising from the thesis

Refereed Journal Articles

1) Leung, M.S.-H.; Yick, K.-L.; Sun, Y.; Chow, L.; Ng, S.-P. 3D printed auxetic heel pads for patients with diabetic mellitus.Comput.Biol. Med.2022,146, 105582 (Published)

2) Leung, M.S.-H.; Yick, K.-L.; Sun, Y.; Chow, L.; Ng, S.-P. "Numerical simulation of pressure distribution for structure design of diabetic footwear insoles." (submitted to Defence Technology Journal)

Conference Publications

1) Leung, M.S.-H.; Yick, K.-L.; Sun, Y.; Chow, L.; Ng, S.-P. (ID 154), "Proceedings of the 3nd World Conference on Advanced Materials for Defense" SCIENCENTRIS, UNIPESSOAL, LDA, ISBN 978-989-54808-7-6

Exhibitions

1) Asia Summit on Global Health (ASGH) 10-11 November 2022, Hong Kong (Organiser: HKTDC)

Acknowledgements

I would like to express my most sincere appreciation and gratitude to my Chief Supervisor, Dr Kit-Lun Yick, Associate Professor of The School of Fashion and Textiles at the Hong Kong Polytechnic University for her continuous support of my MPhil study and related research, and for her patience. Motivation, and immense knowledge. Her guidance helped me throughout time of research and writing of this thesis. Without her insightful advice, and her encouragement and support, this study would hardly have been completed.

Besides, I would like to express my warmest gratitude to my co-supervisors, Dr Yue Sun, Associate Professor of School of Fashion Design & Engineering at Zhejiang Sci-Tech University and Dr Sun-Pui Ng, Associate Division Head of the Division of Science, Engineering and Health Studies at Hong Kong Community College, The Hong Kong Polytechnic University, for their insightful and valuable comments and encouragement.

Finally, I wish to thank my family for their support and love given throughout the study.

Table of contents

List of figures

List of tables

Chapter 1 Introduction

1.1 Background

Diabetes mellitus (DM) is one of the diseases that causes the most concern worldwide because the condition has a significant economic burden on health systems. In 2021, more than 422 million people suffered from diabetes globally and the number is increasing every year[1]. In general, there are two types of diabetes: Types 1 and 2. Type 1 diabetes is mostly inherited and caused by an autoimmune reaction in which the body cannot produce any insulin[2]. Normally, Type 1 diabetes emerges at a very young age. Currently, there are no means of preventing or curing Type 1 diabetes[3]. Type 2 diabetes is when the insulin cannot be used properly so that the high blood sugar levels cannot be controlled[4]. Type 2 diabetes mainly originates from an unhealthy diet and lifestyle and mostly develops in adults or the elderly[5]. However, both types of diabetes have similar symptoms; for example, blurred vision, slow healing of injuries, diabetic foot, etc.[6, 7]. Around 50% of the population of diabetes suffer from neuropathy[8]. Due to the loss of the protective sensation that is associated with neuropathy, diabetic patients have difficulties in responding to pressure, wounds and/or injuries[9]. Wounds could quickly become infected with a long recovery duration, thus leading to foot ulceration and even foot amputation which greatly deteriorates the quality of life[10]. More than 15% of the diabetic community have developed a diabetic foot ulcer during their lifetime[11]. It is believed that the main reason for diabetic foot ulcers is excessive plantar pressure, which can result in necrosis or even amputation of the foot or the entire calf[12, 13]. Considering the above-mentioned consequences, diabetics use many different ways to protect their feet. For instance, they use diabetic insoles, and wear diabetic shoes and diabetic socks to reduce the plantar pressure and protect the plantar foot from injury[14].

Diabetic footwear is commonly worn by diabetic patients to protect their feet at all times including during both static and dynamic movements and recommended to wear all kinds of diabetic footwear once the patent is diagnosed [15, 16]. Generally, diabetic footwear has a longer shoe length and extra depth which can allow the toes to move freely without adding any unnecessary pressure compared to regular footwear[17]. Apart from that, the insole in diabetic footwear is one of the most important elements to protect the plantar foot from injury[18]. Custom-fabricated footwear insoles that are anatomically engineered to reduce the magnitude of exposure to pressure are one of the primary means to manage diabetic foot problems[19]. By using a well-designed diabetic insole, the contact area between the plantar foot and the insole can be increased, however, the contact pressure can be reduced[20]. Also, shock-absorbing, and soft material like foam, gel and leather are often used as the insole material[17] (**Figure 1.1**). Nevertheless, the efficacy of insoles varies with the stress-strain performance of the insole material which requires maintaining constant contact between the foot-insole interface and allowing effective control of plantar pressure[20]. Yet related scientific knowledge is minimal, whilst the mechanisms behind the different structures of the insoles in relation to the mechanical stress that acts tangential to the plantar surface are still unclear. To better understand the role of plantar pressure, more in-depth analyses on the foot-insole pressure and the interaction between the plantar soft tissues and insole materials are therefore necessary for engineering the design of orthotic insoles for diabetic patients[21]. However, it is important to develop insoles with a different internal structure that can increase the contact area and reduce the pressure on the plantar foot [22]. The aim of this study is to develop a diabetic insole that reduces the dynamic plantar pressure. The study will also use a finite element model (FEM) to predict the dynamic plantar pressure distribution so as to enhance the design of diabetic footwear.

Diabetic insoles are generally custom moulded. The plantar soft tissue of the diabetic foot has a slower recovery compared to non-diabetics. The geometry of the foot is one of the key factors for producing a diabetic insole. Yet related scientific knowledge on the dynamic changes to the foot shape is limited. The foot morphology of each individual patient is taken into consideration in the fabrication of custom-made insoles, in order to offer suitable support that would reduce the magnitude of induced pressure and redistribute the plantar weight forces by facilitating total contact with the plantar surface of the foot, thus reducing the development of diabetic foot ulcers[23]. An accurate representation of the shape of the foot at the foot-insole interface is the first priority in fabricating total-contact insoles, which affects the success of the goal of pressure relief. A mismatched or poorly fitting insole design can result in undue pressure on the foot, thus causing discomfort or even foot pain[24]. Despite recent developments in 3D scanning technologies, the protocols and measurement approaches used to characterise the plantar of the foot surface to design diabetic insoles are still limited.

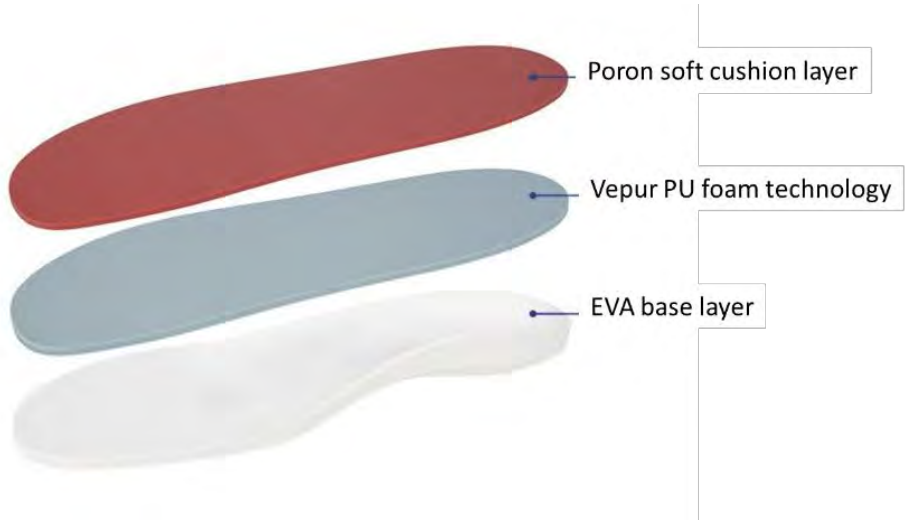

Figure 1. 1 An example of a diabetic insole with three layers of different material

1.2 Problem statement

Diabetic foot insoles are typically used for the treatment of foot ulceration in patients with diabetes. Nonetheless, there are two main problems associated with diabetic insoles which influence the quality and efficacy of treatment. They are the control of the plantar pressure in relation to the fabrication and structural design of the insole material and the 3D dynamic foot shape and fit of the insoles.

(1) Control of plantar pressure and structural design of insole materials

First, the relationship between the geometry of the plantar of the foot and pattern of the diabetic insole needs to be further examined and optimised. Generally, there are three layers with different materials that are used in a diabetic insole. Furthermore, standard diabetic insoles usually have a thicker layer in the heel and metatarsal head which can offer extra protection to those areas[25]. Since the heel and the metatarsal head of the plantar of the foot have the most contact pressure, they can become injured very easily which leads to foot ulceration[26]. The performance of diabetic insoles in preventing diabetic foot ulcers during walking is not well understood. It is believed that reducing the peak pressure and improving the pressure distribution can reduce the risk of injury. Therefore, the efficacy of currently available diabetic insoles varies with different structures and materials. However, the manufacture of diabetic insoles is specific to the wearer since there are no instructions on choosing the right diabetic insole. In other words, it is challenging to fully understand the effect of a diabetic insole in protecting the plantar of the foot from injury.

(2) Three-dimensional dynamic shape of foot and fit of insoles

As discussed above, an accurate protocol and measurement approach to obtain the foot shape with particular focus on the plantar of the foot is crucial for designing diabetic insoles. Traditionally, foot shape geometry is obtained with patients in the standing position. A standing position allows the plantar of both feet to balance the weight. However, the foot shape continuously deforms upon weight bearing and locomotion. For instance, during the heel strike position, most of the body weight is supported by the heel of the plantar, while during forefoot strike, most of the body weight is supported by the metatarsal of the plantar foot[27]. The characterisation of foot shape geometry and plantar deformation during walking is challenging with the use of traditional 3D scanning technology. Diabetic insoles that are designed from an upright standing position may therefore result in poor conformity of the foot-insole interface during dynamic movement. Therefore, this study aims to offer a scientific approach which addresses the intricacies of diabetic insoles and reliable guidelines to predict the resultant performance of diabetic insoles which would be invaluable for both research and practical purposes, thus facilitating more effective management of the diabetic foot.

1.3 Research objectives

The research objectives of this study are as follows:

1. To establish a thorough scientific basis for understanding the physiological mechanisms, particularly the foot geometry changes during walking and the contact interface between the foot skin and the footwear of diabetic patients in order to protect the diabetic foot against impact and pressure.

2. To characterise the mechanical properties of insole materials such as shock absorption, friction, stiffness, bending, etc. which affect the plantar pressure distribution in different loading conditions during walking.

3. To analyse the contact mechanics of heel strike between the heel and the insole and formulate biomechanical models to simulate the pressure distribution of the heel in relation to different the structures and features of insole materials.

4. To propose a new insole material structure and undertake laboratory wear trials to validate finite element models that analyse and numerically simulate the administration of plantar pressure, so as to accurately and reliably alleviate plantar pressure, thus reducing the risk of foot ulceration of diabetic patients.

1.4 Originality and significance of the study

With the increasing prevalence of diabetes, prevention and management of diabetic ulceration have become a leading public health challenge. Diabetic foot ulceration is one of the most detrimental and costly complications experienced by diabetic patients with 15-25% of those who suffer from foot ulcers at risk of lower limb amputation[28]. One of the major causes of ulceration is the high plantar pressure during locomotion since there are increased load and strain on the plantar skin and soft tissues[29]. Therefore, by using custom-design orthotic footwear, diabetic patients have an excellent means of evenly supporting their foot and reducing the peak pressure (up to 50-70%)[30]. They are generally made of a leather upper, with a wide and deep toe box, a rocker sole which is designed to reduce foot pressure, extra foam interlining that moulds to the natural curves of the foot and superior shock absorption for maximum comfort, wide heel base for stability, and a light and flexible sole[17].

However, there is still much ambiguity in terms of the insole fit and control of plantar pressure, thus increasing the risk of ulceration[31]. The footwear and insole prescription parameters such as the type of material and its compression, resilience, and stress-strain behaviour induced by repetitive plantar stresses are not fully studied. The changes in the foot shape and the corresponding change in plantar pressure during locomotion have been largely overlooked.

A diabetic insole that is anatomically engineered and fabricated remains challenging, thus there is currently wear discomfort, poor fit and low adherence with the use of orthotic insoles, particularly at home. Wearing poorly fitting footwear and insoles may

further worsen the foot conditions as it increases the risk of falls, thus leading to serious morbidity and mortality. This project therefore offers a scientific approach to address the intricacies of footwear for diabetics, thus advancing the design process and the choice of fabrication. Biomechanical simulation models to predict the interface pressure between the plantar of the foot and insole to control excessive plantar pressure will be established, thus facilitating effective prevention of diabetic foot ulcers. The output of this project can contribute to the development of other daily and active footwear for diabetics, and add a new dimension to footwear design, orthotic treatment and/or medical garments. More importantly, the output can be used to protect the foot and reduce the risk of ulcers, and thus preserve the mobility of diabetic patients.

1.5 Outline of the report

The structure and framework of this study is presented in Figure 1.2. The thesis is divided into seven chapters. The outline of each chapter is summarized below.

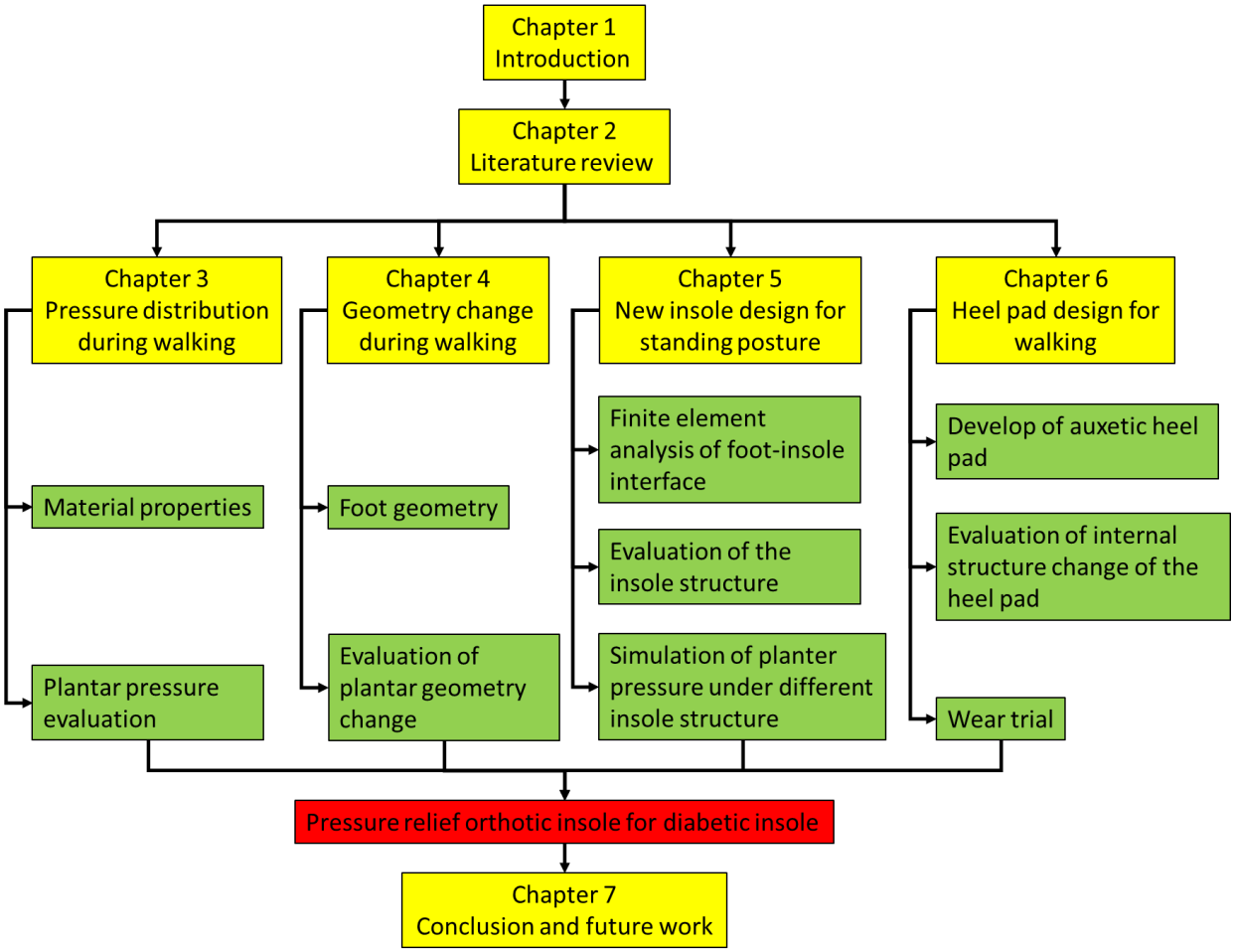

Figure 1. 2 Thesis structure and framework

Chapter 1 is the introduction of this study. This chapter provides the background information, conceptualisation and rationale, and objectives of this study. Thus, the originality and significance of this study are provided. At the end of this chapter, the outline of the chapter has been provided.

Chapter 2 is the literature review which includes a review of studies on the development and treatment of diabetic plantar ulceration, customised orthotic insoles and associated problems, foot geometry measurements and foot-insole interface pressure measurements. Also, the numerical simulation by using finite element analysis has been reviewed. It provides useful guidelines for understanding the gap knowledge and formulate a scientific approach in this study.

In chapter 3, the physical and mechanical properties of the insole materials are explored, which are the key element to determine the performance of the diabetic insoles. The effects of different insole materials on redistribution of plantar pressure during standing and walking are investigated. By using the in-shoe Pedar® system, the offloading performance of different insole materials are compared. The findings will contribute to the material selection for insole design.

Chapter 4 investigates the foot measurements and geometry changes during human walking. It aims to provide an accurate and reliable foot anthropometric data in dynamic situations for enhancing the fit and comfort of footwear and insoles. By using a novel

dynamic 3D foot scanning system, the 3D geometry shape of the foot including the plantar during walking are continuously scanned and characterized.

With reference to the excellent offloading performance of the braced frame structures, new structures of the insole material are proposed in Chapter 5. The application of braced frame structure insole for diabetic patient can effectively improve the shear stress, the contact area as well as the contact pressure of the plantar during standing posture. A FE foot model including soft tissues and bone has been developed to simulate the standing posture. The braced frame structure enhances the pressure reduction of the insole which can reduce the risk of ulcerations for the diabetic patients.

Chapter 6 explicates the development of 3D printed auxetic heel pads for the diabetic patients. The application of auxetic structure for insole development can effectively improve the contact area and contact pressure of the heel during heel strike posture. A FE model of the foot heel has been developed that the effect of the auxetic heel pad on the peak contact force, total contact point and mean pressure of the heel were simulated. The auxetic structures proposed in the study would not limit to the diabetic foot heel pads, but also various personal protective gears for optimal cushioning and protection from impact forces.

In Chapter 7, the conclusion of this study and the future research direction related to the diabetic insole for diabetic patient are proposed. The investigation and discoveries of the study will be clearly organized in this section. After that, the outlook of the development of diabetic insole of diabetes will be given.

Chapter 2 Literature Review

2.1 Introduction

Diabetic insoles are a protective solution for diabetic patients to prevent diabetic foot ulcers. In this chapter, an overview on diabetic plantar ulceration and different types of diabetic insoles is presented. The development of the insole and problems correlated with them, and their materials are reviewed. Moreover, current types of foot geometry measurements are discussed. The equipment and applications of measured plantar pressure will also be reviewed.

2.2 Diabetic foot ulceration

2.2.1 Formation of diabetic foot ulceration

Diabetic foot ulcers are a main complication of DM, and also one of the main injuries of the diabetic foot. Normally, when the body experiences an injury, the skin and/or tissues break open. This external or internal injury is called a wound. Normally, the wound will then start to heal, which is an innate immune response[32]. During the wound healing process, the extracellular matrix directs repair to replace the damaged tissues, which is a key step that produces the largest part of the dermal skin layer[33, 34] (**Figure 2.1**). Since neuropathy involves the loss of the protective sensation , the diabetic patient has a very low or no response to pressure, temperature, and any type of injury to his/her foot. As a result, diabetic patients frequently suffer from foot injuries like minor cuts or pressure injuries[35, 36]. Normally, when there is a wound, the platelets aggregate in the wound area. The activated platelets release cytokines and growth factors which further cause their activation to eventually form a haemostatic

plug. Neutrophils are important cells in the immune system that help to prevent bacterial infections. They trap and remove pathogens and dead tissue. After that, the granulation tissues, which are the new connective tissues, replace the aggregated platelets. The tensile strength of the granulation tissues then increases to that of regular skin. However, this formation process of the granulation tissues is slower for diabetics, which is why the wounds of diabetics have a very high risk of infection and then become ulcers[37, 38] **(Figure 2.2)**. Diabetic foot ulcers are frequently found in areas with high contact pressure over bony prominences of the plantar surface of the forefoot and the heel[39].

The causes of peripheral diabetic neuropathy or nerve damage is not only due to long-term hyperglycaemia (high blood sugar), but also, the blood vessels and the local tissues are pathologically changed [40, 41]. The soft tissues of the plantar of the foot can absorb compressive stresses like a cushion that can absorb energy especially in the plantar heel [28]. Nevertheless, the high blood glucose means that the skin of the feet of diabetic patients is dry, thick, and stiff. Compared to non-diabetics, the plantar soft tissues of diabetic patients have a significantly lower peak strain, but higher peak stress and Young's modulus, thus resulting in low shock absorption efficiency to dampen the effects of impact forces during gait [42, 43]. The changes in the mechanical properties of plantar tissues with impaired cushioning ability could eventually reduce their capacity to uniformly distribute load during locomotion. Of which, the heel is the first part of the plantar of the foot that is subjected to high impact forces from body weight. The altered mechanical properties of the plantar soft tissues of diabetics with repetitive and excessive loading beneath the heel, together with poor vascular supply and nerve

damage in the diabetic foot may eventually result in cell and tissue death, and thus, a high risk of heel ulceration[44].

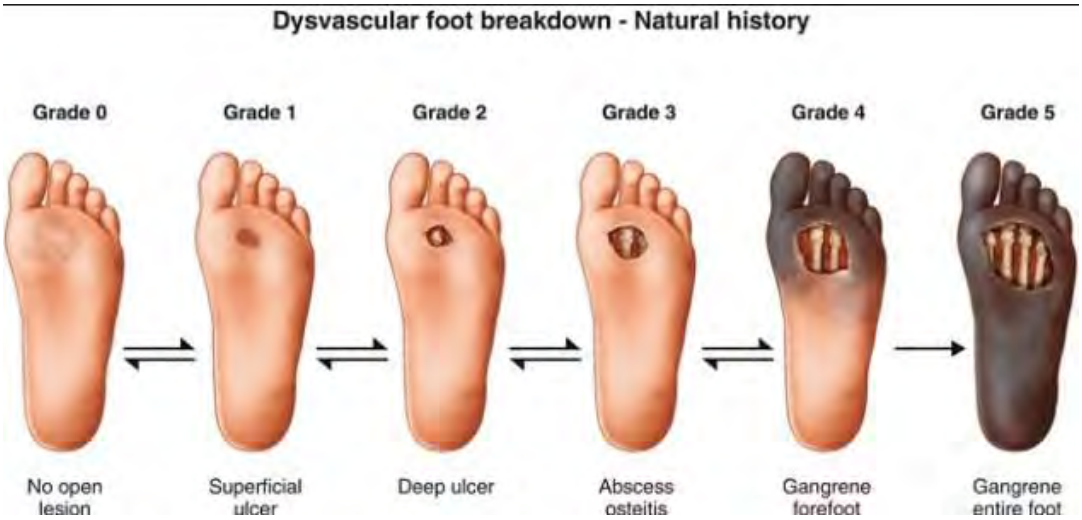

Figure 2. 1 A diabetic foot severity grade.[34]

Figure 2. 2 Immature diabetic foot ulcer[36]

2.2.2 Problems and impacts of diabetic foot ulceration

Diabetic foot ulceration can have a serious deleterious effect on quality of life including negative impacts on both career and personal life. Diabetic foot ulceration can cause loss of mobility which seriously affects many routine tasks like bathing[45] [46]. Due to limited mobility, leisure activities may not be a viable option and there is always the concern of an increased infection and deterioration of the ulcer. If the ulceration is not addressed, necrosis might occur or even the amputation of the foot or the lower leg. Although many patients can recover from such ulcers within a year, the rate if recurrence is very high[16]. Once there is ulceration, even if the ulcers are treated, recurrence is very common[47]. For example, Kim et al. [48] found in their study in South Korea that around 40% of patients have a recurrence in the same area within one year after healing and nearly 70% within their lifetime.

The problems and impact of diabetic foot ulcers are magnified for the elderly and smokers[49]. Calluses and cracked skin are commonly found in those who suffer from foot ulceration. The unhealed wound increases the humidity of the in-shoe environment which contributes to the risk of infection[50]. The usual locations of diabetic foot ulcer are over dorsal portion of the plantar especially in the metatarsal head and heel region.

2.2.3 Treatment for diabetic foot ulceration

Diabetic insoles are therapeutic insoles that are specifically made to accommodate the foot morphology, thereby facilitating its total contact with the plantar surface of the foot. The function of orthotic insoles is to reduce the transmission of elevated plantar loads from the plantar bony prominences and redistribute plantar pressure over a wider surface area, thus reducing the risk of ulceration[15, 51, 52].

Nowadays, there are several treatments for foot ulcers. In Taiwan, Oneness Biotech launched a novel topical medication called Fespixon cream, and the trial phase has commenced in the US with the aim for a global launch in 2030[53]. Also, antibiotics can be used to reduce the severity of the infection, which can stop the wound from further deterioration[54]. Moreover, there are many types of wound dressings that can be used to treat diabetic foot ulcers, such as exosome and hydrogel dressings [55, 56]. However, most related treatments can only reduce the infection of the wound[57]. The best solution is to protect the foot well and prevent the foot from injury.

2.3 Diabetic insoles

2.3.1 Principles of diabetic insole

Custom-fabricated orthotic footwear and/or insoles are commonly used for optimal fit and reducing the magnitude of the plantar pressure. The main design characteristics of orthotic footwear and insoles, such as the geometric contours, fit and material properties, which directly affect the interfacial interactions between the foot and the insole. It is anticipated that the 3D design of orthotic footwear and insoles and the choice of footwear materials have a major impact on the fit and comfort, which leads to increased

compliance with treatment to prevent ulceration of the neuropathic diabetic foot. Foot deformations and biomechanical inefficiencies can be reduced with the use of orthotic insoles, in which the plantar load from the plantar bony prominences and the peak contact pressure can be reduced by distributing the plantar pressure throughout the entire insole. Therefore, orthotic insoles can protect the plantar of the foot and reduce the risk of diabetic foot ulcers[58] (**Figure 2.3**). Diabetic insoles have the most contact with the plantar of the foot and used to evenly distribute the pressure through the entire plantar. Normally, the forefoot and the heel of the plantar are subjected to the most pressure during standing and walking[59]. When standing barefoot, there is no contact between the arch and the ground, and all the pressure is exerted onto the forefoot and the heel[60]. During barefoot walking, the process can be simply divided into 3 parts, i.e., the heel strike, mid stance and toe off. During heel strike, all the body weight is supported by the heel of one foot and the forefoot of another foot. During mid stand, all of the body weight is supported by one foot, and mainly by the heel and the forefoot. During toe off, all of the body weight is supported by the forefoot[61]. Therefore, diabetic foot ulceration[62] mainly occurs at the forefoot and heel. On the other hand, arch support can provide contact with the arch. In order to reduce the contact pressure of the foot, the contact area between the insole and plant should be increased [17]. An additional pad that offers extra cushioning to the forefoot and the heel is commonly found in diabetic insoles. Therefore, diabetic insole should be used anytime to prevent the foot from getting injury.[63]

Apart from dividing the insole into the forefoot, arch and heel, there are diabetic insoles that contain different layers with different types of materials. There is a diabetic insole that contains a triple-layer structure (**Figure 2.4**). Each layer has its own characteristics

that protect the foot of the diabetic patient. The top layer is built with perforated polypropylene (PP) material that is very soft and the primary role of this layer is to evenly distribute the plantar pressure and reduce the peak force of the insole since it is directly in contact with the plantar of the foot. The middle layer is made of ethylene vinyl acetate (EVA) which is used as a cushioning material to absorb the impact forces during walking. The bottom layer of the insole is made of polyethylene (PE) material which is relatively harder than the materials of the other two layers to provide stability during walking. Therefore, the multiple layers of materials used for the insole can provide different properties that reduce the plantar pressure and prevent diabetic foot ulcers[64].

Figure 2. 3 Example of insole structure for foot deformities

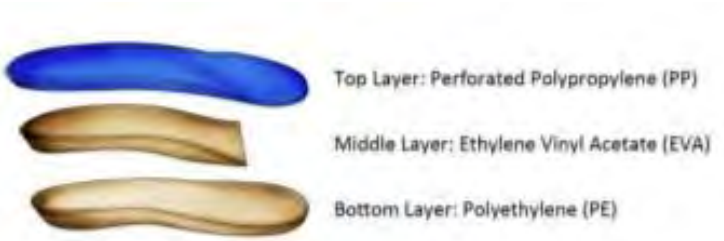

Figure 2. 4 Triple-layer structure of a foot orthopaedic insole for diabetic patients[64]

2.3.2 Properties of insole materials

As discussed in the previous section, diabetic insoles are generally made of a plurality of materials, such as PP, EVA, PE, microcellular rubber (MCR), etc. EVA such as Nora® Lunalastik and Lunairflex is available in a wide range of hardness and densities, and levels of durability. Low density EVA is generally soft and resilient which provides good cushioning, shock absorption and walking comfort, whilst high density EVA provides dimensional stability, support and control. EVA can also be formulated in open or closed cell structures. EVA with an open cell structure is pervious to liquids because the foam cells are broken so that air can permeate them more easily. Thus, open cell foam can absorb humidity since each foam cell is porous and absorbent. On the other hand, EVA with closed cell structures is less permeable to liquid, vapour, and air, but more durable due to the isolation of each foam cell. However, the EVA material is not durable. It may become very hard after some period of time, especially it is not often used.

PEs such as Pe-Lite® are soft and heat-formable in applications and offer reasonable amount of cushioning and shock absorption. PEs are a polymer with a lower density and molecular weight. These materials have a relatively smaller stiffness-to-thickness

ratio which causes permanently high compression set and rapid shape deformation. PU foams such as PORON® have excellent cushioning and pressure distribution properties, as well as high energy absorption behaviour. Soft PU foams are usually adopted in orthotic insoles for spot cushioning which not only provide excellent resistance to ground reaction forces when walking, but also high resistance to bottoming out under pressure, shock, and shear. However, the PE and PU material after several times of bending, it is easy to fracture since they have poor elongation. MCR excels at absorbing shocks from external forces. The hardness of MCR is Shore A 15 and its unique manufacturing process gives MCR the ability to spring back to its original shape when the pressure is released, which prevents high pressure points and plantar ulcers[65]. This material has not yet appeared in mass production since there are manufacturing in scaling up for large scale production, it is very difficult to ensure every product is the same.

Many studies have evaluated the effectiveness and applications of different types of insole materials on various clinical applications[66-70]. However, there is little information available on the most suitable type of insole materials for diabetic patients. Due to the scarcity of standardised guidelines for material selection, the use of materials for manufacturing insoles is highly subjective and entirely reliant on the experience of practitioners.

2.3.3 Development of diabetic insole

Traditionally, there are a total of 7 steps that are carried out to produce a diabetic insole (**Figure 2.5**). To begin with, it is important to understand the foot problems and the daily use of the insole of diabetic patients. For instance, they may have foot or knee

pain. Then the bone of the foot of the patient has to be analysed by using a 3D foot scanner. That step is to understand the lower leg alignment problem and the weight distribution patterns of the diabetic patient[71]. After understanding the alignment problem of the lower leg, the patient has to understand the correct standing posture, in which the weight distribution should be evenly placed on both feet. The next step is to use two rubber bags filled with fine silicon sand to obtain an imprint of the shape of the foot. The entire plantar of the foot including the forefoot, arch and heel, should have full contact with the rubber bag. This process can provide a perfect footprint to make the insole. Then the insoles would be produced based on the footprint. After that, stabilising is needed. The moulded insole then has to strengthen the arch area and stabilise the rear foot. Moreover, an extra layer is added underneath the parts of the insole for the heel and the metatarsal heads. Also, arch support would be added to the insole. In addition, a finishing process is required so that the insole can fit into personal footwear[72]. Lastly, the diabetic patient has to use the insole and provide feedback about the insole. Nowadays, improved technology has facilitated many new types of equipment to produce an insole. The plantar pressure during walking can be measured by using a pedograph platform including the direction and the amount of the force as well as the pressure in different gait cycles[73]. This technology can help to understand the changes in the plantar pressure[74]. Furthermore, based on the result of the plantar pressure measurements, a suitable insole can be generated by inputting the information into a computer software programme. Then by using three-dimensional (3D) printing technology, the entire insole can be printed out and the geometry of the insole can match that of the plantar of the foot.

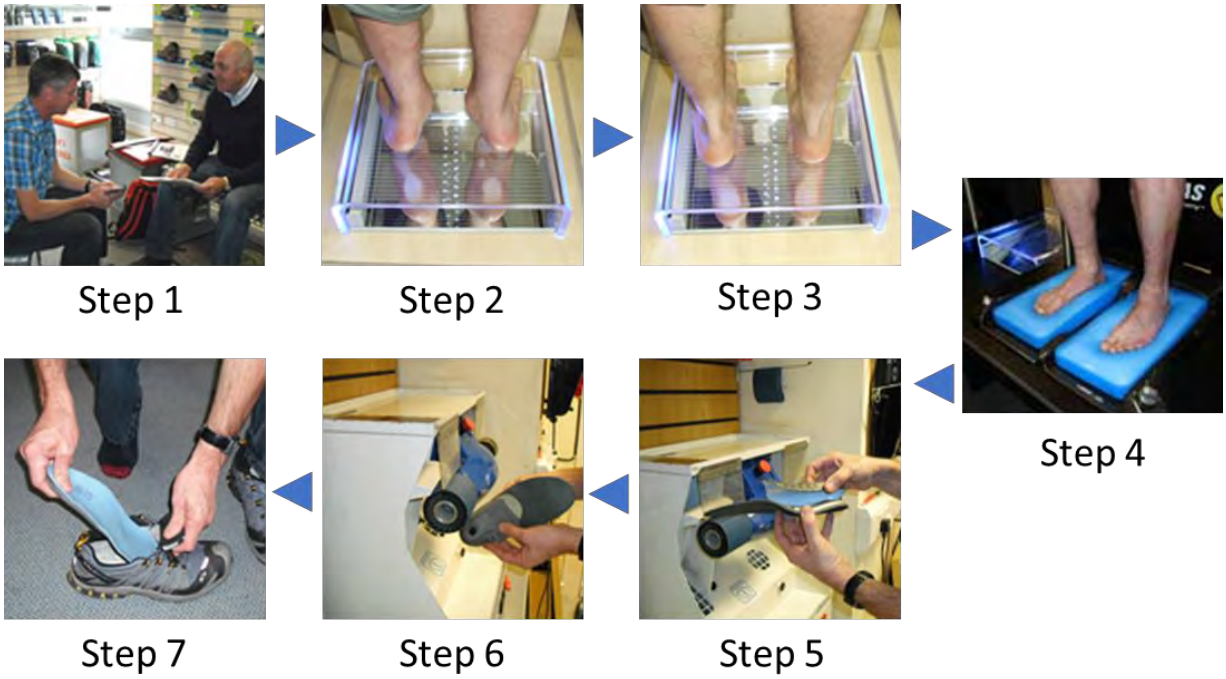

Figure 2. 5 Steps of customising a diabetic insole

2.3.4 Evaluation of plantar pressure

Recently, a number in-shoe devices have been made available and commercially and clinically adopted, as well as in examined academically, to measure the interfacial pressure between the foot and insole[75]. Pedobarography is a method to measure the pressure between the foot and a surface including floor-based systems, such as the Strideway system (Tekscan) which is a modular platform full of sensors (**Figure 2.6A**). The subject can walk on this platform and the pressure distribution during walking is measured. The key limitation of this modular platform is that only the barefoot condition can be used to measure the pressure distribution. When the subject is wearing footwear, the plantar pressure cannot be measured. The most frequently used device is the Novel Pedar® in-shoe pressure measurement system (Novel GmbH) which has

been conventionally used to measure the plantar pressure[76] (**Figure 2.6B**). The Novel Pedar® is an in-sole based system in which the insole with a matrix of pressure sensors will be inserted into a shoe. The insole can precisely and accurately receive the real time size and position of the pressure between the plantar and the footwear. There are in total 99 Pedar sensors in the insole and each sensor has a pressure range of 15 – 600 kPa. Due to the large number of sensors, the pressure distribution and centre of force that act on the foot over time can be easily obtained. The thickness of the sensors is 1.9 mm which would not affect the comfort sensation of the insole. In addition, Pedar® system has a Bluetooth® system inside and that can provide a real time data and that wireless device can provide a high flexibility and mobility for the experiment.

In previous studies, by using the in-shoe pressure measurement systems to identify the behaviour of different types of in-shoes interventions, like the shoe lacing, custom-made insole and arch support etc., on the plantar pressure distribution and loading patterns of participants with different foot problems. With the benefit of the custom-made foot orthoses and insole can redistribute the plantar pressure along the whole foot. However, the effectiveness of insoles that relieve plantar pressure may vary due to the different materials used[77-80]. There are some studies by using in-sole pressure measurement sensors to understand the performance of different material and shoe type on reducing the force and plantar pressure in different activities so as to find the best footwear that provide the best force reduction, mainly the athletes [38, 81, 82]. Therefore, there are a very wide application to collect the insole plantar pressure data. Those methods can provide a very high efficiency and accurate information for data analysis.

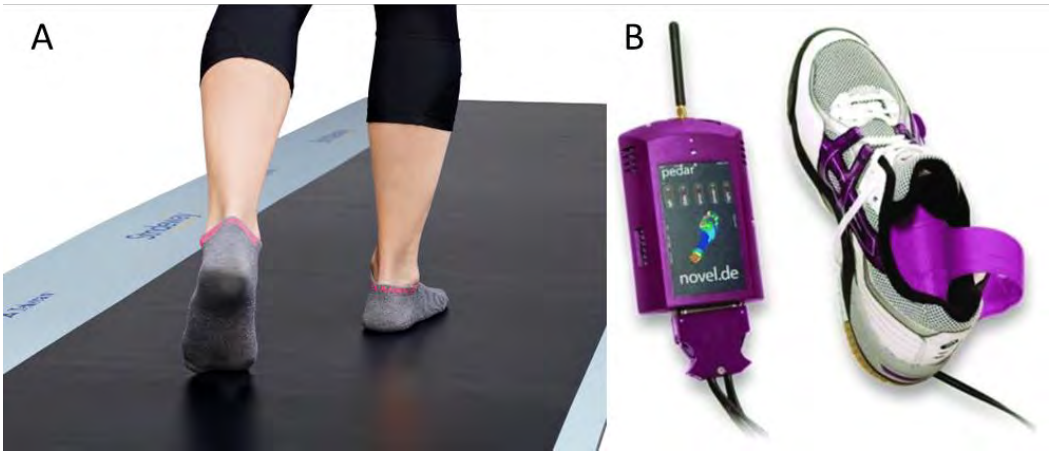

Figure 2. 6 Foot-pressure monitoring system (**A**). Modular platform, Strideway System (**B**). Pedar insole system[76]

2.3.5 Prediction of plantar pressure

Research studies have also attempted to use pressure prediction models or systems to predict the contact pressure between the plantar of the foot and the insole with the aim to reduce the individual differences and potential trials and errors during human wear trials[83]. As the production of diabetic insoles is costly and time consuming, the use of prediction models can reduce the need for extensive experiments with improved data accuracy and reliability. Also, the production model can provide a large amount of data such as the pressure on the bones, internal changes of the insole, etc.[61]. Basically, mathematical model approach as well as the computational modelling and simulation analysis method are commonly used to predict the contact interface pressure.

2.3.5.1 Mathematical model

Due to the length of time required for pressure measurements and the costly equipment, mathematicians recommend and have created different prediction models to predict the interfacial pressure[84]. Laplace's law is one of the most eminent fundamental principles developed by different researchers. Laplace equations are a nonlinear partial differential equation that explains for the continuous capillary pressure that differ at the interface between two static fluids, because of the effect of the surface tension[85]. For instance, there is an equation developed to use in diabetic plantar pressure analyses through image fusion. Image fusion was used for the wavelet transform and compared with Laplace's law [86]. Chattopadhyay and Bera [87] suggested a new mathematical method based on the principle of energy, which can predict the result of the fabric tube in the foam cylinder provided. As compared to the conventional Laplace's law, the new model has improved prediction accuracy. Although researchers have validated the accuracy of the mathematical models when comparing experimental results with the real situation, this approach is limited to cylindrical body parts. It is noted that mathematical models are not commonly used in hospitals, due to the complex mechanical properties of different textile materials.

2.3.5.2 Computational modelling and simulation analysis

Following the advancements in both the software and the hardware of computers, more complex simulation modelling approaches have been developed, which has resulted in high accuracy. Recently, the finite element method has been widely used in solving different biomechanics problems and footwear research[75, 88]. Since there are many components in the human body such as the complex structures of the bones, hyperelasticity of the tissues and complex geometry of the body surface, large,

complicated structures or geometry of the human anatomy can be simplified into finite elements in the form of triangles or quadrilaterals[89]. Based on the geometry of the foot, different material properties of the insole and foot including the bones, soft tissues and muscles can be built into the simulation[90] (**Figure 2.7**). By defining the boundary conditions on the finite elements, the plantar pressure can be estimated, and the distribution of the pressure can be shown on the plantar surface[91]. The plantar pressure and the distribution are very helpful for developing a diabetic insole so that the result of different parameters such as the insole material properties and the shape of the insole can be observed by changing the value of the input model[92].

Finite element modelling is an effective means to systematically evaluate the parametric design effects of the proposed diabetic insole and biomechanical response of the foot under different loading conditions in different stance phases, as well as with different shape and material variations, but without the need to fabricate prototypes and undergo wear trial evaluations. For example, Shaulian et al.[93] investigated the use of an FEM to simulate a foot in the heel strike position when changing the depth of the off-loading hole under the foot ulcer in the insole. It is found that a large offloading radius, large radius of curvature and large depth of the hole can reduce the most pressure and reduce the risk to the lowest for diabetic ulcers. By using an FEM, the patient does not need to try on the insole numerous times, which can reduce the experiment time and the risk of the diabetic patients of diabetic foot ulcers[15].

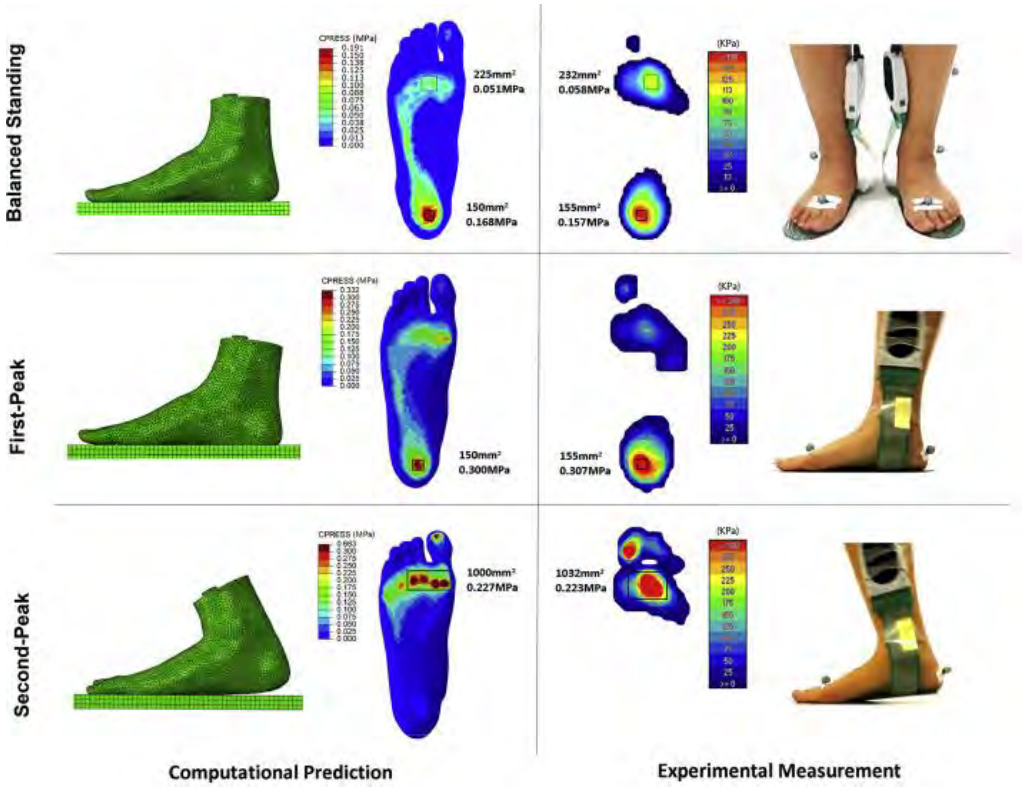

Figure 2. 7 A pressure prediction of normal subject wearing insole by using FEM and a comparison between real situation[94]

2.4 Foot anthropometric measurements

The human foot is an important organ for weight bearing and locomotion. Over the past decades, a number of studies have tried to establish a reliable and definitive foot anthropometric measurement framework that can best describe the shape, size, and proportion of the foot. Nevertheless, the foot characteristics and geometry change with posture in different weight bearing condition. For example, the plantar of the foot becomes flatter when the patient is standing on one foot, and the plantar curvature also deforms with increased body weight on the foot. Xiong et al.[24] showed that the foot length increases by about 15% when there is no to full body-weight placed onto the foot. The foot also increases in weight, reduces in height and rotates to the medial side

upon loading. Foot anthropometric measurements during dynamic walking can provide realistic 3D foot information and plantar geometries for practical use of footwear which can advance the design of diabetic insoles for improved fit and wear comfort.

Foot measurements are usually made based on the following dimensions: length, width, height, and girth of the foot. Foot length measurements include the foot, arch, heel to medial malleolus, heel to lateral malleolus and heel to 5^{th} toe lengths. Foot width measurements include the foot, heel, width, bimalleolar and mid-foot widths. Foot height measurements comprise the medial malleolus and lateral malleolus heights and height at 50% foot length[95]. For foot girths, the ball, instep, long heel, short heel, ankle and waist girths are taken.

2.4.1 Conventional methods for taking foot measurements

Foot measurement devices such as calipers and podographs are traditionally used for measuring the length and the width of the foot. Calipers are often used to measure the height of the foot and goniometers are used to measure the angle of the foot[96]. Normally, those measurement devices are easy to use and do not require much training to use them. However, they are normally low in accuracy and require a long time to use. Since they can only provide some general data, the complex anatomical sites of the dorsal and plantar of the foot are not considered in the measurements. Moreover, it is very common to have a large measurement error due to several reasons. First, the foot is flexible and soft where the position and the size of each bone and muscle may have a large difference which causes a large variation in the measurement. Also, the marked scale of each piece of equipment may not be the same due to quality control. Moreover,

the landmarks on the foot which are used to find the corresponding location for measurement might be erroneous depending on the practitioner skills. Therefore, the reliability of such equipment is questionable. In order to reduce errors and improve the accuracy of the measurement, researchers have used plaster casting to obtain the geometry of the entire foot (**Figure 2.8**). To create a plaster casting, the subject is first required to place the foot inside a container with clearance from the sides and bottom. The mixed alginate, which is used to construct the mould, is then poured into the container. After that, the subject slowly removes his/her foot from the container to help prevent air bubbles. Next, the foot is immersed again slowly and held until the mixed alginate sets to a firm solid gel. Then the foot is removed from the top of the mixed alginate. After forming the mould, the liquid form of the plaster is poured into the mould and the plaster is left to dry. Lastly, the plaster is removed from the mould and the plaster foot is formed. As the plaster foot is hard and kept in the same position, the measurement can be more accurate. However, this method requires a long processing time and only a non-weight bearing foot geometry can be obtained. In order to obtain the geometry of the plantar of the foot, podographs are commonly used and two-dimensional footprints are collected (**Figure 2.9**). Based on the footprint from the podograph, measurements such as foot length, width and angle can be taken. However, using these discussed measurement methods may have a negative effect on the diabetic foot since all of the measures require a great deal of contact with the equipment. Also, these methods may cause discomfort because it is difficult to keep the foot in the same position for a long period of time, which affects the accuracy of the measurement. Therefore, a less invasive method that requires little or no contact with the foot should be used to obtain the foot geometry.

Figure 2. 8 Example of casted foot.

Figure 2. 9 Footprint result using podograph

2.4.2 3D foot image analysis methods

Apart from the conventional measurement methods, 3D image analysis is widely used in which digital images of the human anatomy are examined. Three-dimensional scanning is becoming popular as this method can quickly capture all of the physical measurements from scanning an object. During the scanning process, there is no contact with the subject which can avoid any unnecessary injuries. Also, all of the scanned images can be stored in a digital form and retrieved when needed. As the 3D scanned images can only provide the surface geometry, it is necessary to place landmarks on the

object in order to obtain the measurements. The 3D foot images are obtained in digital form[97]. Three-dimensional surface registration is required to form a 3D image[98]. Nevertheless, the image quality is greatly influenced by light reflection. During scanning of the foot in an upright standing position, the plantar surface and the edge of the toes cannot be collected as a result of shading. On the other hand, 3D foot scanning systems with the aid of software programmes are specially designed to capture foot images so that the accuracy of data extraction can be precisely controlled. Standard foot measurements for footwear and insole production, such as the heel width, arch height, foot girth, etc. can be efficiently obtained[99, 100] (**Figure 2.10**). This not only shortens the foot scanning process, but also provides data on the plantar surface. Nevertheless, the feet are still measured or scanned during static standing or sitting in a non-weight-bearing condition.

While 3D foot scanning technologies have been gaining more attention in research studies, researchers have started to realise the limitations of scanning systems. To date, specific information on the geometric characteristics of the plantar of the foot which affect the 3D design and shape of the footbed is particularly scarce. Inherent ambiguity is also found in the foot dimensions and the 3D foot shape geometry changes during locomotion due to changes in body weight and balance. An anatomically engineered design and fabrication of orthotic insoles for diabetic patients therefore remain challenging. With advances in scanning technologies, a novel 4D foot scanning system has been developed to capture dynamic 3D foot images during a gait cycle (**Figure 2.11**). The 4D foot scanning system has numbers of modular camera units synchronized with a robust LED lighting system that used to capture the foot image together. Provides 360-degree full foot coverage. Records foot articulation and a range of actions in 4D.

The capture speed is up to 40 frames per second. It is anticipated that the dynamic scanning system provides a scientific approach to address the intricacies of footwear design which incorporates precise 3D foot shape and plantar geometries and human locomotion to improve the fit, wear comfort and adherence of the use of diabetic insoles. However, there are some limitations in using 4D scanning is that during a gait, the foot that is in swing phase may block the camera. During that moment, the 3D image of the foot during stance phase may have defect.

Figure 2. 10 (**A**) 3D laser scanner; (**B**) FotoScan scanner; (**C**) 3D foot model using 3D scanner[100]

Figure 2. 11 Example of a 4D scanning system: 3dMD (US)

2.5 Finite element analysis

Finite element analysis (FEA) is one of the commonly used computation approaches to understand and to settle the engineering problem. The first prediction method was developed in the 1800's. John William Strutt Rayleigh is the first scientist created a method to predict natural frequency of some simple structures[101]. The deformation of a structure and/or the shape changes can be quantified by minimizing the distributed energy in the structure. Unfortunately, this approach was very complicated for complex shapes since the number of possible shapes grew with complexity. However, this prediction method is important for the development of subsequent finite element analysis algorithms[102]. In the 1950s, team of Boeing used triangular stress elements to model airplane wings, and an in-house program was developed for structure analysis

in computer[103] (see **Figure 2.12**). The basic idea of finite element was thus developed, although the process was full of limitation and very time consuming. With the advances of the digital computer, the finite element analysis begins to commercially use[104]. This is a very popular computational simulation method that used to solve the numerical problem arising in engineering and mathematical modelling and to enhance the understanding of biomechanical applications[105]. Hence, the use of FEM in the biomechanical research in very common and success due to the efficient of modeling structures with asymmetric geometries and complex material properties[106]. Since it provides vivid simulation of in vivo conditions, Finite element model (FEM) can simulate load distribution and deformation of systems. It allows flexible changes of input parameters and material modifications so as to investigate their effects [107-109]. The use of FEM can overcome experimental limitations of clinically relevant applications. It is an effective approach that provides additional clinical information and generates results in a cost and time effective way for better understanding of the geometry and mechanical behaviour of the foot [93, 110]. The FEM is an ideal clinical tool to understand the foot behaviour in different situations and explore the design of different forms of footwear. Moreover, the use of FEA can reduce the risk of getting injury for the DM patients and avoid the danger of repeating experiments. In the light of the preventative measures for COVID-19, FEA can reduce the contact between each other [111, 112].

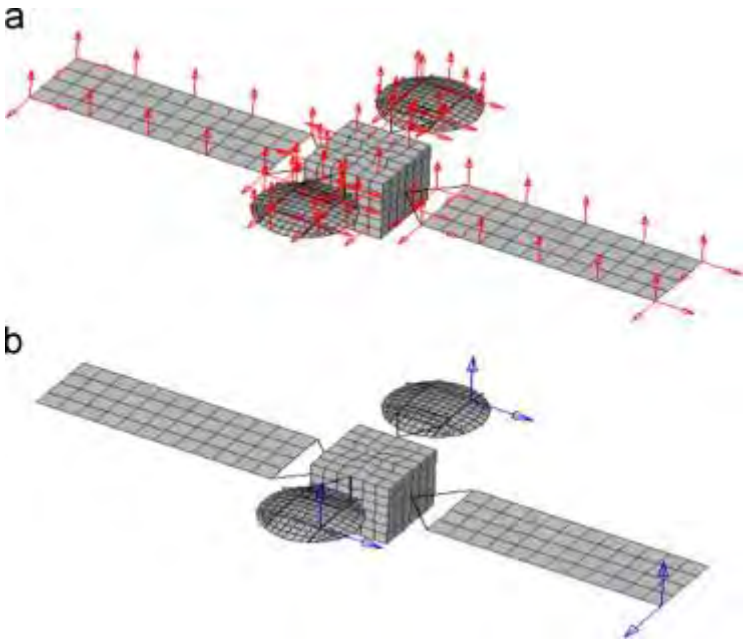

Figure 2. 12. Communication satellite with core body, rectangular photovoltaic arrays, and circular reflectors. Accelerometer layout of 124 sensors in (a) and force layout of 6 actuators in (b)

2.5.1 Principle and characteristics of finite element analysis

FEA is a famous method for numerically solving differential equations that arise in engineering and mathematical analysis. Apart from traditional problems of structural analysis, heat transfer, fluid flow, mass transfer and electromagnetic, FEA can be used to enhance the understanding of biomechanical applications. The finite element model (FEM) (**Figure 2.13**) is a general numerical method to solve partial differential equations of two or three spatial variable, for example different boundary value problem[113]. To simplify the equation problem, FEM divided some large systems into smaller and simpler parts which is called finite elements. This is achieved by discretizing a specific space in the spatial dimension, which is achieved by building a grid of objects; numerical deterritorialization with a finite number of points. The

formulation of finite element methods for boundary value problems eventually led to the creation of systems of algebraic equations. This method approximates an unknown function in the domain. The finite element that modelled by some simple equations are then combined into a larger system of equations to model the entire problem. The FEM then uses a variational approach to approximate a solution that minimizes the associated error function.

In the biomechanical applications, FEM provides a clear image that simulate the vivo condition. By using FEM, the prediction of the pressure change, temperature change, geometry change in vivo can be found easily. Once the models are developed, different experiment can be done by changing the material properties and boundary conditions, which do not have to put extra cost like the production cost of the product, or the risk of getting injury of the patients (see **Figure 2.14**). Apart from the benefit of the cost, FEM can provide more experimental results than conducting complex experiments in the real world. Hence, the FEM has been widely adopted in biomechanical research for unlimited geometry and complicated material characteristics.

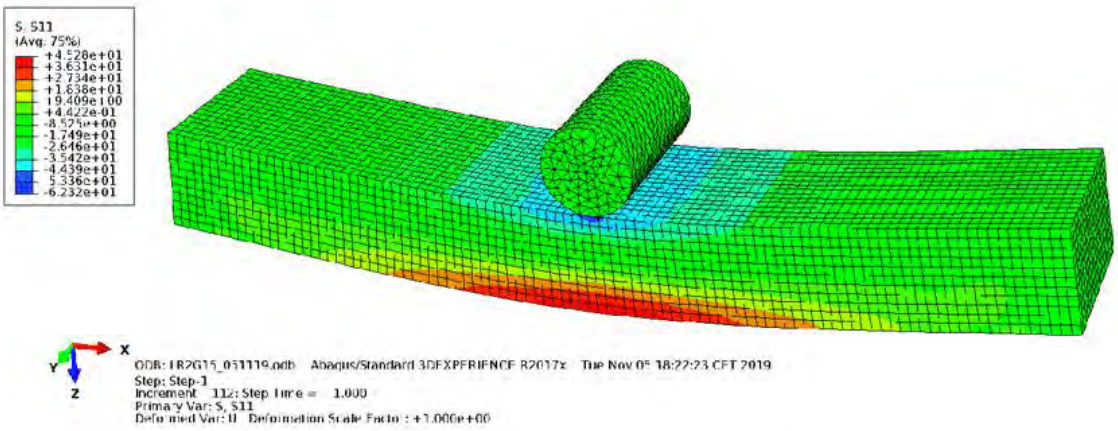

Figure 2. 13. Stress field obtained from the finite element method (FEM) analysis

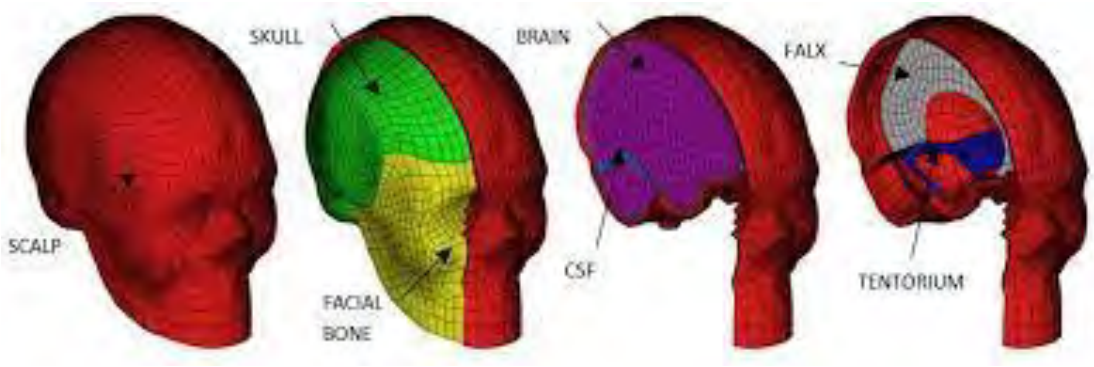

Figure 2. 14. Strasbourg University Finite Element Head Model[114]

2.5.2 Application of finite element analysis on bio-medical engineering

As there are many benefits of using FEA, many researchers have used it to develop biomedical goods and their effects on the human body. For example, a well-developed biomechanical FEM was used to simulate the contact pressure of the foot-insole interface. The soft tissue, foot bones, ankle, tendon and insole can be developed in the FEM. In order to simulate the standing posture, the boundary conditions of the model were set to applied on the Achilles tendon toward the insole and the foot bones were connected with the muscle[115]. The result of the FEM showed the plantar pressure distribution and the internal stress-strain of the bones and soft tissue structure under different boundary conditions and various of insole structure and material. Franciosa, et al.[116] integrated a FEM and a parametric study to determine the effect of the sole on the contact pressure of the foot (**Figure 2.15**). Although many researchers developed foot model to find the plantar-insole pressure by using FEA, traditional insole materials are generally used while the complex insole structure is largely neglected.

Figure 2. 15. Initial shoe design[116]

2.6 Internal structure design

Insole material structures and parameters such as stress-strain behaviour and shear force are not fully studied. Literatures on insole shear stress between the plantar-insole interface indicated that shear stresses on the diabetic foot not only show a close correlation with thermal changes in response of walking [117, 118], but also contribute up to 30% of the vertical loading on the foot[119]. Analysis of the material parameters is therefore important to better understand the insole materials for precise control and management of the plantar pressure for optimal foot protection. Therefore, in this part, braced frame structure and auxetic structure will be included.

2.6.1 Braced frame structure

Braced frame structure is traditionally used to prevent excessive lateral loading under the influence of lateral loads by providing diagonal steel members or shear cores in building construction. The structural system can resist wind and earthquake forces in the field of civil engineering building [120]. Normally, the members in a braced frame cannot be moved in lateral direction. Beams and columns in the braced frame are rated under vertical loads, assuming that the bracing system contributes to all the loads in lateral direction[121]. There is a wide range of braced framed structures, such as V-braced, X-braced and multi-storey-X-braced (**Figure 2.16**). The V-braced frame structure was design to protect the maximum unbalanced vertical and horizonal loads when there is buckling and yielding adding to the beam. However, the beam of the V-braced structure has to be very strong to keep the stability. While the X-braced and the multi-storey-X-braced structures have low peak inter-storey drift ratio, they can induce balanced forces to the beams when there are buckling and yielding. In considering the reduced shear force energy with improved stability of the braced frame structures[122], the potential use of X-braced and multi-storey-X-braced structures for insole material is investigated in this study. These two structures have a very low peak inter story drift ratio in all different braced framed structure, which means they are more stable than the others[123].

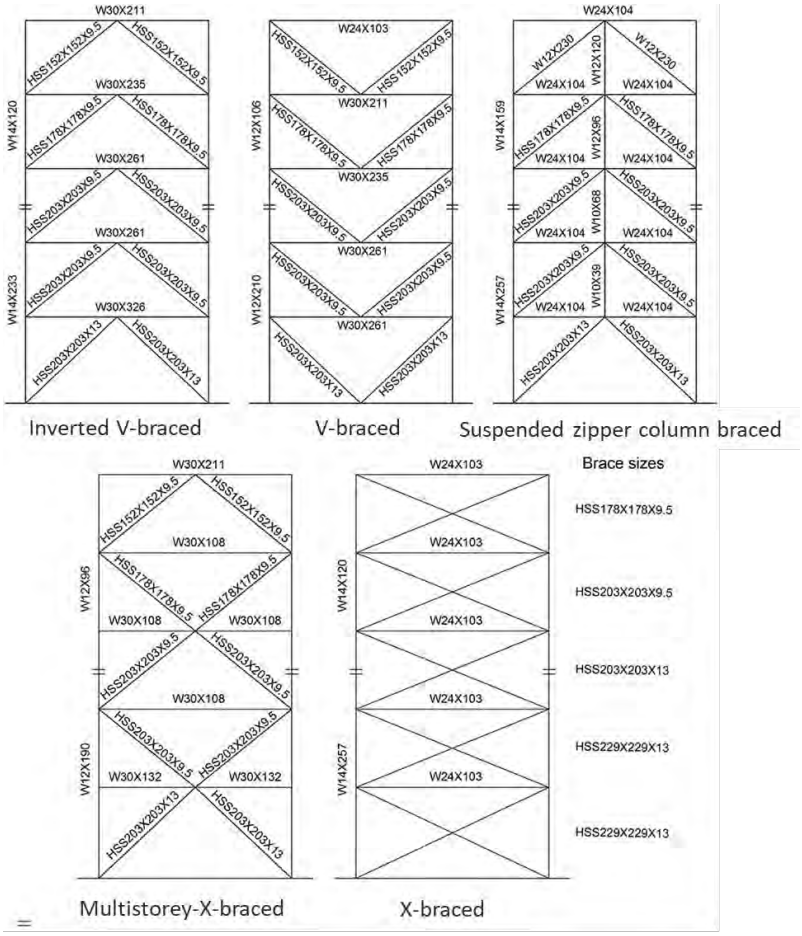

Figure 2. 16 Centric Steel Braced Frames with High Ductility

The density of insole materials is strongly associated with the energy absorption performance of insoles during wearing. When shear force is applied to the insole, the shear deformation reduces the volume of the insole by using the equation:

$$\rho = \frac{m}{V} \qquad \ldots (1)$$

where ρ is the density, $m$is the mass and V is the volume. The use of the braced framed structure may reduce the shear deformation of insole material [124], while the density of the insole can remain constant for minimal contact pressure between the plantar and the insole [125].

2.6.2 Auxetic structure

Auxetic material can be defined as a material that exhibits negative Poisson's ratio. Poisson's ratio is the ratio of the transverse train and axial strain have negative relationship. For most of the materials, have a positive Poisson's ratio, that if tensile stress is given in the longitudinal direction, the material shrinks in the transverse direction (see **Figure 2.17**). However, an auxetic material enlarge when tensile stress is given[126]. Apart from the transformation of the shape of material, Poisson's ratio is also a key of the mechanical properties that affects the shear strength and modulus of the material. There is a negative relationship between the shearing modulus and Poisson's ratio, that helps the auxetic material can be the suitable material to resist impact [127, 128]. Along with the development of auxetic material, various internal structures and geometries are invented and evaluated its deformation behaviour which can be some particular structures of macroscopic to micro-level or even a single molecule. The auxetic geometries can be summarized as re-entrant hexagons, re-entrant quadrangles, rotating units, chiral structures and foldable structures, different variations can be created based on such basic auxetic geometries to obtain a desired Poisson's ratio at different strains[129]. Together with unique deformation pattern, auxetic materials and structures are increasingly used in various personal protection equipment, seat cushions, vibration dampers, acoustic isolators, etc [86, 130]. The superior properties of auxetics for insoles may improve energy absorption and protect the foot from impact forces and the velocity of locomotion. Under a compression load, auxetic materials tend to move toward the compression point, leading to increased rigidity at the contact area with increased indentation resistance and lower energy absorption[131, 132]. It is anticipated that the increased contact area of between the plantar and the insole can alleviate high plantar pressure, particularly during body movement. As

Scarpa et al. [133] indicated, the energy absorption ability of auxetic foam is ten folds that of traditional foam materials under repetitive compression [133].

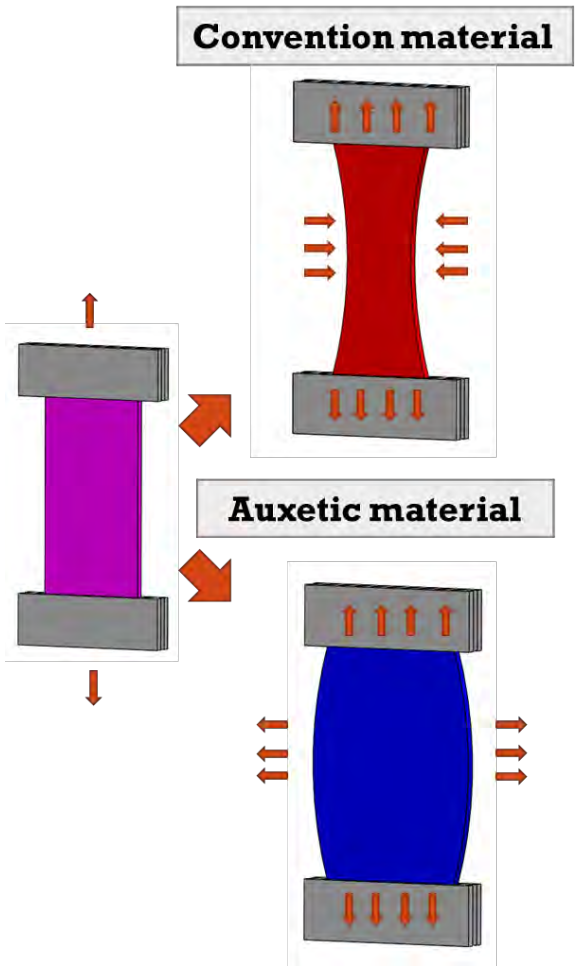

Figure 2. 17 The differences between conventional and auxetic material

2.7 Summary

Diabetic plantar ulceration resultant of elevated pressure affects foot functions and cause the need for amputation. Customised orthotic insoles are used to prevent ulcers by redistributing the plantar pressure over a wider surface area. The choice of insole materials is a key factor in improving treatment effectiveness. However, the pressure reduction performance of insole materials for diabetic patients is somewhat unclear. The material selection process is entirely based on the experience of individual practitioners. The use of a simulation model could precisely predict the performance of different insole materials on the reduction and redistribution of plantar pressure so as to optimise the design of diabetic insoles.

Precise foot geometric measurements are required to custom design orthotic insoles with an optimal fit. Nevertheless, conventional devices used to obtain foot geometry measurements show relatively low repeatability and accuracy with limited postures, while the foot shape and measurements change considerably during locomotion. The lack of foot shape information in various weight bearing conditions during stances may inevitably cause discomfort to diabetic patients who have remarkable deformities or ulcerations, thus adversely affecting the insole fit, treatment efficacy and adherence to treatment. Therefore, a reliable way to acquire 3D images of the foot during dynamic movement is necessary to minimise the problems of insole fit. To improve the efficacy of orthotic insoles, the fit of insole with a consistent contact at the interface between the foot and insole to enable effective control of the plantar pressure are paramount. Finite element models that allowing flexible changes of input parameters and material modifications can reliably simulate the load distribution and deformation of insole systems, providing a new understanding of the geometry and mechanical behaviour of

the foot and the insole. Braced frame structure and auxetic structure will be used in the design of diabetic insole to minimise the contact pressure.

Chapter 3 Pressure distribution under different insole conditions during walking

3.1 Introduction

The function of orthotic insoles is to facilitate the transmission of elevated plantar loads from prominent plantar bony prominences and redistribute plantar pressure over a wider surface area, thus reducing the risk of ulceration. The type of material not only affects the comfort of the patients, but also influences the functional performance of orthotic insoles. Knowledge on the properties of insole materials is essential to understand their behaviour for insole prescriptions. In this chapter, the material properties of different insole materials and their effects on the plantar pressure and gait performance of diabetic patients are investigated.

3.2 Experimental

3.2.1 Insole materials and test methods

A total of 3 traditional insole are sourced from the commercial market, including Lunalastik®, PeLite® and Poron®. Amongst, Lunalastik® is ethylene-vinyl acetate (EVA) and PeLite® is polyethylene foam (PE foam) with a closed cell structure, while Poron® is a polyurethane open cell foam (PU foam) with excellent impact absorption properties. To compare the material properties, ASTM D638 Standard Test Method for Tensile Properties of Plastics was referenced and the Instron 5566 universal mechanical test frame was used. In order to find the energy absorption, Young's modulus and compression strain at preset point, a 5kN load is added to the materials.

3.2.2 Subjects

There are twenty male diabetic subjects participated in this study. Their ages ranged between 60 and 71 (mean: 66.0, SD: 3.0) and BMI was 20.3 to 26.8 (mean: 23.6, SD: 2.3). The selected subjects: (1) are 55 years old or above, (2) no have no foot current foot injury, and (3) able to walk by themselves. The demographics of the participants are listed in **Table 3.1**. The study was approved by the Human Ethics Committee of the Hong Kong Polytechnic University. The participants provided written informed consent before taking part in the study.

Table 3. 1 Subject profile

	Overall N=20 (Mean± S.D.)	Range N=20
Age	66.00 ± 3.00	60-71
Weight (kg)	64.00 ± 8.00	54-84
Height (cm)	164.50 ± 6.50	155-175
BMI	23.6 ± 2.3	20.3-26.8
Foot length (Left)(cm)	40 ± 1	38-42
Foot length (Right)(cm)	39.1 ± 1.1	37-40.5

3.2.3 Plantar Pressure measurement

Subjects were required to walk in barefoot over a distance of 8m at their noraml pace to find the self-selected speed. Two timing gates were placed at the 1 m and 7 m to determine the duration for each trial. A total of 10 trials were carried out to obtain the speed of walking of each participant, which was calculated based on the division of the distance walked (6 m) by the time needed to cover this distance (s). To minimize the error on the plantar pressure due to the various walking speeds, the walking trials were refused if it over 5% of the predetermined self-selected speed [6]. The walking speed that collected from all the subjects is ranged from 0.58m/s to 0.89 m/s [7, 8]. An automatic timing gate (Brower Timing Systems, Utah, USA) is used to capture the walking speed. After recording the walking speed, In-shoe Pedar® system (Novel GmbH, Munich, Germany) was used and located between the plantar and the diabetic insole to collect the walking plantar. The subject was required to walk with their own speed three times with different diabetic insole. There are 99 sensors in the Pedar® insole and the whole insole will divide into 3 part which is the forefoot, midfoot and rearfoot to find the pressure distribution (**Figure 3.1**).

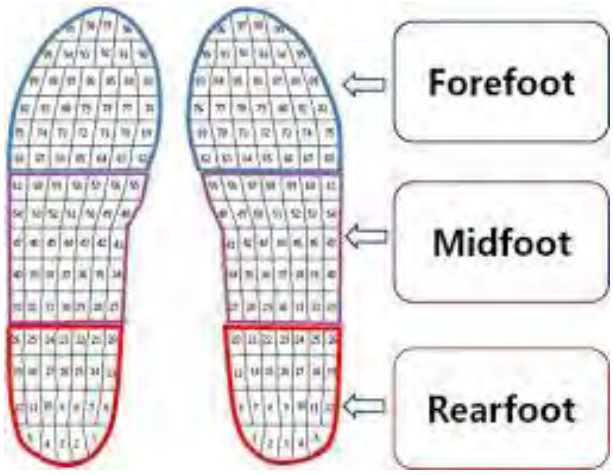

Figure 3. 1 Distribution of the 99 sensors in the Pedar® insole

3.3 Data analysis

All the received data was analysed by Statistical Package for the Social Sciences (SPSS Inc, version 22, IBM, Arnonk, NY). A one-way repeated measures Anova (rANOVA) was used to find the performance of the three insole condition and barefoot condition. Pearson's correlations have been carried out between the left and the right foot, and the mean peak pressure. The significance of the statistical analysis was set at a level of 0.05.

The percentage change of the mean peak pressure between barefoot and insole conditions were calculated with $p = [(b - a)/a] \times 100\%$, where p is the percentage change of peak pressure, b (kPa) is the mean peak pressure of walking under different insole conditions, a (kPa) is the mean peak pressure of standing under barefoot condition.

3.4 Result and Discussion

3.4.1 Material properties of the insoles

The insole material property results are shown in **Table 3.2.** 5 samples were measured for each diabetic insole and the mean were calculated. As shown, PeLite® insole resulted in the highest value in hardness of 44.6A, Young's modulus of 3.28 MPa and compression strain at preset point of 5.36%, while it has the lowest value in density of 0.16 g/cm^3 and energy absorption of 73%. Poron® insole material exhibited the lowest value in hardness of 15.1A, Young's modulus of 0.72 MPa and compression strain at pre-set point of 2.20%, while it has the highest value in density of 0.32 g/cm^3 and energy absorption of 78.60%.

Table 3. 2 A summary of material properties of insole materials

Material	**Lunalastik®**	**PeLite®**	**Poron®**
Hardness (A)	32.8	44.6	15.1
Thickness (mm)	3.12	3.17	2.91
Density (g/cm3)	0.2	0.16	0.32
Energy absorption (%)	75.30%	73.00%	78.60%
Young's modulus (MPa)	1.87	3.28	0.72
Compression strain at pre-set point % (Load=0N)	2.71	5.36	2.20

3.4.2 Overall offloading performance of different insoles

3.4.2.1 Mean peak pressure

Table 3.3 shows the mean peak pressure obtained at various insole and barefoot condition during standing and walking posture. As compared to barefoot, the use of insole has reduced the mean peak pressure by 12.1% (Lunalastik®), 14.3% (Pelite®) and 15.0% (Poron®) respectively during standing. In addition, by comparing to barefoot, the use of insole has reduced the mean peak pressure by 16.0% (Lunalastik®), 13.1% (Pelite®) and 19.8% (Poron®) respectively during walking. By using one-way repeated ANOVA analysis, all the insoles have a significant reduction as compared to barefoot in both standing and walking. Poron® showed the best offloading performance amongst the 3 insole materials studied.

Table 3. 3 Statistical results of the overall mean peak pressure during standing and walking (N=20) [a]

Standing Posture				
	Lunalastik®	**Pelite®**	**Poron®**	**Barefoot**
Mean peak pressure (kPa) ± S.D.	123.3 ± 25.4	120.3 ± 16.8	119.3 ± 20.7	140.4 ± 21.4
Compared to barefoot (p-value)	0.032	0.000	0.000	
Walking Posture				
Mean peak pressure (kPa) ± S.D.	313.9 ± 29.0	324.7 ± 34.0	299.7 ± 29.7	373.8 ± 38.2
Compared to barefoot (p-value)	0.000	0.000	0.000	

[a] Significant value ($p < 0.05$) in red

3.4.2.2 Contact area

Table 3.4 shows the mean plantar contact area at insole conditions and barefoot condition at standing posture, the contact area of the insole-plantar interface increased when insole is used. As compared to barefoot condition, the mean contact area is increased by 24.9% (Lunalastik®), 25.5% (Pelite®) and 25.1% (Poron®) respectively. By using the one-way repeated ANOVA analysis, the increased mean plantar contact area is statistically significant in all insole conditions.

During walking, the contact area of the insole-plantar interface increased when insole is used. The mean contact area is increased by 10.5% (Lunalastik®), 10.1% (Pelite®) and 10.0% (Poron®) respectively. By using the one-way repeated ANOVA analysis, the increased mean plantar contact area is statistically significant in all insole condition with the barefoot condition.

Table 3. 4 Statistical results of the overall contact area during standing and standing (N=20) [a]

	Standing posture			
	Lunalastik®	**Pelite®**	**Poron®**	**Barefoot**
Contact area (cm^2) ±S.D.	160.1 ± 16.7	160.8 ± 13.4	160.2 ± 16.6	128.1 ± 16.7
Compared to barefoot (p-value)	0.000	0.000	0.000	
	Walking Posture			
Contact area (cm^2) ± S.D.	192.9 ± 5.3	192.1 ± 6.9	192.0 ± 6.1	174.5 ± 12.1
Compared to barefoot (p-value)	0.000	0.000	0.000	

[a] Significant value ($p < 0.05$) in red

3.4.3 Regional offloading performance of different insoles

3.4.3.1 Mean Peak Pressure

Figure 3.2, **Tables 3.5** and **3.6** provide the regional mean peak pressure under various foot conditions during standing and walking. During standing posture, the use of Lunalastik® insole has reduced the peak pressures by 11.2% (rearfoot) and 15.8% (forefoot), while Pelite® insole has reduced the peak pressures by 18.1% (rearfoot) and 23.7% (forefoot) and Poron® insole has reduced the peak pressures by 14.8% (rearfoot) and 27.0% (forefoot) respectively. The insertion of 3D arch support has increased the mean peak pressure at midfoot region. During walking posture, the use of Lunalastik® insole has reduced the peak pressures by 18.9% (rearfoot), 11.9% (midfoot) and 14.0% (forefoot), while Pelite® insole has reduced the peak pressures by 18.1% (rearfoot), 5.5% (midfoot) and 12.4% (forefoot) and Poron® insole has reduced the peak pressures by 23.8% (rearfoot), 10.9% (midfoot) and 21.1% (forefoot) respectively.

Through one-way repeated ANOVA analysis, the reduction of mean peak pressure is significant at rearfoot and forefoot in most insole conditions, while the change of pressure at midfoot is statistically insignificant.

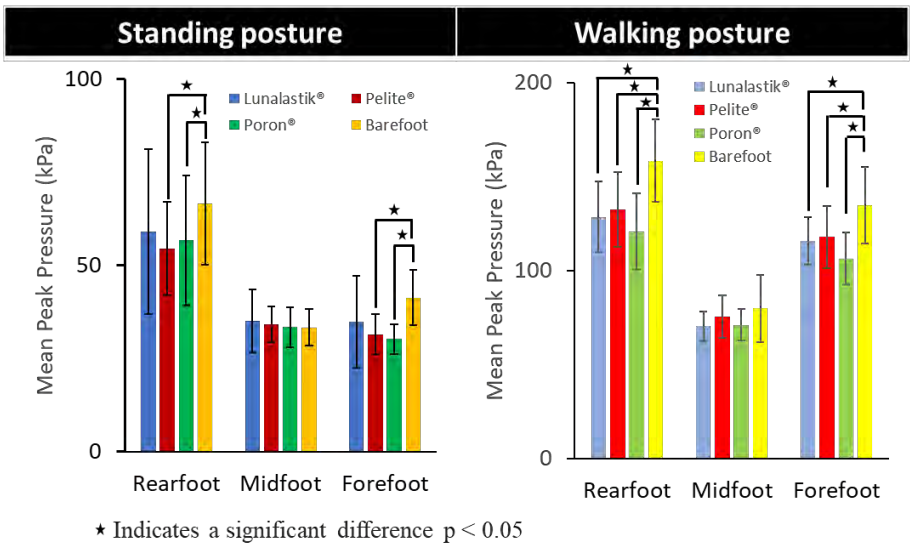

Figure 3. 2 Regional mean peak pressure comparison under insole and barefoot during standing and walking

Table 3. 5 Mean peak pressure and change percentage of each foot region under insole and barefoot conditions

Standing Posture

	Mean peak pressure (kPa) ± S.D.				Percentage change		
	Lunalastik®	Pelite®	Poron®	Barefoot	Lunalastik® VS Barefoot	Pelite® VS Barefoot	Poron® VS Barefoot
Rearfoot	59.1 ± 22.1	54.5 ± 12.5	56.7 ± 17.5	66.5 ± 16.4	-11.2%	-18.1%	-14.8%
Midfoot	35.2 ± 8.5	34.3 ± 4.8	33.4 ± 5.3	33.4 ± 4.9	5.4%	2.7%	0.1%
Forefoot	34.8 ± 12.3	31.5 ± 5.3	30.2 ± 4.1	41.4 ± 7.5	-15.8%	-23.7%	-27.0%

Walking Posture

	Mean peak pressure (kPa) ± S.D.				Percentage change		
	Lunalastik®	Pelite®	Poron®	Barefoot	Lunalastik® VS Barefoot	Pelite® VS Barefoot	Poron® VS Barefoot
Rearfoot	128.4 ± 18.8	132.5 ± 19.8	120.6 ± 20.2	158.3 ± 21.9	-18.9%	-16.3%	-23.8%
Midfoot	70.3 ± 8.0	75.3 ± 11.3	71.0 ± 8.4	79.7 ± 18.0	-11.9%	-5.5%	-10.9%
Forefoot	115.7 ± 12.6	117.9 ± 16.5	106.2 ± 13.8	134.6 ± 20.3	-14.0%	-12.4%	-21.1%

Table 3. 6 Summary of rANOVA results for effect of barefoot vs insoles (mean peak pressure)

Standing Posture					
	Barefoot VS Insoles		df	F	p-value
Rearfoot	Barefoot	Lunalastik®	7.47	4.59	0.722
		Pelite®	12.06	1.99	0.000
		Poron®	9.84	2.28	0.002
Midfoot	Barefoot	Lunalastik®	-1.79	1.75	1.000
		Pelite®	-0.90	1.00	1.000
		Poron®	-0.02	0.93	1.000
Forefoot	Barefoot	Lunalastik®	6.52	3.44	0.440
		Pelite®	9.82	1.42	0.000
		Poron®	11.19	1.74	0.000
Walking Posture					
	Barefoot VS Insoles		df	F	p-value
Rearfoot	Barefoot	Lunalastik®	29.87	2.98	0.000
		Pelite®	25.84	3.43	0.000
		Poron®	37.74	3.05	0.000
Midfoot	Barefoot	Lunalastik®	9.47	3.99	0.169
		Pelite®	4.39	4.07	1.000
		Poron®	8.68	3.62	0.162
Forefoot	Barefoot	Lunalastik®	18.82	3.21	0.000
		Pelite®	16.66	3.65	0.001
		Poron®	28.35	3.83	0.000

[a] Significant value ($p < 0.05$) in red

4.3.3.2 Contact area

Figure 3.3 shows the regional contact area at various insole and barefoot conditions. By using the one-way repeated ANOVA analysis, the use of insoles has significantly increased the contact area amongst the 3 foot regions. During walking, area similar trend is also observed, except the forefoot region.

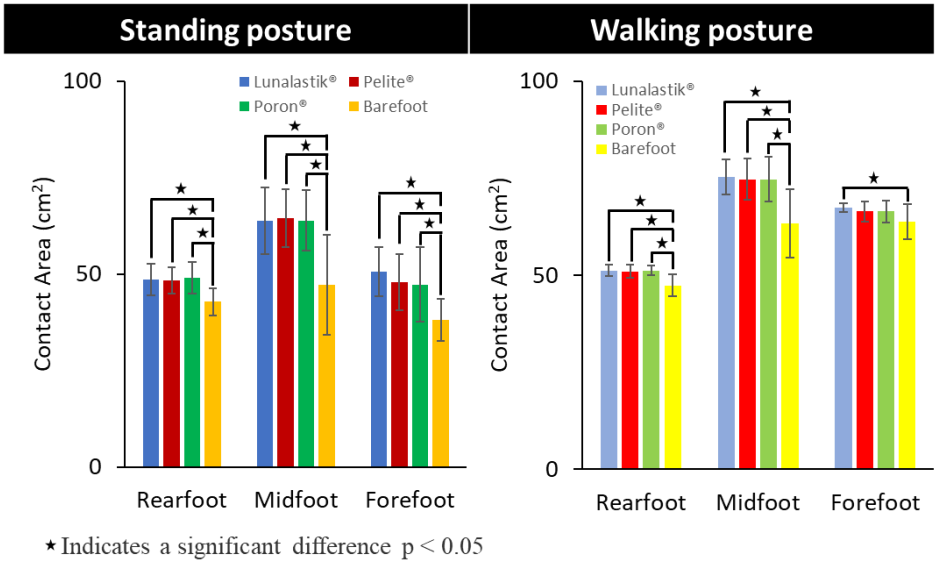

Figure 3. 3 Regional contact area comparison under insole and barefoot conditions

3.5 Discussion

Diabetic insoles are used to redistribute the plantar pressure through the whole planter and avoid peak pressure. The structure and the material property of the insole always reflect to the performance of the insoles. Arch support, metatarsal and heel pad are frequently used to reduce the peak pressure and increase the contact area of the plantar-insole interface. In this study, the material properties of the traditional diabetic insole material are firstly compared. Among the 3 insole materials, Poron® has the highest density, the lowest compression strain and the best energy absorption performance that it tends to readily absorb energy and reduce the plantar pressure. Through laboratory wear trials, Poron® has the best offloading performance in comparison with the other two insoles studied. As compared to barefoot, the use of Poron® insoles has significantly reduced the mean peak plantar pressure in both standing (15%) and walking (19.8%).

When the regional offloading performance is examined, the insoles perform differently at various foot regions. As compared to barefoot, the insertion of insole showed significant reduction of plantar pressure in the rearfoot and forefoot regions. The offloading performance of insole is less apparent in the midfoot region. This may be explained by the 3D arch support of insole with increased contact area in midfoot. Amongst, the rearfoot and forefoot generally share the highest plantar pressure at standing (70% of the total plantar pressure) and walking (80% of total plantar pressure). Therefore, regarding to an insole design, it is very important to divide the insole at least into three parts. Since the features of each insole region needs to provide different needs for the plantar. For the rearfoot and the forefoot, it is important to reduce the contact pressure by improving the material property or structure. At midfoot, arch support can

provide a better fit and increase the contact area. The material for the insole of the midfoot region can be thicker and harder which can redistribute more pressure to the midfoot.

3.6 Summary

In this chapter, the plantar pressure of the diabetic subjects at barefoot and insole conditions was investigated. Amongst the 3 traditional insole materials, Poron® insole is able to readily absorb energy and reduce the plantar pressure. The choice of insole material structure and property is crucial, thus affecting the effectiveness of insoles for optimal cushioning and protection. While the regional offloading performance of insoles perform differently at various foot regions, attention should also be paid at the rearfoot and the forefoot regions that sharing the highest insole-foot contact pressure in design of diabetic insoles.

Chapter 4 Foot Geometric changes of diabetic foot during walking

4.1 Introduction

The fit and design of diabetic insoles greatly affect the protection and performance of footwear. To provide adequate foot protection, consideration should be given to foot measurements during dynamic movement. However, currently available diabetic insoles based the standing stance of the foot have failed to provide optimum fit. The impact of foot movement on the foot dimensions should be investigated to improve the fit and protection of diabetic insoles. Taking the various walking speeds into consideration, the foot geometry for three different walking speeds is analysed in this chapter. Dynamic three-dimensional or four-dimensional (4D) scans of the foot are analysed to examine foot deformation during various foot stances, from the first heel contact, first metatarsal head contact, first toe contact, heel take off to metatarsal head take off. The changes in the manual measurements with various walking speeds are then statistically analysed.

4.2 Methodology

4.2.1 Subjects

A total of fourteen male diabetic subjects participated in this study. The selected subjects: (1) are diabetic patients, (2) have no history of foot wounds, and (3) are able to walk by themselves. The demographics of the participants are listed in **Table 4.1**. The study was approved by the Human Ethics Committee of the Hong Kong Polytechnic University. The participants were informed about the study contents in Cantonese and provided written consent before taking part in the study. The Chinese language consent forms are shown in **Figure S1.**

Table 4. 1. Participant demographics

	Male N=14 (Mean ± S.D.)	Range N=14
Body height (cm)	167.11 ±7.06	157 – 181
Body weight (kg)	66.36 ± 7.27	54 – 82
BMI (kg/m^2)	23.77 ± 2.22	20.48 – 26.78
Foot length (cm)	25.43 ± 0.86	23.40 – 26.90
Age (years old)	68.00 ± 3.00	60 – 71

4.2.2 4D scanning approach

Dynamic 3D scanning was used to obtain the foot dimensions in 5 different foot stances during gait at 3 different walking speeds. Dynamic 3D scanners can accurately capture the geometry and profile of the body with detailed information during movement. A 3dMDfoot^{TM} System Series was used to capture foot models during walking. This system provides 360-degree full foot coverage including the plantar of the foot. The system offers a maximum capture speed of 40 frames per second (fps), a total of five modular camera units and a powerful light emitting diode (LED) system. The 3D sensing of surface images offers a linear accuracy range of 0.7 mm. Scanned images are processed by the system to output 3D files of objects. The subjects are required to walk on a walkway, and the cameras then capture the foot geometry on the scanning area (see **Figure 4.1**).

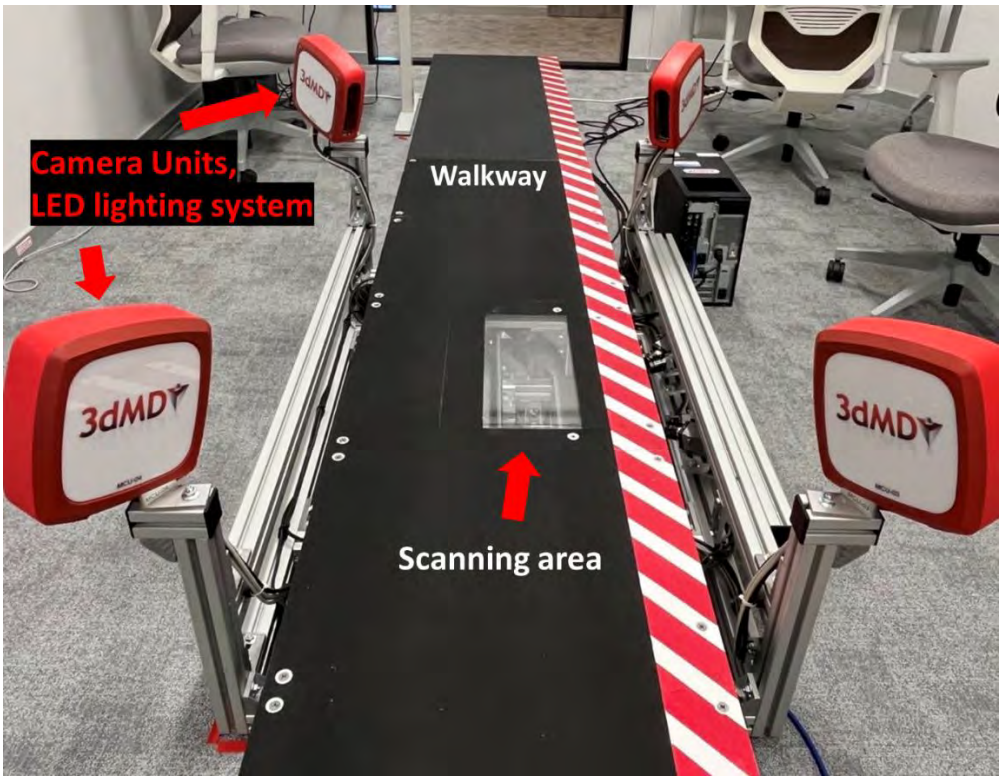

Figure 4. 1 Setup of 4D foot scanning system.

4.2.3 Landmarks and foot measurements

Before scanning, 14 coloured markers (landmarks) that are 5 mm in diameter are adhered to the foot of each subject to ensure reliable measurements for different frames during walking, as shown in **Figure 4.2**. In order to reduce the measurement error and maximized the accuracy of the data, small and flat markers are used. There are 13 measured areas, including 3 length dimensions, 2 height dimensions, 3 width dimensions, 3 angles and 2 girths, as listed in **Table 4.2** and shown in **Figure 4.3**.

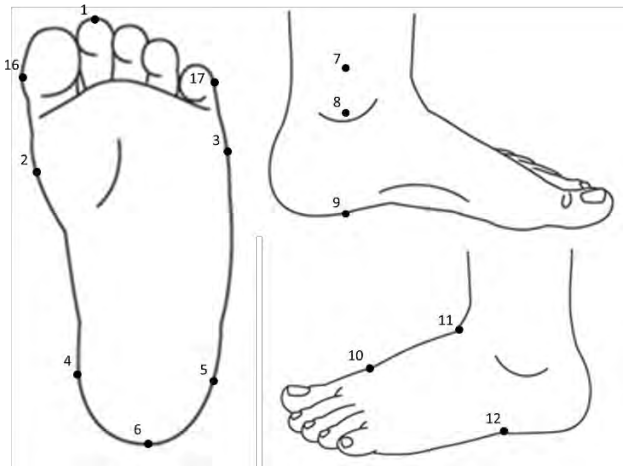

Figure 4. 2 Landmarks of foot

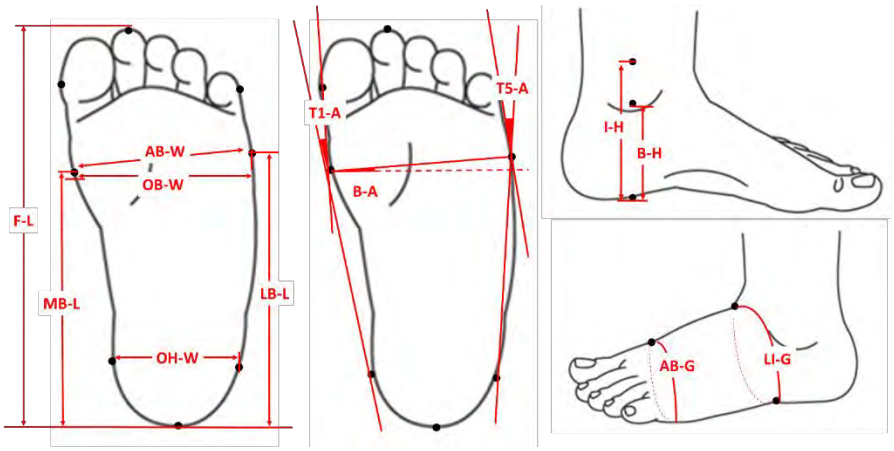

Figure 4. 3 Anthropometric measurements of foot taken from 3D images

Table 4. 2 Foot measurements for insole design [a]

Dimension type	Abbre-viation	Dimension	Description	Landmarks
Length	F-L	Foot Length	Distance between most posterior point of the heel and foremost point of the longest toe	1 – 6
	MB-L	Medial Ball Length	Distance between most posterior point of the heel and most medial point of MTH1	2 – 6
	LB-L	Lateral Ball Length	Distance between most posterior point of the heel and most lateral point of MTH5	3 – 6
Height	I-H	Instep Height	Highest point of the foot at 50% of the foot length	7 – 9
	B-H	Ball Height	Highest point of the foot at the golden ratio (61.8% of foot length)	8 – 9
Width	AB-W	Anatomical Ball Width	Distance between most medial point of MTH1 and most lateral point of MTH5	$2_{xy} – 3_{xy}$
	OB-W	Orthogonal Ball Width	Distance between most lateral and most medial points of the forefoot measured orthogonally	$2_x – 3_x$
	OH-W	Orthogonal Heel Width	Distance between most lateral and medial points if the heel measured orthogonally is between 14 and 20% of foot length	4 – 5
Angle	B-A	Ball Angle	Angle between the connecting line of MTH1 and MTH5 and the x-axis	∠3 – 2 – x axis
	T1-A	Toe 1 Angle	Angle between the connecting line of most medial point of the heel and MTH1 and the connecting line of most medial point of Toe1 and MTH5	⦤16 – 2 – 4
	T5-A	Toe 5 Angle	Angle between the connecting line of most lateral point of the heel and MTH5 and the connecting line of most lateral point of Toe5 and MTH5	⦤17 – 3 - 5
Girth	AB-G	Anatomical Ball Girth	Girth around anatomical landmarks MTH1 and MTH5	10 – 3 – 10
	LI-G	Last Instep Girth	Girth around the point detected on the last at an angle of 22^o relative to the vertical	11 – 12 – 11

[a] MTH 1: first metatarsal head; MTH 5: fifth metatarsal head.

4.2.4. Walking speed

The subjects were required to walk on a 6-metre-long platform. Two Brower Timing Systems were used to record the walking time of the subjects, and the 4D foot scanner was placed at the centre of the walking platform to capture the 3D images. The subjects were required to walk on the platform 10 times to record their normal walking time. The average time of those 10 walks was then used as the reference time for the subject. Three different walking speeds (m/s) were used: slow (6(m) / 1.2 x reference time (s)), normal (6(m) / 1.0 x reference time (s)) and fast (6(m) / 0.8 x reference time (s)). The left and right feet of each participant were scanned at those three walking speeds. If the subject walked over 5% of the predetermined self-selected speed, that scanning progress will be refused. The participants were scanned in their bare feet. Basically, five different stances of walking were captured for the different foot measurements (see **Table 4.3**). They are the first heel contact, first metatarsal head contact, first toe contact, heel take off and metatarsal head take off. The 3D images of each frame are shown in **Figure 4.4**.

Table 4. 3. Foot measurement in different walking posture

Foot measurement	First Heel Contact	First MTH Contact	First Toe Contact	Heel Take Off	MTH Take off
Foot Length		✓	✓	✓	
Medial Ball Length **Lateral Ball Length**		✓	✓	✓	
Height Measures		✓	✓	✓	
Ball Width		✓	✓	✓	✓
Heel Width	✓	✓	✓	✓	
Girth Measurement		✓	✓	✓	

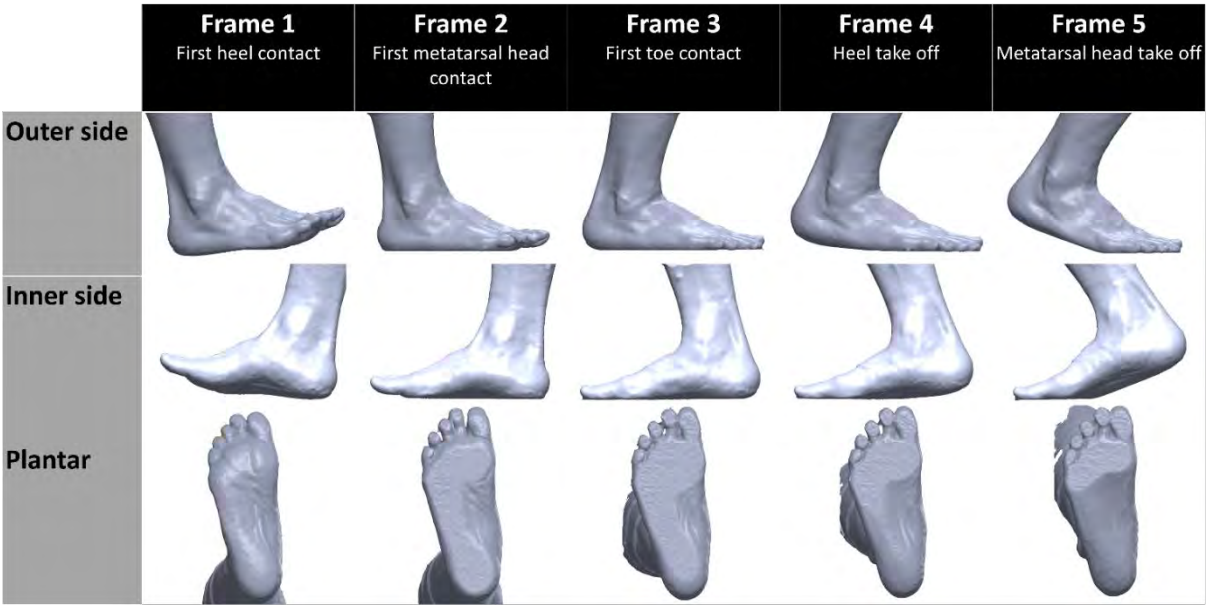

Figure 4. 4 Example of a measured 3D foot shape during gait.

4.3 Data analysis

The Statistical Package for the Social Sciences (SPSS Inc, version 22, IBM, Armonk, NY) was used to analyse the data. A repeated-measures analysis of variance (rANOVA) was performed to observe the effects of the three walking speeds as well as the foot stance on each foot measurement. The significance of the statistical analysis was set at a level of 0.05.

The foot deformation during the different stances of walking based on the foot measurements was calculated by using the deformation ratio, which is determined by using $\delta = [(Max - Min) / Min] \times 100$, where δ (%) is the foot deformation ratio, Max (mm) is the maximum measured foot dimensions and Min (mm) is the minimum measured foot dimensions for all the stances of walking.

4.4 Result

4.4.1 Differences in foot dimensions during walking

The result with different walking speed is shown in **Table 4.4.** According to the result of rANOVA result, there are no foot measurement have a significant difference among the three different walking speeds. On the other hand, 12 of the 13 foot measurements show significant differences among the 5 different walking foot stances, including in the 3 length dimensions, 2 height dimensions, 3 width dimensions, 3 angle dimensions and 2 girth dimensions (see **Table 4.5**).

Table 4. 4 Foot measurement result in different walking speed.

	Fast		**Normal**		**Slow**	
No.	Male N=14 (Mean ± S.D.)	Range N=14	Male N=14 (Mean ± S.D.)	Range N=14	Male N=14 (Mean ± S.D.)	Range N=14
F-L (mm)	253.43 ±8.46	240.16 - 269.29	251.19 ± 6.37	239.53 - 260.84	250.85 ± 8.17	238.82 - 265.65
MB-L (mm)	179.13 ± 4.85	171.30 - 187.88	181.80 ± 3.87	174.28 - 189.25	181.54 ± 5.33	171.48 - 188.38
LB-L (mm)	155.28 ± 5.26	146.80 - 163.45	156.24 ± 5.91	147.34 - 163.76	156.69 ± 5.23	146.50 - 163.64
AB-W (mm)	108.17 ± 7.20	100.16 - 127.40	108.30 ± 8.64	97.01 - 130.35	106.91 ± 6.40	100.08 - 124.96
OB-W (mm)	101.00 ± 4.37	94.17 - 108.36	100.46 ± 4.37	94.09 - 109.51	100.26 ± 4.36	94.87 - 108.26
OH-W (mm)	52.01 ± 5.64	45.75 - 63.40	52.56 ± 4.96	45.69 - 60.23	51.44 ± 5.30	44.67 - 60.51
I-H (mm)	69.12 ± 4.96	61.69 - 76.44	70.64 ± 5.59	62.71 - 79.29	69.20 ± 5.41	59.53 - 76.72
B-H (mm)	54.01 ± 5.05	46.25 - 60.85	55.21 ± 5.59	48.23 - 65.49	53.29 ± 3.90	47.53 - 58.75
B-A (°)	74.25 ± 10.90	58.47 - 89.55	77.29 ± 8.98	59.84 - 88.19	76.00 ± 10.71	61.97 - 89.81
T1-A (°)	20.49 ± 4.53	7.94 - 24.96	21.39 ± 4.05	10.99 - 24.90	19.59 ± 3.80	13.16 - 24.15
T5-A (°)	13.83 ± 3.48	8.03 - 19.88	14.96 ± 4.66	5.31 - 19.65	15.60 ± 3.71	6.96 - 19.36
AB-G (mm)	221.65 ± 14.55	202.40 - 244.46	219.29 ± 14.41	200.94 - 244.12	219.51 ± 13.48	200.93 - 236.96
LI-G (mm)	235.22 ± 14.76	213.68 - 259.68	231.79 ± 14.93	210.63 - 253.52	231.14 ± 14.30	209.91 - 254.04

Table 4. 5 Summary of rANOVA results for the effect of three different speed and five different frames on each foot measurement (N=14) [a]

Speed					Frame				
No.	**df**	**F**	**p-value**	**η2**	**No.**	**df**	**F**	**p-value**	**η2**
F-L	2.000	2.826	0.078	0.179	F-L	2.000	32978.45	0.000	1.000
MB-L	2.000	2.095	0.143	0.139	MB-L	2.000	13907.08	0.000	0.999
LB-L	1.359	0.386	0.606	0.029	LB-L	2.000	2347.863	0.000	0.994
AB-W	1.140	0.258	0.650	0.019	AB-W	1.006	252.340	0.000	0.951
OB-W	2.000	0.936	0.405	0.067	OB-W	1.041	201.926	0.000	0.940
OH-W	2.000	0.202	0.819	0.015	OH-W	1.375	23.648	0.000	0.645
I-H	2.000	3.314	0.052	0.203	I-H	1.024	835.109	0.000	0.985
B-H	2.000	1.835	0.180	0.124	B-H	1.092	352.125	0.000	0.964
B-A	2.000	0.593	0.560	0.044	B-A	3.000	7.817	0.000	0.376
T1-A	1.432	0.198	0.749	0.015	T1-A	2.144	1.177	0.326	0.083
T5-A	2.000	0.413	0.666	0.031	T5-A	3.000	5.274	0.004	0.289
AB-G	2.000	0.428	0.656	0.032	AB-G	1.245	11409.250	0.000	0.999
LI-G	2.000	0.795	0.462	0.058	LI-G	1.416	36708.340	0.000	1.000

[a] Significant value ($p < 0.05$) in red

4.4.2 Foot deformation between the walking postures

The foot deformation ratio was calculated and compared between the slow, normal and fast walking speed. The three different speeds (fast, normal and slow) and the mean result of the foot deformation ratio of the 13 foot measurements are listed in **Table 4.6**. According to the equation, a high foot deformation ratio means that the length, or the angle of the foot, undergoes a substantial change during the stances of walking. The foot deformation ratio of the length, width, height and girth is between 1.1% to 9.1%, 1,1% to 9.0% and 1.1% to 8.6% at fast, normal and slow walking speeds, respectively.

From the result, the deformation ratio of the width is the highest when comparing the length, height, and girth, as shown in **Figure 4.5**. **Figure 4.6** shows an example of the change in girth measure under different foot stances.

Comparing the change (percentage) in the angular measurements, Toe 5 angle (T5-A) shows a very large foot deformation during the different stances of walking. The deformation ratio is 58.2%, 48.9% and 56.8% at fast, normal and slow walking speeds, respectively, as shown in **Figure 4.7**. The result of the Paired T-test showed that the result of the left and right feet among all the measurement has no significant difference (**Table 4.7**).

Table 4. 6 Foot deformation ratio (%) at three different walking speeds and mean of foot measurements.

Foot deformation ratio (%) (N=14)				
Foot measurement	**Fast speed** (Mean ± S.D.)	**Normal speed** (Mean ± S.D.)	**Slow speed** (Mean ± S.D.)	**Mean** (Mean ± S.D.)
Foot length (F-L)	2.51% ± 0.10%	2.55% ± 0.11%	2.56% ± 0.09%	2.51% ± 0.10%
Medial ball length (MB-L)	2.15% ± 0.09%	2.10% ± 0.12%	2.08% ± 0.12%	2.15% ± 0.09%
Lateral ball length (LB-L)	1.10% ± 0.09%	1.14% ± 0.11%	1.14% ± 0.11%	1.10% ± 0.09%
Anatomical ball width (AB-W)	9.07% ± 1.89%	8.91% ± 1.99%	8.59% ± 2.18%	9.07% ± 1.89%
Orthogonal ball width (OB-W)	4.63% ± 0.89%	4.66% ± 0.85%	4.48% ± 1.01%	4.63% ± 0.89%
Orthogonal heel width (OH-W)	4.00% ± 1.27%	3.72% ± 1.78%	4.41% ± 1.69%	4.00% ± 1.27%
Instep height (I-H)	6.99% ± 1.88%	6.58% ± 1.36%	7.46% ± 1.40%	6.99% ± 1.88%
Ball height (B-H)	3.66% ± 0.78%	3.99% ± 0.79%	4.03% ± 1.14%	3.66% ± 0.78%
Anatomical ball girth (AB-G)	1.75% ± 0.12%	1.73% ± 0.14%	1.77% ± 0.15%	1.75% ± 0.12%
Instep girth (LI-G)	2.75% ± 0.20%	2.80% ± 0.20%	2.79% ± 0.22%	2.75% ± 0.20%
Ball angle (B-A)	11.65% ± 5.52%	13.39% ± 7.36%	18.79% ± 11.02%	14.61% ± 7.97%
Toe1 angle (T1-A)	50.27% ± 30.75%	49.97% ± 26.53%	41.12% ± 26.22%	47.12% ± 27.83%
Toe5 angle (T5-A)	58.19% ± 25.58%	48.93% ± 25.62%	56.84% ± 31.91%	54.65% ± 27.71%

Table 4. 7 The paired T-test result of left and right foot.

Paired T-test (Sig.)				
No.	**Frame**	**Fast**	**Normal**	**Slow**
F-L (mm)	1	/	/	/
	2	0.904	0.932	0.921
	3	0.936	0.940	0.914
	4	0.958	0.929	0.931
	5	/	/	/
MB-L (mm)	1	/	/	/
	2	0.903	0.913	0.939
	3	0.928	0.953	0.962
	4	0.942	0.911	0.903
	5	/	/	/
LB-L (mm)	1	/	/	/
	2	0.933	0.928	0.909
	3	0.943	0.949	0.924
	4	0.919	0.953	0.931
	5	/	/	/
AB-W (mm)	1	/	/	/
	2	0.972	0.936	0.952
	3	0.932	0.965	0.962
	4	0.925	0.951	0.944
	5	0.927	0.909	0.918
OB-W (mm)	1	/	/	/
	2	0.923	0.930	0.946
	3	0.933	0.951	0.915
	4	0.962	0.945	0.942
	5	0.917	0.904	0.927
OH-W (mm)	1	0.912	0.916	0.905
	2	0.942	0.933	0.922
	3	0.918	0.941	0.929
	4	0.936	0.913	0.922
	5	/	/	/
I-H (mm)	1	/	/	/
	2	0.953	0.962	0.963
	3	0.948	0.957	0.935
	4	0.937	0.944	0.926
	5	/	/	/
B-H (mm)	1	/	/	/
	2	0.941	0.925	0.912
	3	0.945	0.943	0.921
	4	0.962	0.938	0.933
	5	/	/	/
B-A (°)	1	/	/	/
	2	0.965	0.961	0.938
	3	0.938	0.953	0.951
	4	0.925	0.918	0.934
	5	0.912	0.907	0.922

T1-A (°)	1	/	/	/
	2	0.942	0.944	0.935
	3	0.947	0.926	0.951
	4	0.958	0.939	0.922
	5	0.941	0.928	0.933
T5-A (°)	1	/	/	/
	2	0.937	0.931	0.943
	3	0.925	0.933	0.916
	4	0.939	0.921	0.946
	5	0.938	0.942	0.928
AB-G (mm)	1	/	/	/
	2	0.935	0.944	0.941
	3	0.912	0.925	0.923
	4	0.921	0.936	0.937
	5	/	/	/
LI-G (mm)	1	/	/	/
	2	0.914	0.905	0.922
	3	0.951	0.954	0.931
	4	0.943	0.917	0.939
	5	/	/	/

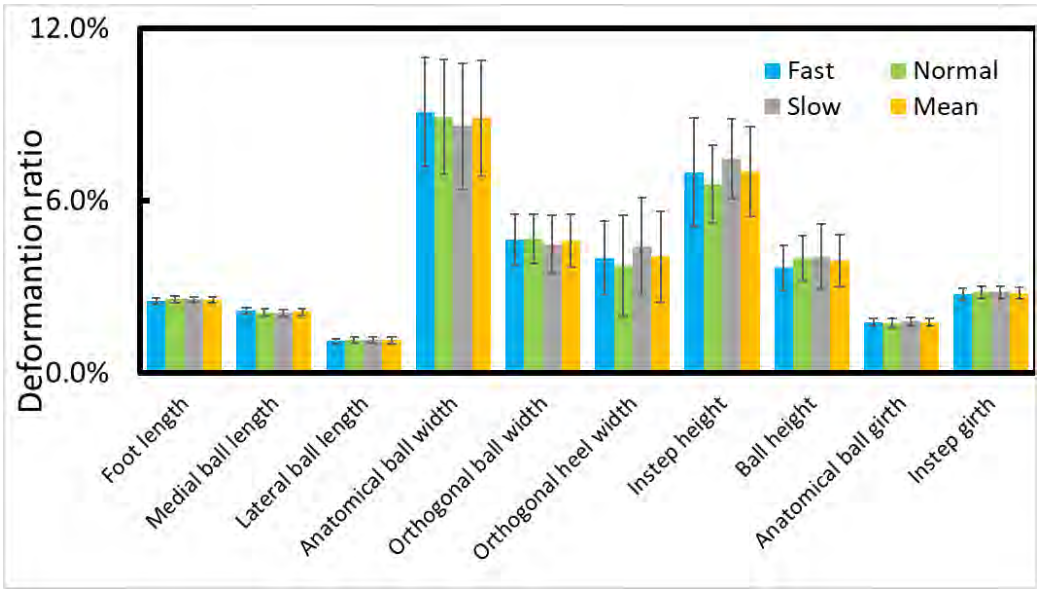

Figure 4. 5 Foot deformation ratio (%) of length, width, height and girth measurements during three different walking speeds and the mean of foot measurements.

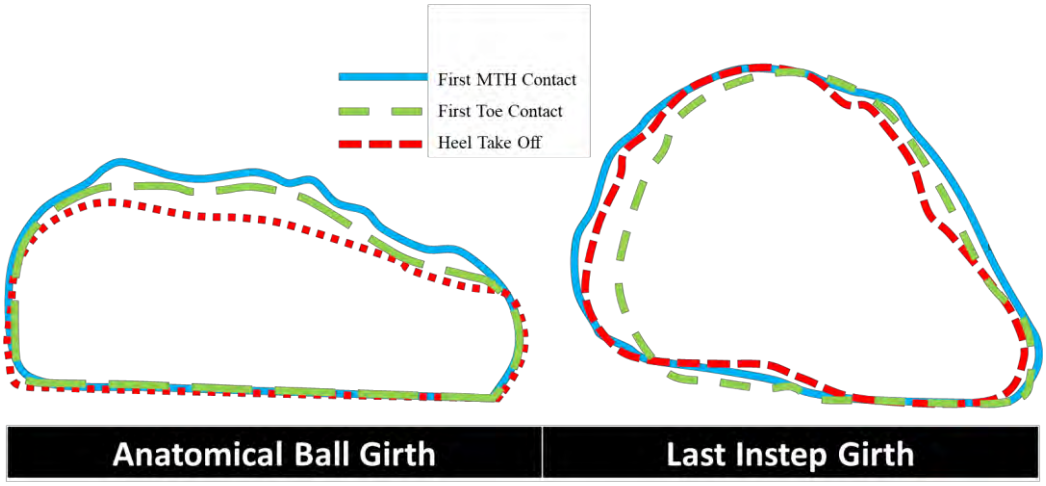

Figure 4. 6 Example of girth measurement with different stances

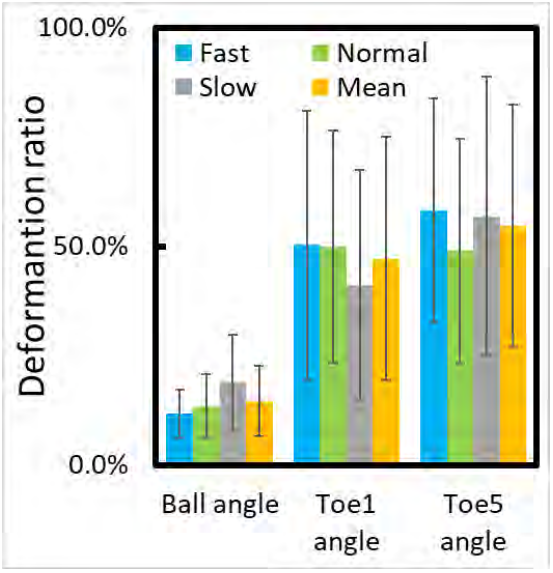

Figure 4. 7 Foot deformation ratio (%) of angle measurement during three different walking speeds and mean of foot measurements.

4.5 Discussion

According to the SPSS result, the changes in walking speed in this study do not show a significant effect on the foot measurements. However, as indicated by Burnfield et al. [134], there are significant changes in the plantar pressure with different walking speeds due to acceleration and the associated impact forces. According to Simmonds et al. [135], the weight bearing percentage during walking at a normal speed is increased from 56.1% to 64.9% with increase in walking speed. The findings of Houston et al. [136] and Tsung et al. [137] showed that there is no significant change between 50% and 100% weight bearing. Therefore, the changes in walking speed in this study (±10%) may be too subtle to induce significant foot deformation as compared to previous works. Moreover, the frame of the foot during walking stances is significant in all of the foot measurements except for Toe 1 angle (T1-A). This shows that the geometry of the foot changes with different walking stances, which aligns with the findings of Novak et al. [138]. In choosing the right footwear, there should be some tolerance for the overall deformation during dynamic situations. Wen et al. [139] found that in a group of 80 subjects, there are no significant differences in the foot measurements between the left and right feet, which is in agreement with the findings in this study. This infers that foot measurements are not influenced by foot dominance. In an orthotic insole design, it is therefore not necessary to develop left and right foot insoles individually.

Moreover, Zhang et al. [140] compared the foot dimensions at the non-weight and half weight bearing conditions of 48 subjects, and found that the length deformation is very small. In considering the five categories of foot measurements, the changes in length dimensions are the lowest (1.1% - 2.5%), while major deformations are also found in the angular dimensions (14.6% - 54.7%). Since the traditional insole design only

concerns the length of the foot, diabetic patients only focus on the length of their foot for selecting an insole or footwear. The angular dimension changes of the foot have not been considered, therefore inevitably affecting the movement of the toes during walking, especially in the area of Toes 1 and 5. The results also show that the deformation of the medial ball length is much higher than that of the lateral ball length. In footwear design, the medial foot should have more space to accommodate foot deformation.

The anatomical ball width has the highest deformation ratio (8.9%) and the highest deformation among all of the foot measurements except for the angular dimensions. In Chapter 3, it was found that the contact pressure of the forefoot is very high during walking, which correlates with the deformation ratio of the anatomical ball width. In the selection of insoles, the width of the insole is not considered, which is based on the ratio of the measured length. However, the deformation ratios of foot width are consistently higher than those of the foot length, thus leading to poor fit of footwear and even foot injury [141].

Moreover, the angular dimensions have the highest deformation ratio (14.6% to 54.7%), where T5-A has the highest deformation ratio of 54.7%. It was found that the original angle measurements are very small, especially the T1-A (18^{o}) and T5-A (10^{o}) angles. Therefore, a slight change of the angular measurement leads to a large percentage change. So it is important to provide more space to the toes to allow the toes to move freely without contact with the footwear.

4.6 Summary and Recommendation

Diabetic footwear fit is essential to facilitate foot movement during walking, as well as provide protection to the foot. Detailed foot measurements from this chapter can help to produce an optimal fitting diabetic insole that minimises the long-standing problem of insole fit in different dimensions. By using the advanced technology of a 4D scanning system, foot measurements at various loading conditions during walking can be precisely captured and measured. The 3D foot images provide valuable information for diabetic insole design with improved fit. The deformation ratio can be used to provide a better understanding of the foot deformation that advances the design and development of diabetic insoles when insoles are worn in daily activities.

Chapter 5 Numerical simulation of pressure distribution for structure design of diabetic footwear insoles.

5.1 Introduction

In this chapter, we propose a new type of insole structure which aims to reduce the maximum plantar pressure of the diabetic patients. A FEM of foot with bone models is constructed and slowly compressed to the insole under half bearing of body weight to simulate a standing posture. By using finite element analysis (FEA), the influence of the proposed insole internal structure on the redistribution of plantar pressure have been simulated and the results are compared with traditional insole structure with material of PE foam and PU foam.

5.2 Methodology

5.2.1 Design of the braced frame structures and construction of insole sub-model

A total of three different braced frame structures are used as the internal structure of the insole material, including a square structure (SQ), a X-braced frame structure (XBF) and a Multi-storey-X-braced frame structure (MXBF) respectively. Their corresponding geometry and dimensions of the unit cell are shown in **Figure 5.1**. They are prepared with dimensions of 120 mm in width, 300 mm in length and 36 mm in height for insole applications [142]. The dimensions of the unit cells and the insole are kept constant, while the volume of the insoles varies with different internal structure designs (**Table 5.1**). Their mechanical properties and the pressure reduction performance are also compared with two traditional insole materials, including a PU foam (Poron®) and a PE foam (PeLite®).

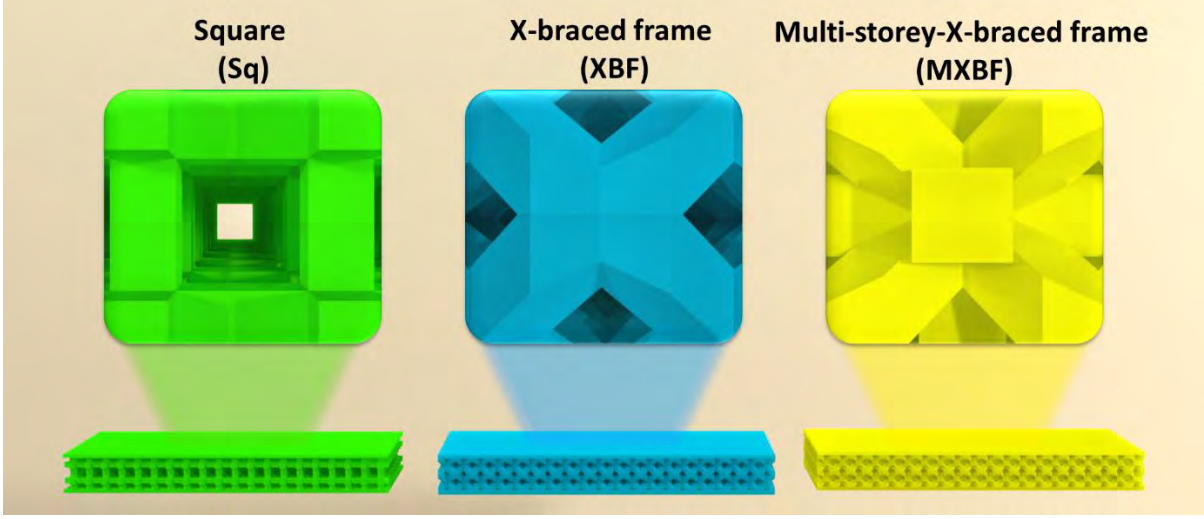

Figure 5. 1 Internal structures of insole in a Square (Sq), a X-braced frame (XBF) and a Multi-storey-X-braced frame (MXEF) structure.

Table 5. 1 Volume of the insole with different internal structures

Insole Structure	Volume (mm^3)
Square (SQ)	496,000.00
X-braced frame (XBF)	755,133.72
Multi-storey-X-braced frame (MXBF)	897,045.70
Original (as control)	1,296,000.00

5.2.2 Mechanical characterization of the insole material

The compression properties of two traditional types of insole materials, PU foam (Poron®) and PE foam (PeLite®), were first measured. The ASTM D575 Standard Test Method for rubber properties in compression was referenced and the Instron 5566 universal mechanical test frame was used. The specimens are 28.5 mm in diameter and 12.5 mm in thickness. The results were then inputted into the FEM to simulate the interface pressure distribution during insole compression.

5.2.3 Three-dimensional scanning and modelling of foot sub-model

A structured light handheld 3D scanner (Artec Eva, Luxembourg) was used to obtain the geometry and shape of a non-weighted foot (28 cm) of a healthy 26-year-old male subject. The complex geometry and shape of the foot can be scanned accurately with this scanner. This handheld 3D scanner has a 3D point accuracy up to 0.1mm, a 3D resolution up to 0.2mm and a 3D reconstruction rate up to 16fps. By transforming the raw scanning data to a 3D model, Artec Studio 13 was used. After obtaining the 3D model of the foot, the sub-model of the foot bones including distal phalange, metatarsal, cuboid, talus, calcaneus and tibia, as well as the designed insole and the foot were constructed into a mesh model by using MSC Apex software. After the meshed model was developed, then it was input into a FEA software (MSC Marc 2019.2.0, US) and which is known as the FEM (**Figures 5.2A** and **5.2B**). The material properties of the foot and bones were obtained with reference to Gefen et al. [143] (**Table 5.2**). The Young's modulus and Poisson's ratio for the bones and soft tissues are 7300 MPa and 0.3, 0.3MPa and 0.4 respectively. The element type of the insole is a structural 3-D solid element type 127, the foot and the bones are structural 3-D solid element type 134

[88], while the insole material is regarded as an Ogden elastomer model [144]. The following equation is used to determine the strain energy:

$$W_{deviatoric}^{ogden} = \sum_{k=1}^{N} \frac{\mu_k}{\alpha_k}\left(\bar{\lambda}_1^{\alpha_k} + \bar{\lambda}_2^{\alpha_k} + \bar{\lambda}_3^{\alpha_k} - 3\right) \quad \ldots(1)$$

where $\bar{\lambda}_1^{\alpha_k} = J^{-\frac{\alpha_k}{3}}\lambda_i^{\alpha_k}$ is the deviatoric stretch ratio while μ_k and α_k are the moduli and exponent constants obtained from the curve fitting of the experimental data. To validate the accuracy of the FE contact model, a compression test was done so that the simulated result was compared with the experimental compression result based on the ASTM D575 standard test method.

Table 5. 2 Material properties and element type of the finite element model

Component	**Element type**	**Young's modulus E (MPa)**	**Poisson's ratio ν**
Bone	3D-tetrahedra	7300	0.3
Soft tissue	3D-tetrahedra	0.3	0.4

To evaluate the plantar pressure in the standing position, an external force of 350 N (half weight of the subject) was applied onto the insole (see **Figure 5.2C**). To ensure all the force can be evenly applied onto the insole, a rigid link (RBE2) was set where each node on the bottom surface of the insole was rigidly connected to a corresponding node that was set under the insole, while the degree of freedom in all directions was also fixed. The nodes above the ankle of the foot were fixed in all directions and the

bones inside the foot were set as a rigid body. The friction force tolerance was set to be 0.22 [145]. The shear stress, maximum contact force and total contact area of the plantar under the different structures of insole material were systematically investigated and compared.

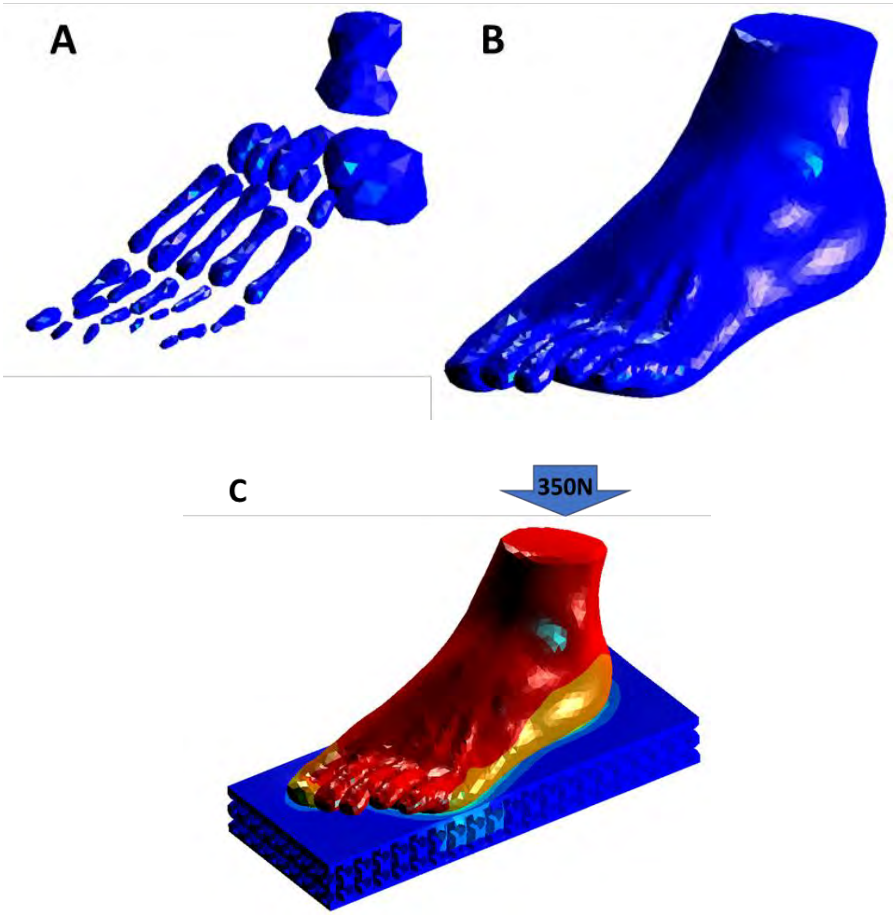

Figure 5. 2 The FE foot models including (**A**) bone and (**B**) soft tissue that (**C**) its shear stress, contact area and contact force with the insole sub-model can be simulated and optimised through FEA

5.3 Result and discussion

5.3.1 Compression properties

In order to withstand the deformation loads and retain the original shape of the insole material to reduce the plantar pressure, the compressive stress of the insole material is an important parameter. The stress-strain behaviour is one of the criteria to determine the performance of the insole. With a low Young's modulus, the insole can be easily deformed to absorb energy. The stress-strain cycle of traditional insole material is plotted in **Figure 5.3** and the Young's modulus and Poisson's ratio values are listed in **Table 5.3**. The PE foam has a higher Young's modulus than that of the PU foam. PE foam tends to have better shape retention with less deformation as compared to the PU foam. The Young's modulus and Poisson's ratio values are applied to the FEM.

Table 5. 3. Material properties of the insole material

Material	Young's modulus E (MPa)	Poisson's ratio v	Density ρ (kg/m^3)
PU foam (Poron®)	1	0.35	52.5
PE foam (PeLite®)	3	0.34	73.5

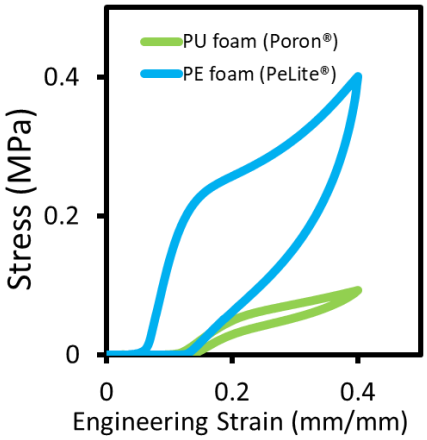

Figure 5. 3 Potted material compression properties: stress-strain of PU foam vs PE foam

5.3.2 Validation of material properties: stress-strain of PU foam vs PE foam

First, the reliability of the FEM is validated to confirm its ability to accurately predict the material compression behaviour by using a FEA. A compression test was carried out and the simulation results were compared with the experimentally obtained compression displacement values. The solid specimens for the FEM are 28.5 mm in diameter and 12.5 mm in thickness. A compression force of 350 N was applied to the specimens to measure their displacements. The results showed that the FEM can accurately predict the compression displacements of the PU and PE foams. As shown in **Figure 5.4**, the compression displacement results obtained from the simulation model is slightly higher than those from the experiments, but with less than a 3% discrepancy, while the friction during the experiment is negligible in the FEM.

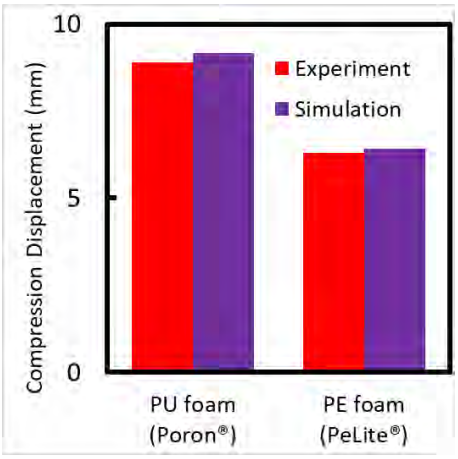

Figure 5. 4 Validation of the developed FEM. Comparison of experiment and simulation results for PU foam and PE foam.

5.3.3 Effect of insole internal structures on the insole-plantar interface

The FEM was then used to predict the influence of the proposed internal structure of the PU and PE foams on the plantar of the foot. The shear stress, contact area, as well as contact forces between the insole and plantar interface were then systematically analysed.

5.3.3.1 Shear stress

A 3D geometric sub-model of the human foot was developed to predict the shear stress of the soft tissues of the foot, the interface pressure between the foot and insole and the contact conditions during standing, when the different insoles are worn. The mean shear stress between the foot and the insole is shown in **Figure 5.5A**. The results indicate that the PU foam insoles show a lower shear force compared to the PE foam insoles by an average of 12%, which may be associated with the deformation behaviour of PE insoles. In both foams, the proposed braced frame structure results in a major reduction of the shear stress (21% or higher). As compared to the MXBF structure, the results show that the XBF structure has a lower shear stress. The shear stress reduction performance of the non-braced frame structure (Sq) is less effective, as compared to the braced frame structures (XBF and MXBF). The shear stress distribution between the foot and the insole for the various insole conditions is also obtained through simulation.

As shown in **Figures 5.5B** and **5.5C**, high shear stresses are found along the edge of the heel, metatarsals and the great toe, where the plantar soft tissues deform the most, thus leading to a high risk of foot pain and injury. The peak shear stress on the edge of the PU foam insole is lower than that of the PE foam insole (17% and higher). The

braced frame structure has a low peak shear stress as compared to the non-braced frame structure (Sq). Therefore, the braced frame structure can reduce the peak and the mean shear stress of the plantar of the foot, which can greatly reduce the risk of becoming injured from shearing forces.

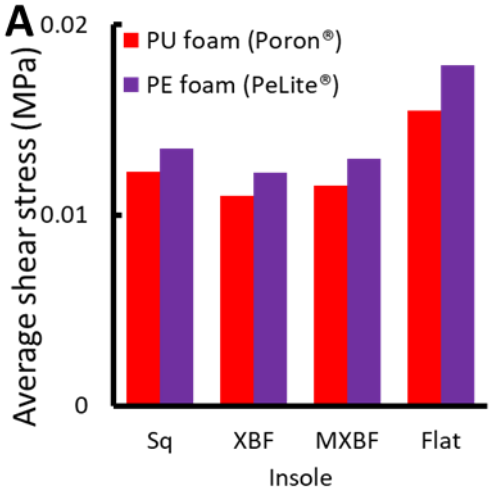

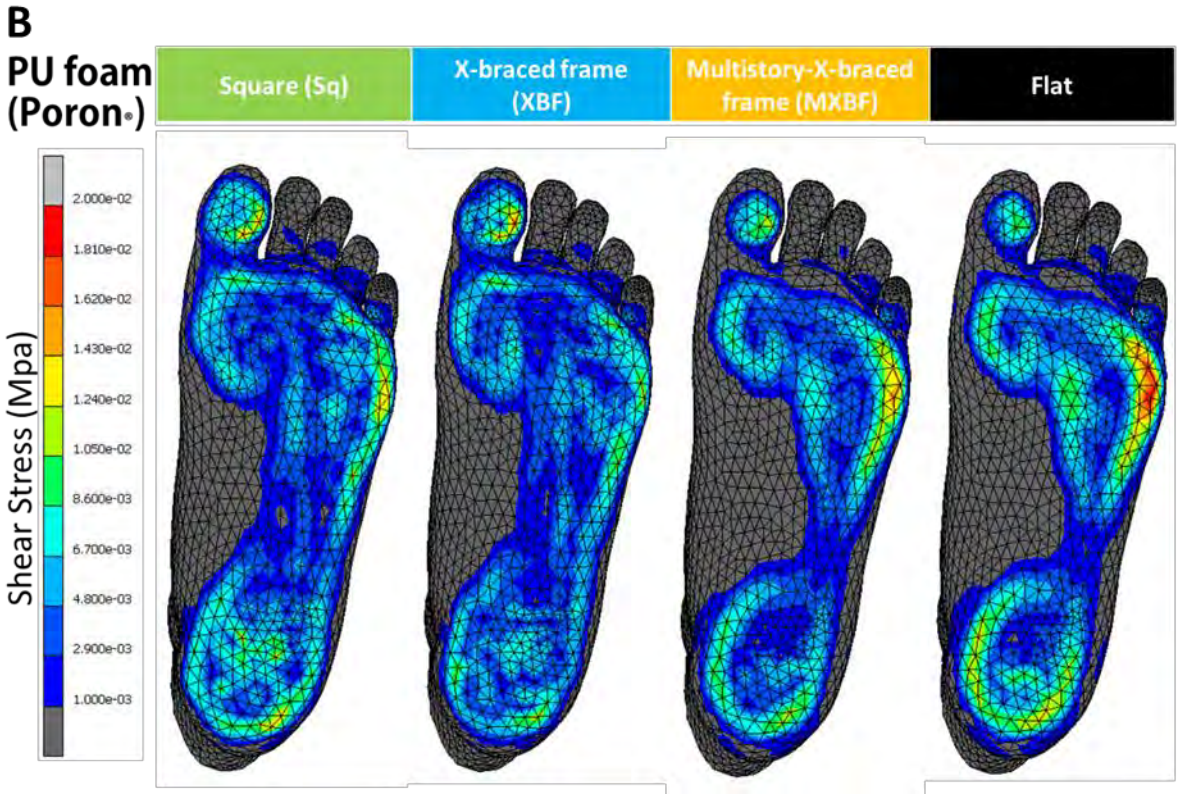

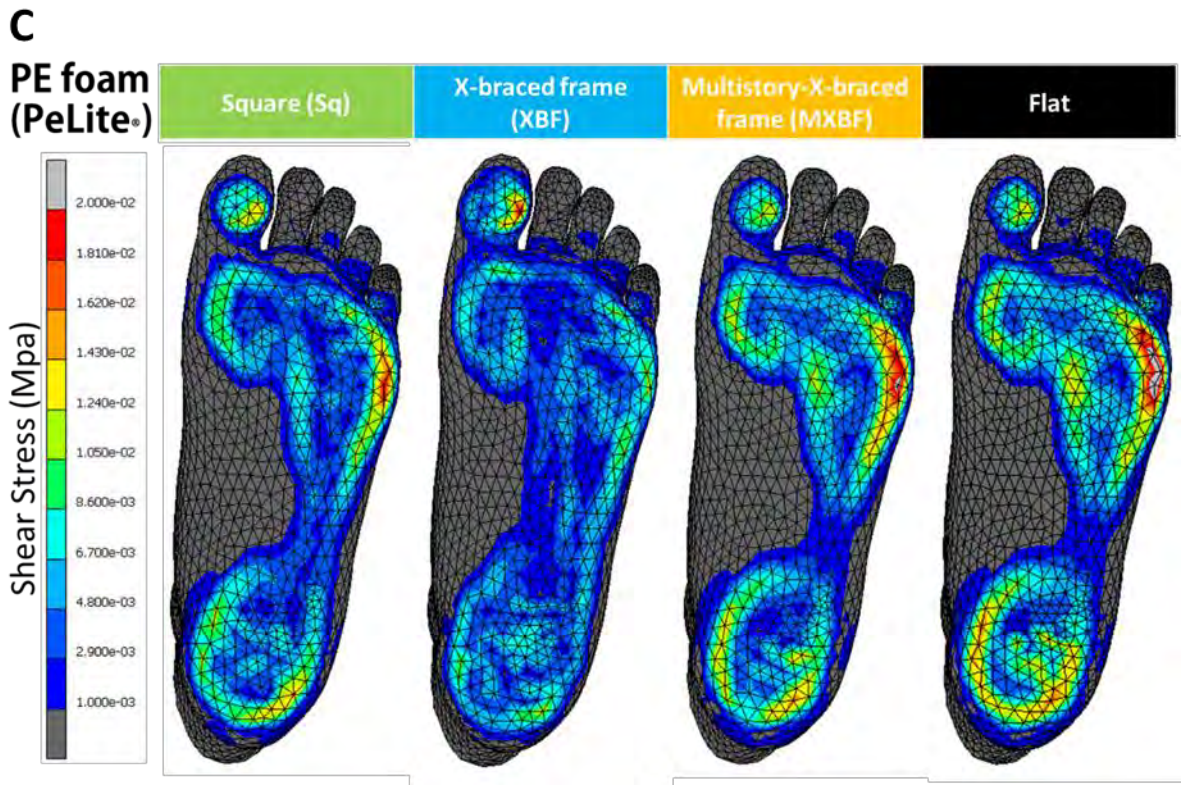

Figure 5. 5(**A**)Shear stress of PU and PE insoles in different internal structures; (**B**) Shear stress distribution of the foot plantar at various PU insole structures and (**C**) PE insole structures.

5.3.3.2Contact area

Apart from the shear stress, insole designs with increased contact area between the insole and the plantar are primarily adopted to redistribute the plantar pressure, particularly during body movement for optimal foot protection from excessive plantar pressure and even ulcerations for diabetic patients. The contact area is determined by:

$$P = \frac{F}{A} \qquad \ldots(2)$$

where P is the pressure, F is the magnitude of the normal forces and A is the area of the surface on contact. As shown in **Figure 5.6A**, XBF shows a very high contact area in both the PU and PE foams while Sq and MXBF show a similar result in the total contact area. The original structure of the PU and PE insoles provides the smallest total contact area. As compared to the control, the braced frame structure of XBF tends to increase the contact area by 64% in the PU insole and 90% in the PE insole, at a load of 350 N. Therefore, XBF increases the contact area more effectively than non-braced frame structure (Sq) in both the PU (20%) and PE insoles (46%) (see **Figure 5.6B**).

The percentage changes in volume between XBF and the non-braced frame structure (Sq) were then compared. The results showed that the volume of XBF is 52% larger than that of Sq. The changes in the internal structure between the two insoles are shown in **Figure 5.6C**. Under a compression load of 350 N, the space in the beam of the XBF insole is substantially reduced as compared to the Sq. The XBF insole structure can readily accommodate the curved interface of the plantar of the foot, hence leading to an increased contact area with the plantar.

A simple FE simulation was carried out to obtain the compression behaviour of the insole structures. A compression force was applied onto a PU foam cuboid (length: 5 mm, width: 5 mm, and height: 10 mm) along two different directions (see **Figure 5.7A**). To compress a cuboid of 1 mm, a total force of 3.47 N is required while to bend a cuboid of 1 mm, the total force required is only 0.22 N. Apart from the FE, a mathematical analysis was done to compare the forces for compression and bending. The equation for compression stress is:

$$\sigma = \frac{\Delta L}{L_o} \mathrm{E} \qquad \ldots(3)$$

where σ is the compression stress, ΔL is the change in the length, L_o is the original length and E is the Young's modulus of the material. It was found that a force of 2.5 N is needed to compress 1 mm of cuboid. The equation for the bending stress is:

$$\sigma = \frac{Mc}{I} \qquad \ldots(4)$$

$$\mathrm{I} = \int_Q r^2 dm \qquad \ldots(5)$$

where σ is the bending stress, M is the bending moment with respect to the centroidal axis, c is the radius of the centroidal axis, I is the bending moment of inertia, r is the distance to some potential rotation axis, and the integral is over all the infinitesimal elements of mass, dm, in a three-dimensional space occupied by object Q. The bending moment of the cuboid is $\frac{1}{3}ML^2$. Therefore, the force required to bend 1 mm of cuboid is 0.16 N. Both the FE and mathematical results show that 1500% less force is needed to bend than compress 1 mm of cuboid (see **Figure 5.7B**). Therefore, the XBF insole can be readily deformed with increase in contact area between the plantar and the insole.

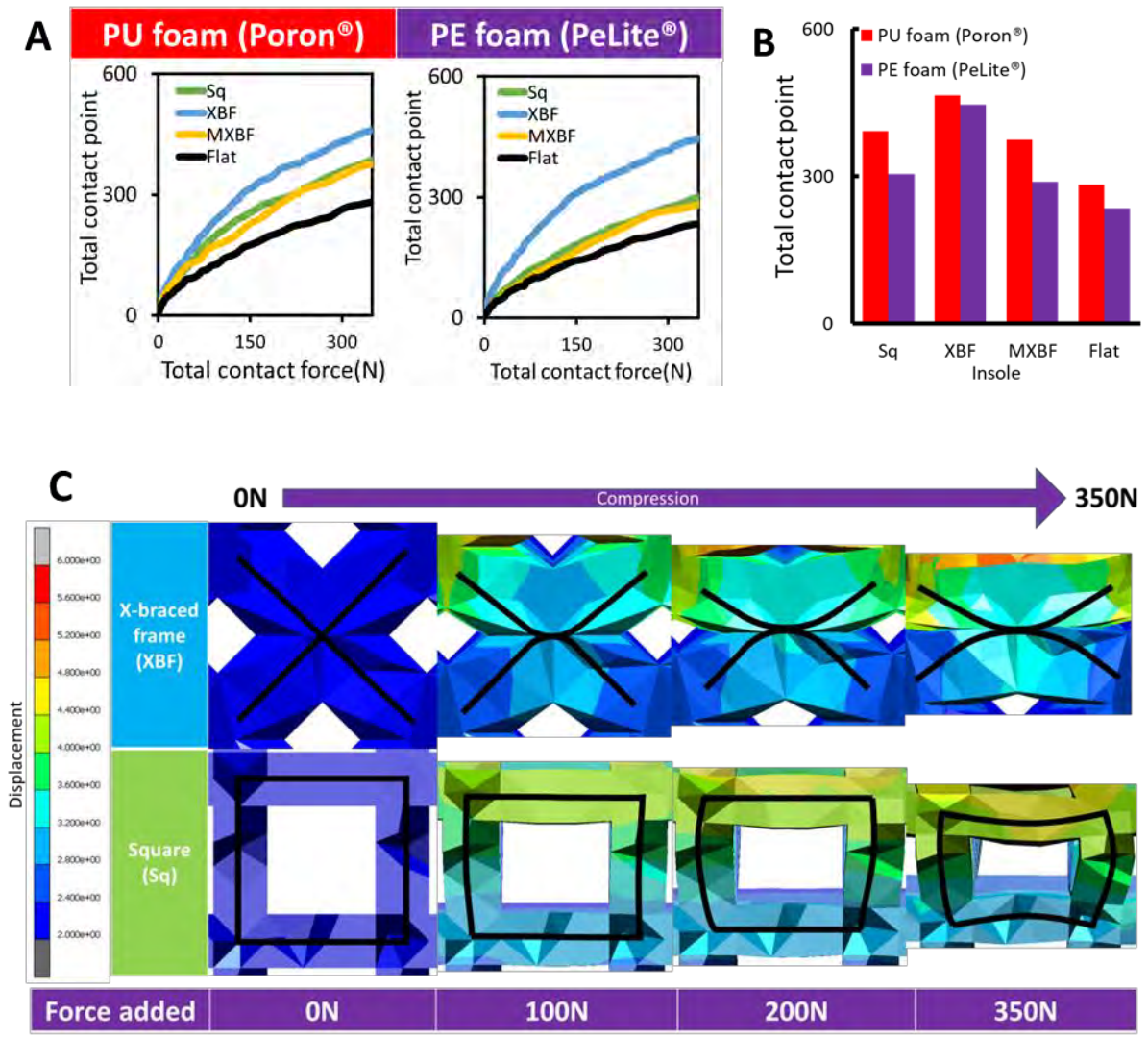

Figure 5. 6(**A**) Comparison of contact area of PU foam and PE foam with different intern structure. (**B**) Difference contact area of PU foam and PE foam with different intern structure under 350N. (**C**) Illustration of FEM developed in this study to predict changes with XBF and Sq insole.

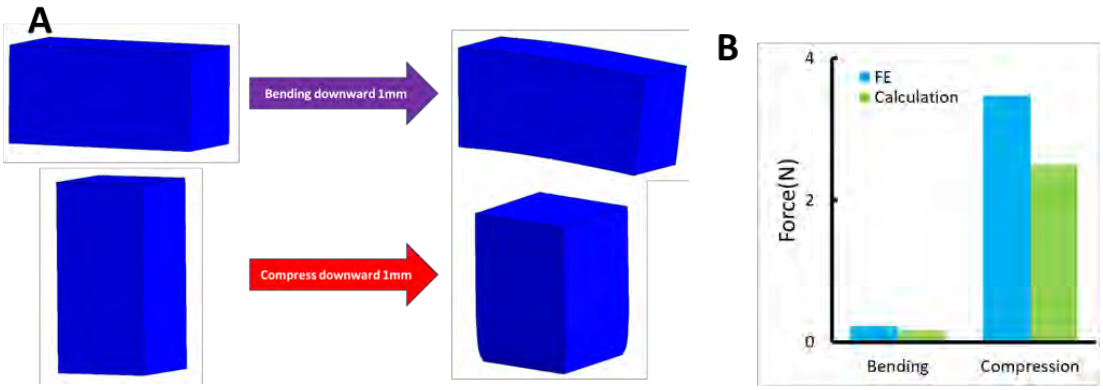

Figure 5. 7. (**A**) Illustration of FEM changes in bending and compression. (**B**) Comparison of force of Bending vs compression.

5.3.3.3 Contact pressure

The braced frame structure has a lower maximum contact force than that of the control condition; see **Figure 5.8A**. The maximum contact force of the XBF structure is 55% lower with the PU foam and 86% with the PE foam. Due to the smaller contact area of the non-braced frame structure (Sq), the maximum contact force is 4% higher in the PU foam and 8% higher in PE foam in comparison with XBF. The influence of the internal structure on the trajectory of the maximum contact force is negligible with both the PU and PE foams; see **Figure 5.8B**. It has been found that pressure is directly proportional to the applied force, but inversely proportional to the contact area. A material with a low Young's modulus tends to reduce the maximum contact force. In this study, PE foam with an XBF structure has a lower maximum contact force (54% or less) than the PU foam with a non-braced frame structure - (Sq and the control. The effect of the internal structure on material deformation is more apparent than the Young's modulus, which leads to the reduction of the insole-foot contact pressure. By looking at **Figures 5.8C** and **5.8D**, a large amount of contact force is found at the heel and the metatarsals. The trend of the contact force pattern is similar to the distribution of the shear stress in

the heel and the metatarsals which may result in potential foot pain and injury. As compared to the control insole, the proposed braced frame structure enables a better force distribution throughout the plantar with lower maximum contact forces.

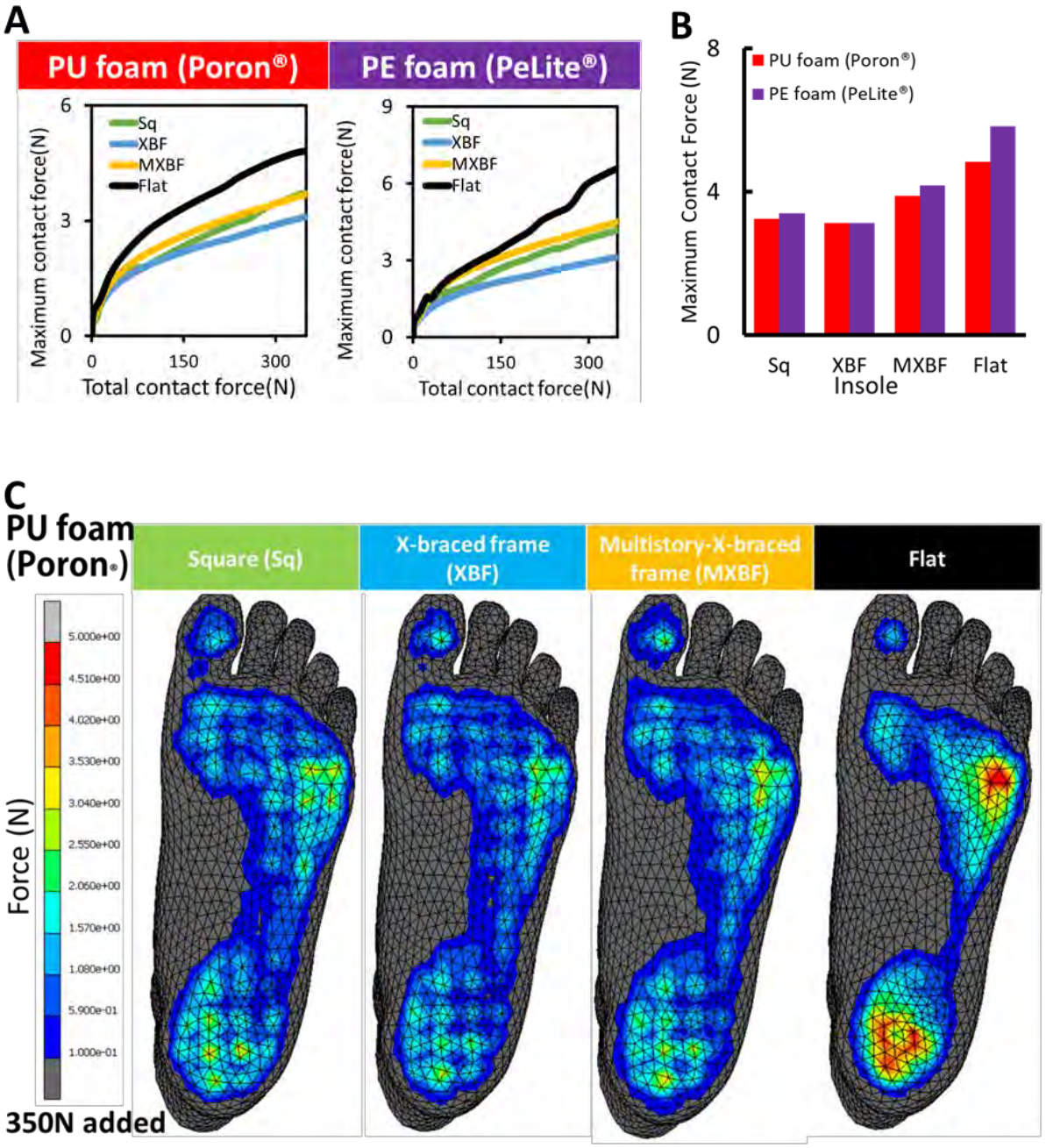

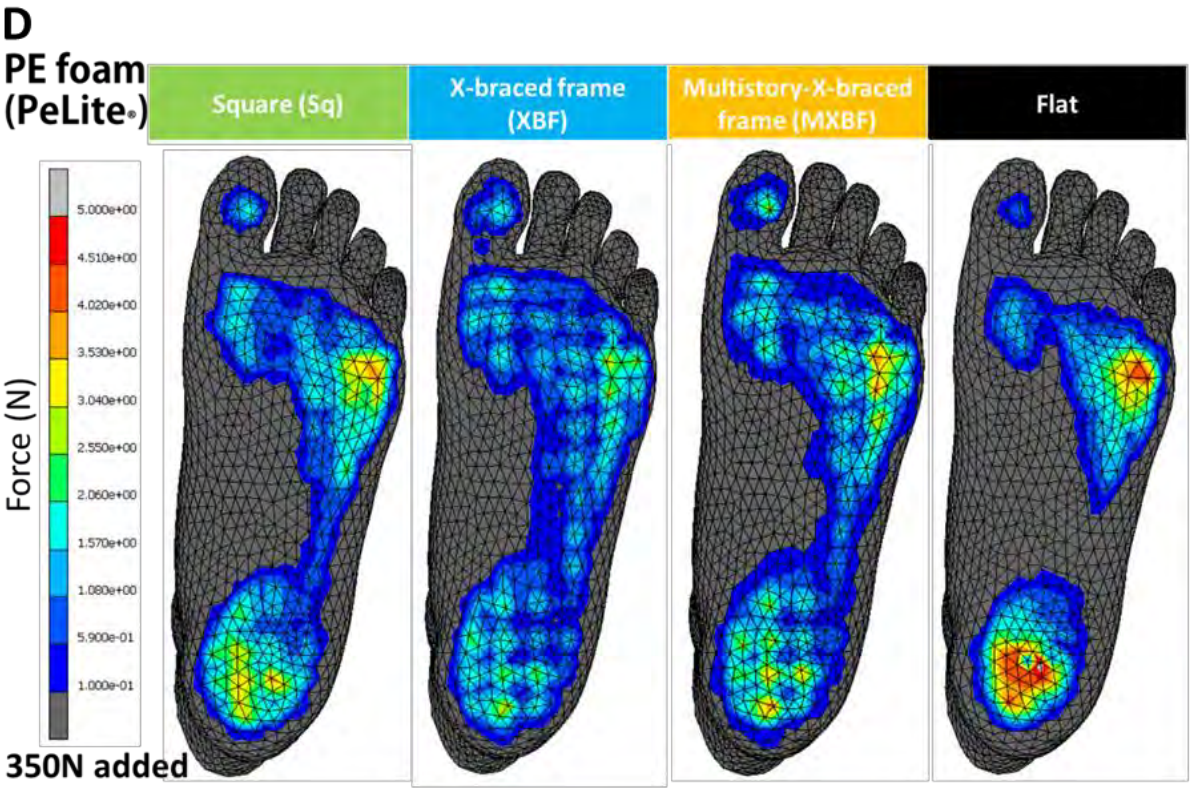

Figure 5. 8. (**A**) Comparison of maximum contact force of PU foam and PE foam with different intern structure. (**B**) Difference maximum contact force of PU foam and PE foam with different intern structure under 350N; The contact force distribution of the plantar using: (**C**) PU foam insole, (**D**) PE foam insole.

5.4 Summary

In this study, two novel braced frame structures are proposed to reduce the shear stress and the pressure interface between the insole and the plantar. An FEA is used to systematically determine the influence of the braced frame structures on shear stress, contact area and maximum contact force of the insole. A load of 350 N to simulate a standing posture is applied to the foot model. The results show that XBF can effectively reduce the shear stress and the maximum contact force, as compared to the control. The X-shape beams of the XBF structure can be readily compressed, thus conforming to the curvature of the foot with increased contact area.

Chapter 6 3D printed auxetic heel pads for diabetic patients

6.1 Introduction

The heel is the first part of the plantar that is subjected to high impact forces from the weight of the body [11, 29, 59, 146]. The altered mechanical properties of the plantar soft tissues of the diabetic foot with repetitive excessive loading beneath the heel, together with poor vascular supply and nerve damage may eventually result in cell and tissue death, and a high risk of heel ulceration [147]. Nevertheless, the efficacy of such insoles varies with the stress-strain performance of the insole material which needs to provide consistent contact at the interface between the foot and insole and facilitate effective control of the plantar pressure [16, 17, 59, 73]. Yet related scientific studies have been minimal, whilst the mechanisms behind the different structures of insoles in relation to the mechanical stress that acts tangential to the plantar surface are still unclear.

In this study, we examine the potential of a heel pad with a 3D printed auxetic structure to minimize the peak plantar pressure of DM patients. The conventional re-entrant honeycomb cell is arranged in a circular structure which contributes to increasing the contact area between the heel and the heel pad during walking. The influence of the internal angle of the re-entrant honeycomb cells on the contact pressure of the heel is investigated. Due to the progression of changes in the mechanical properties of the plantar soft tissues of DM patients, the effect of different hardness of the heel on the received contact pressure is also varied in this study. The designed heel pads are 3D printed and compressed by using a hemisphere to simulate the heel strike in the gait cycle. The FE approach is applied to observe the internal structural changes of the heel pad and the pressure distribution of the hemisphere which cannot be experimentally

observed. We also compare the pressure relief performance of the conventional insole (PU foam) and proposed auxetic heel pads through an FEA and a wear trial.

6.2 Material and Methods

6.2.1 Design of the auxetic heel pads

Re-entrant cells with three different internal angles (60 °, 80° and 90°) are used in this study. Note that the re-entrant honeycomb cells lose their auxetic property once their internal angle is 90 ° or above. Therefore, the three heel pads are labeled A60, A80 and N to denote an auxetic with an internal angle of 60°, auxetic with an internal angle of 80° and non-auxetic and internal angle of 90°, respectively. Their corresponding geometry and the dimensions of each unit cell are shown in **Figures 6.1 A**, **6.1 B** and **6.1 C**. The honeycomb structures are fabricated in a circular shape to form the 3D heel pads which are shown in **Figures 6.1 D**, **6.1 E** and **6.1F**. The length and the thickness of the cell as well as the diameter and height of the resultant heel pad are kept constant so that the total volume of the heel pads vary with different re-entrant angles (**Table 6.1**). The designed heel pads have a diameter of 56 mm, height of 15.4 mm and wall thickness of 0.7 mm.

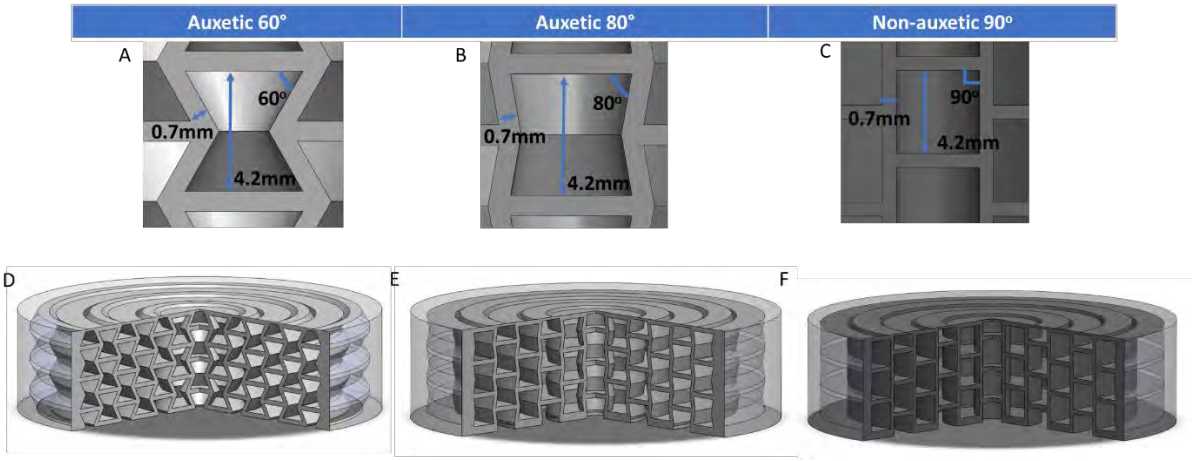

Figure 6. 1. Internal structure of the designed heel pads: (**A**), (**B**), (**C**) The internal angle of the heel pads; (**D**), (**E**), (**F**) heel pads with the internal structure.

Table 6. 1. The volume of each designed heel pads and PU foam heel pad

Designed heel pad	**Volume V (mm^3)**
Auxetic 60°	18601.84
Auxetic 80°	16146.25
Non-auxetic 90°	15287.95
PU foam	37775.69

6.2.2 Additive manufacturing of modelled structures

The 3D models of auxetic 60°, auxetic 80° and non-auxetic 90° were constructed by using SolidWorks® 2015 program. The samples (**Figure 6.2 B**) were then printed by using a 3D printer (Envisiontec Perfactory® P4), which is based on stereolithography (SLA) printing technology [148]. SLA printing technology allows the fabrication of complex internal structures with excellent accuracy. A flexible resin (E-shore A80) was used to print the heel pads. In the standard range, the separation distance is 15000µm and the separation velocity is 1850µm/s. In the burn-in range, the separation distance is 20000µm and the separation velocity is 800µm/s. The pads were exposed to ultraviolet (UV) light for 6 s to cure the resin and 4 s was allowed to elapse prior to the next exposure to the UV light. The energy of the UV light is 180 mW/dm^2.

A hemisphere of 50 mm in diameter was 3D printed by using a Stratasys Polyjet J750™ Digital Anatomy™ 3D printer to simulate the heel (**Figure 6.2 A**). The 3D print material used is photopolymer flexible resin with varying degrees of hardness. Four different hardness - Shores A30, A60, A85 and D86 were used to simulate the individual differences in the stiffness of the skin of the heel amongst the diabetic patients.

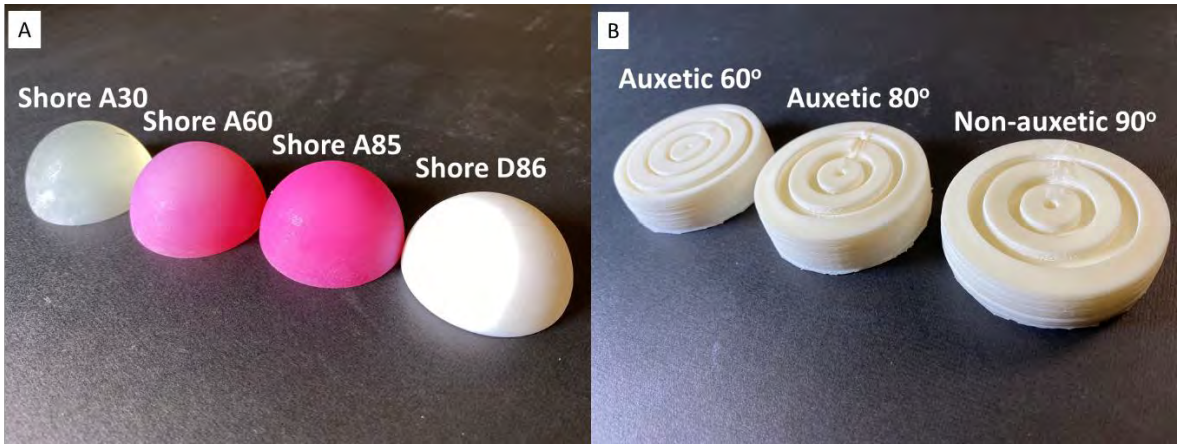

Figure 6. 2. (A) 3D printed hemispheres with Shores A30, A60, A85 and A86 hardness, and **(B)** 3D printed heel pads: auxetic 60°, auxetic 80° and non-auxetic 90°.

6.2.3 Mechanical characterization and FE modeling

ASTM D638 Standard Test Method for Tensile Properties of Plastics was referenced and the Instron 5566 universal mechanical test frame was used to obtain the tensile properties of the 3D printed and PU foam material. Dog bone shaped samples with nominal dimensions of 33 mm (L) x 6 mm (W) x 3.2 mm (T) were used for the tensile test. The compression test was done by Instron 5566 universal mechanical test frame to compare the result with the tensile test. ASTM D575 Standard Test Methods for Rubber Properties in Compression was referenced. The standard test specimens were 28.6mm in diameter and 12.5mm in thickness. The results were then inputted into FE software to simulate compression.

To evaluate the heel pressure in the heel strike position, a hemisphere was used to simulate the heel of the plantar. The Instron 5566 universal mechanical test frame equipped with a 10-k N load cell was used to compress the curved surface of the

hemisphere together with the designed heel pads (**Figure 6.3 A**) [89] and 750 N was applied onto the hemisphere to simulate the average body weight of a Chinese male [148]. The test was conducted at 25ºC and a crosshead speed of 10 mm/min.

A commercial FE modelling software (MSC Marc 2019.2.0, US) was used to simulate the compression process. The 3D models were meshed by using MSC Apex software and the mesh size of the FE models is 1 mm. The material modelling of both the hemisphere and heel pad is assumed to be isotropic. The resin and the PE foam models were based on Ogden formulation [149]. The tensile test result was fitted to the third order deformation model according to the following strain energy function:

$$W = \sum_{n=1}^{N} \frac{\mu_n}{\alpha_n}\left(\lambda_1^{\alpha_n} + \lambda_2^{\alpha_n} + \lambda_3^{\alpha_n} - 3\right) + \sum_{n=1}^{N} \frac{\mu_n}{\beta_n}(1 - J^{\beta n}) \qquad (1)$$

where μ_n, α_n, βn, are material constants. When all terms βn are equal to zero, the second part of in the Equation above is omitted. The material properties are shown in **Table 6.2** For the boundary condition of the FEM, a node was added on top of the hemisphere. By using rigid link (RBE2) where a number of entities are rigidly connected to a retained entity, that node was set to be the retained entity and the top surface of the hemisphere tied to the retained entity. All the degree of freedom is fixed. 750N was applied and onto the hemisphere the experimental process. The nodes at the bottom surface of the heel pads were fixed in all directions (**Figure 6.3 B**). Friction was neglected in the FEM. The peak contact force, total contact point and mean pressure

of the hemisphere were measured. The changes of the internal auxetic cell structure were compared among the different samples.

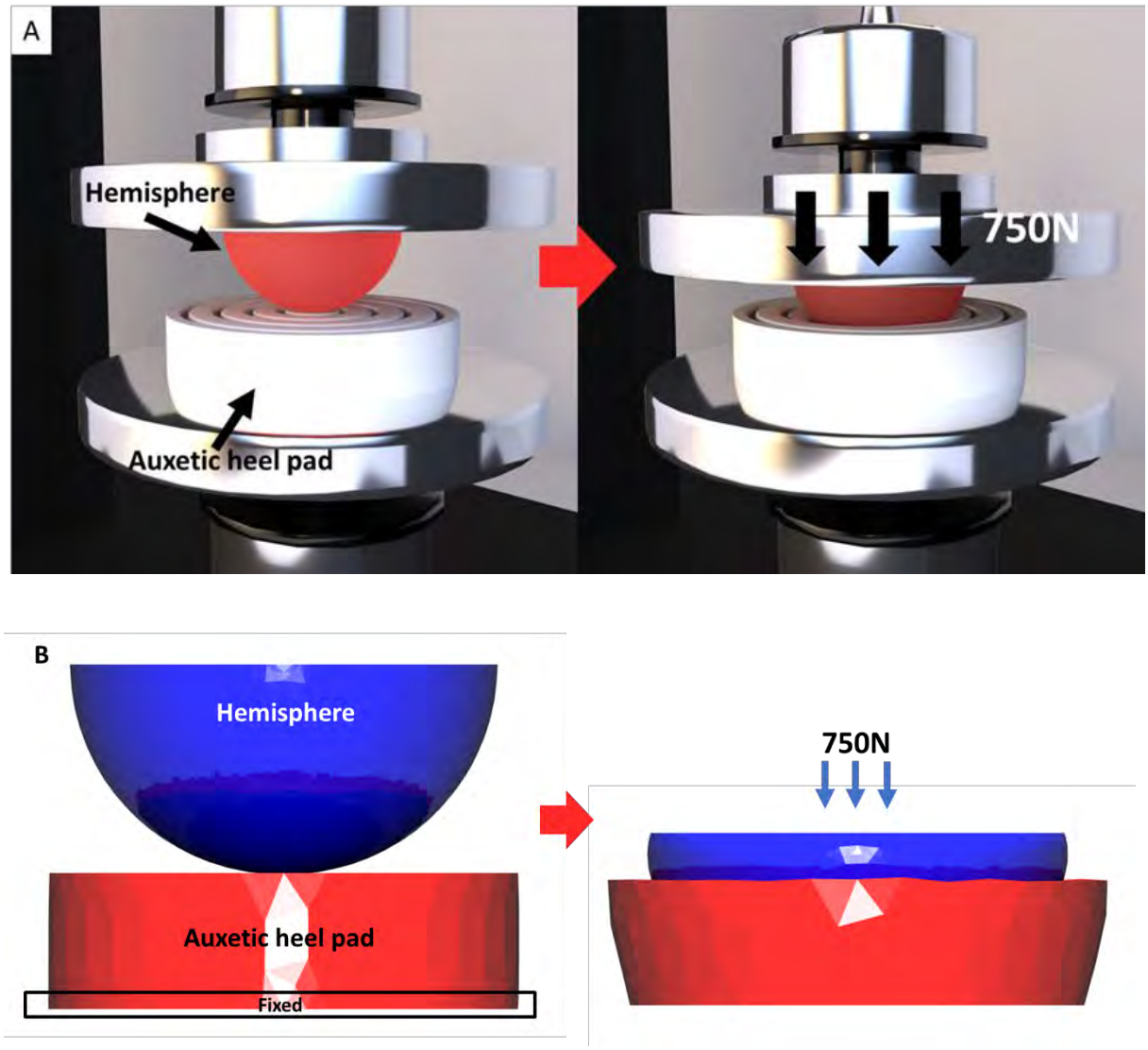

Figure 6. 3. (A) Schematic of compression experiment to simulate heel strike. **(B)** Simulation through FEA

6.2.4 Wear trial of the developed auxetic heel pad

To characterize the pressure relief performance of the heel pads with practical use during gait, a NOVEL Pedar system was used to evaluate the distribution of plantar pressure for various heel pad conditions. The system is insole shaped with 99 pressure sensors in the insole and each sensor has a pressure range of 15-600 kPa. The size of the Pedar insole is 42/43 EU and its thickness is 1.9 mm. A healthy male subject (age 25) with a shoe size of EU 43 and body weight of 72 kg was recruited for the wear trial which would compare the proposed heel pad (A80) and a PU foam. The subject was first instructed to wear a pair of sport shoes with the proposed heel pad. After that, the subject was requested to walked 15 meters in a straight line. The walking speed of the subject was kept constant throughout the wear trial based on the own walking pace. The peak pressure was recorded during the wear trial.

6.3 Results and Discussion

6.3.1 Tensile properties

The modulus is one of the key factors of an insole because its deformation allows the insole to organically accommodate the shape of the plantar, thus resulting in a more even pressure distribution. The stress-strain behaviors of the different heel pads and hemisphere materials are plotted in **Figures 6.4 A** and **6.4 B**. The flexible resin shows a higher Young's modulus than that of the PU foam. In other words, the flexible resin is less deformation than the PU foam when the same force is applied. As shown in **Figure 6.5 A** and **6.5 B**, a similar trend of results is also found from the tensile test. The flexible resin proposed in this study has a higher Young's modulus than the traditional PU foam.

The stiffness of the soft tissues of the feet can change due to different severity of the diabetes. The performance of the heel pads can thus be affected by different soft tissue stiffnesses. Hence, hemispheres with 4 different hardness were used. The stress-strain in ascending order is Shores A30, A60, A85 and D86. Their corresponding mechanical properties are listed in **Table 6.2**.

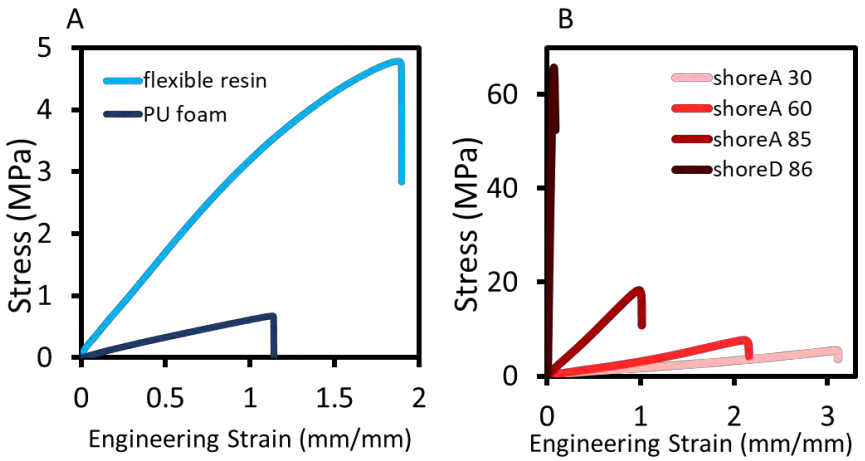

Figure 6. 4. Plotted material tensile properties: **(A)** stress-strain of flexible resin vs. PU foam, and **(B)** stress-strain of hemisphere with Shores A30, A60, A85 and D86.

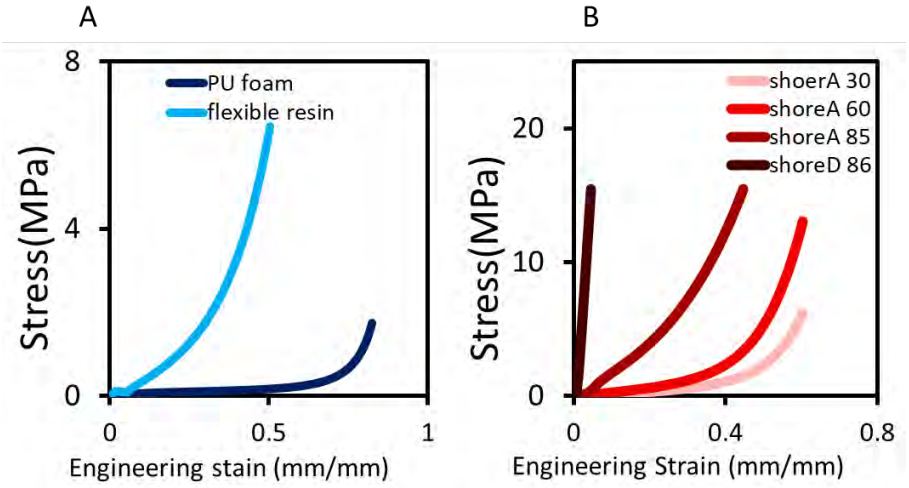

Figure 6. 5. Plotted material compression properties: (**A**) stress-strain of flexible resin vs. PU foam, and (**B**) stress-strain of hemisphere with Shores A30, A60, A85 and D86.

Table 6. 2. Material properties of each hemisphere and heel pads.

Material	Young's modulus E (MPa)	Poisson's ratio v
Agilus 30 (Shore A 30)	0.85	0.35
Agilus 30 (Shore A 60)	1.6	0.33
Agilus 30 (Shore A 85)	20	0.31
Vero (Shore D 86)	1000	0.3
PU foam	1	0.35
Flexible Resin	4	0.33

6.3.2 Evaluation of experiment and simulation result

To evaluate the experimental and simulation results, a comparison of the maximum compressive displacement values of the samples with an applied load of 750 N was made. Both experimental and simulation results are similar for all of the samples (see **Figure 6.6**). The difference in percentage between the experiment and simulation results is around 3%. This small error can be attributed to the 3D printer, the orientation of the 3D printing and assumption of isotropic material. For instance, there may be a layer that shifted which caused some of the layers to move from their original position. Also, the hemisphere might not have been perfectly aligned with the heel pads in the experiment, thus causing variations in the contact position and structural changes to the honeycomb cell. It is noted that due to the anisotropic property of 3D printed part caused by the layering of 3D printing technique, it was assumed as isotropic in the FEA model.

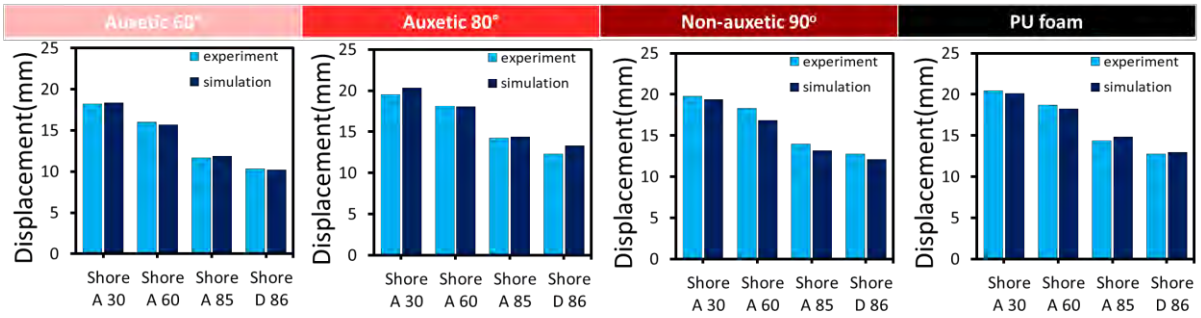

Figure 6. 6. Validation of the developed FEM. Comparison of experimental and simulation results for auxetic 60°, auxetic 80°, non-auxetic 90° and PU foam heel pads.

6.3.3 Effect of auxetic heel pads

6.3.3.1 Heel contact area

The hemisphere is meshed homogeneously, which means that every mesh has the same surface area. Therefore, the contact point of the hemisphere can be an indication of the contact area between the heel pad and the hemisphere. According to **Figure 6.7 A**, the contact point of the heel pads with an auxetic structure is significantly higher than that of pads without an auxetic structure. Auxetic 80° shows the highest contact point which is around 15% higher than that with non-auxetic 90°. The internal auxetic cell structure could be the major reason that causes an increase in the contact area. Due to the curved surface of the hemisphere, the contact pressure is concentrated in the center of the heel pads. As a result, the inner and outer elastic rods of the re-entrant honeycomb structure have different degrees of bending, where the inner rods bend more than the outer rods. **Figure 6.7 B** illustrates the differences of the structural changes of the samples when subjected to different loads. The inner elastic rods bend more than the outer elastic rods, which causes the tilting of the bridging beam. Hence, the heel pad can more easily

accommodate the curved surface and has a higher contact area with the hemisphere. Unlike the re-entrant cell of auxetic 80°, the rod of non-auxetic 90° is not V-shaped which imparts extra elasticity to the structure. Therefore, more force is required to bend the straight rods as opposed to the V-shaped rods. Therefore, larger forces are needed to deform non-auxetic materials to achieve the same contact area with the hemisphere.

When considering the effect of the hemisphere hardness on the contact area, softer materials facilitate a higher contact point (refer to **Figure 6.7 A**). **Figure 6.7 C** illustrates the internal structural changes of the heel pads which are compressed by hemispheres of different degrees of hardness. Note that hemispheres with a hardness of Shores A30 and A60 have a lower Young's modulus than the heel pad material. The deformation of these hemispheres is more obvious and results in a smaller curvature. As such, the heel pad can accommodate a hemisphere with a lower compressive force.

The results from this study showed that the insole material structures have major influence on the heel-insole contact area. The auxetic structure proposed in this study deforms readily to accommodate the foot heel, leading to reduced heel pressure and improved foot protection. It is also noted that the heel-insole interface and the corresponding offloading performance of insole is not only affected by the choice of insole materials, but also the mechanical properties of the plantar soft tissues of DM patients.

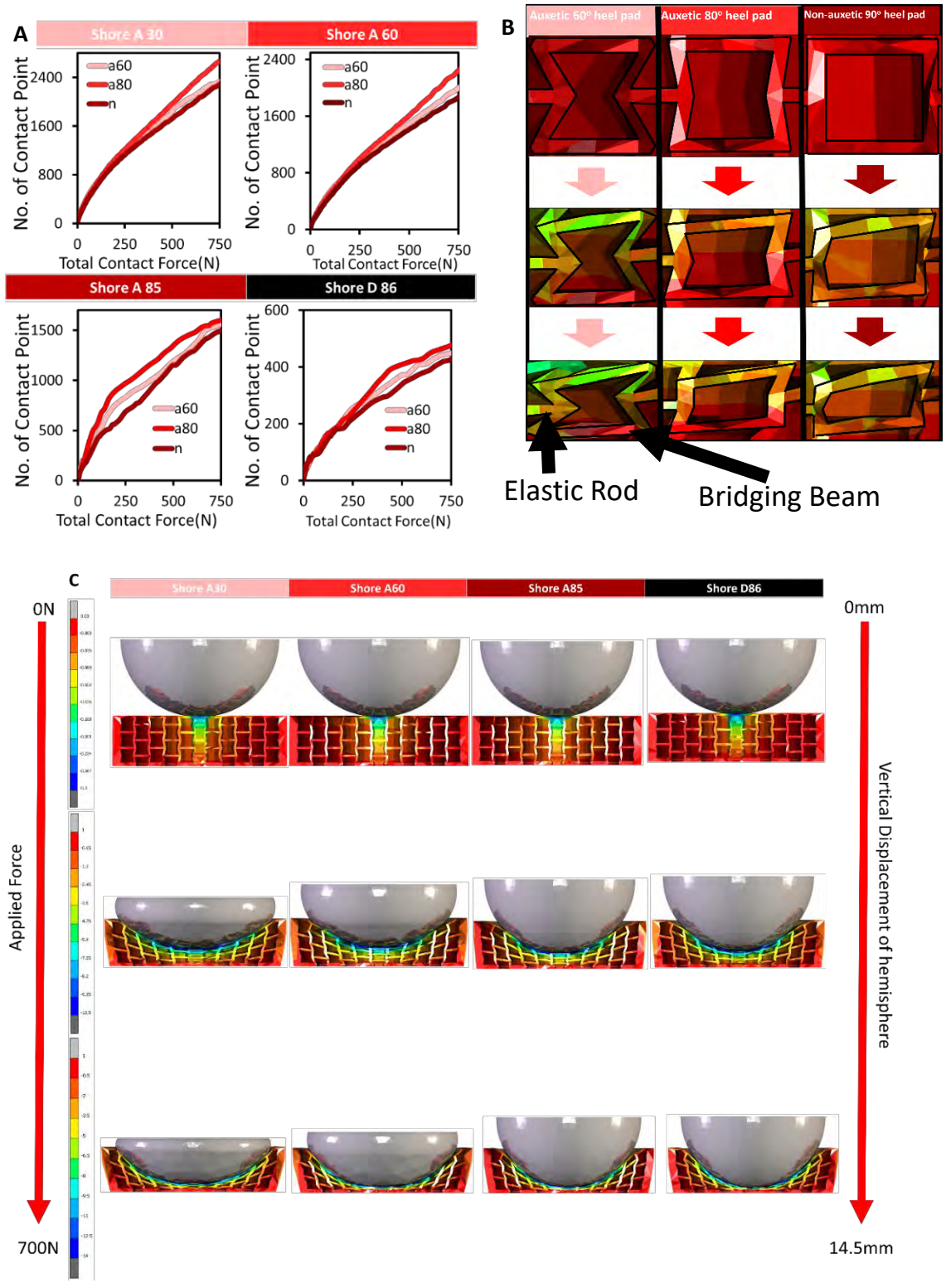

Figure 6. 7. (A) Comparison of contact area of auxetic vs. non-auxetic heel pads with hemisphere of different degrees of hardness. **(B)** Deformation of internal structure of auxetic

60°, auxetic 80° and non-auxetic 90°. **(C)** Illustration of FEM developed in this study to predict changes in hemisphere with auxetic 80°.

6.3.3.2 Plantar heel pressure

According to **Figures 6.8 A** and **6.8 B**, the heel pads with an auxetic structure show a lower peak contact force and mean pressure in comparison to non-auxetic 90° The auxetic sample with a larger internal angle (A80) shows approximately 37% and 16% reduction in peak contact force and mean pressure respectively in comparison to non-auxetic 90°. When considering the effect of the internal angle, the peak contact force and mean pressure of auxetic 80° is around 23% and 11% lower than auxetic 60°.

Regarding the hardness of the hemisphere, the radius of the curvature of the hemisphere made with softer materials is significantly increased under loading, thus resulting in increased contact area between the heel pad and hemisphere. As a result, the hemisphere made with a hardness of Shore D86 has the fewest contact points and highest peak force and mean pressure among the four samples (see **Figures 6.8 A** and **6.8 B**). To reflect the real situation of DM patients, the progressive hardening of the plantar soft tissues may further exacerbate the problem of excessive load and lead to higher risk of foot ulcers.

In comparing the optimal sample (A80) with the PU foam sample for pressure relief, the auxetic sample shows more contact points (19%), even though the PU foam has a much lower Young's modulus than the heel pad material (resin). This shows that the effect of the internal cell structure is comparable to that of the stiffness of the insole

material for compression. The large number of contact points resulted in approximately a 33% and 17% drop in peak force and mean pressure respectively.

With increased heel-insole contact area, the proposed auxetic structures result in reduced peak plantar pressure. Results indicate that the use of auxetic 80° provides a larger contact area compared to the PU foam heel pad. Although PU foam material has a lower Young's modulus, the contact area is still smaller than that of auxetic 80°. Furthermore, a smaller contact area means that the peak contact force and the mean pressure of the PU foam are also higher than those of auxetic 80° (**Figures 6.8 D** and **6.8 E**). The peak contact force and the mean pressure of auxetic 80° are reduced by 32.77% and 16.71% compared to the PU foam heel pad. Therefore, auxetic 80° which has an auxetic structure can provide a superior reduction of the peak force as opposed to the conventional softer PU foam insole. The auxetic re-entrant honeycomb structure, particular auxetic 80° for heel pad applications can effectively increases the heel-insole contact area and reduces the peak plantar pressure, thus reducing the potential of heel ulcerations for diabetic patients.

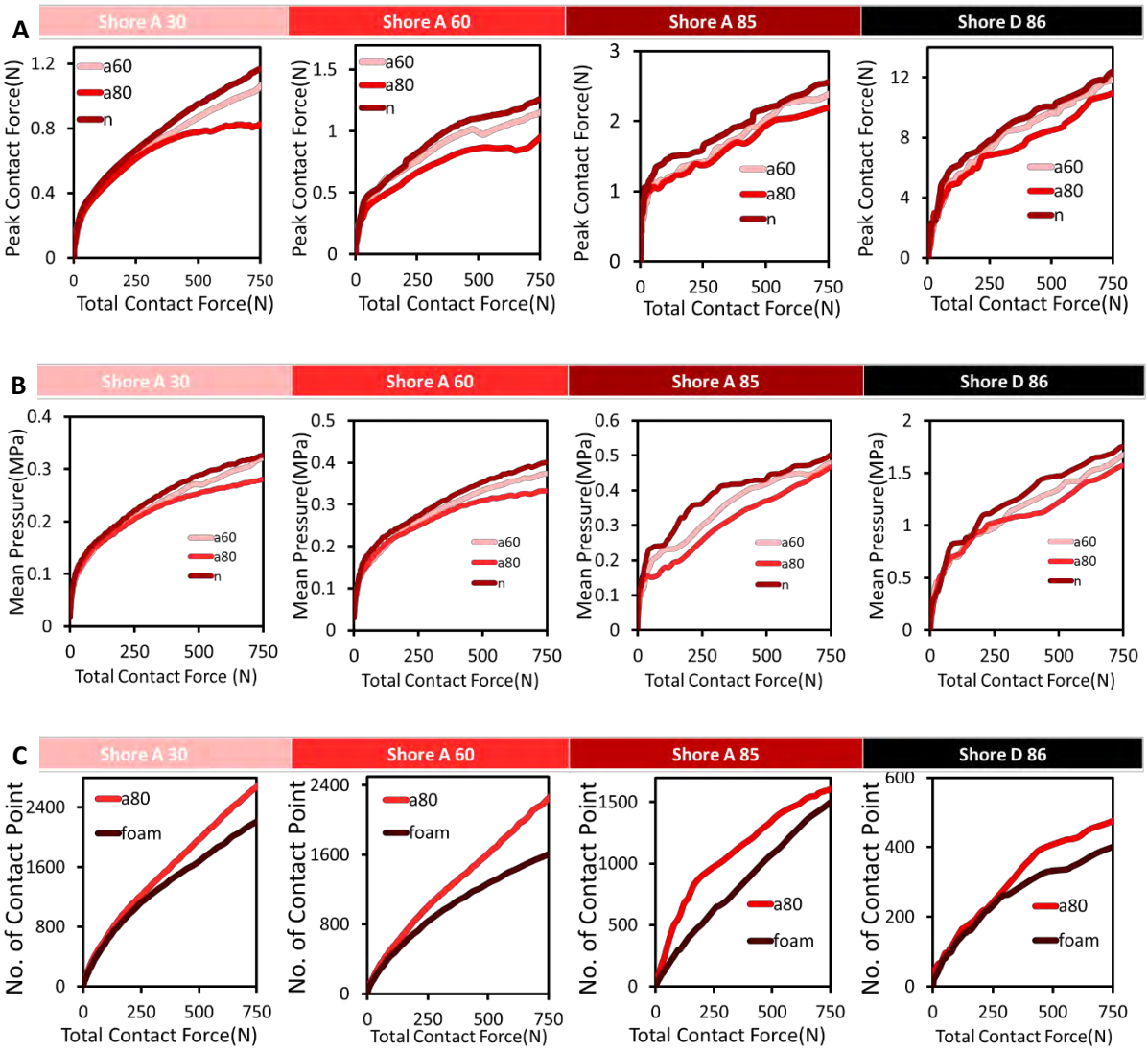
A
Shore A 30
Shore A 60
Shore A 85
Shore D 86
Peak Contact Force(N)
Total Contact Force(N)
a60
a80
n
B
Mean Pressure(MPa)
Total Contact Force (N)
Total Contact Force(N)
C
No. of Contact Point
a80
foam
Total Contact Force(N)

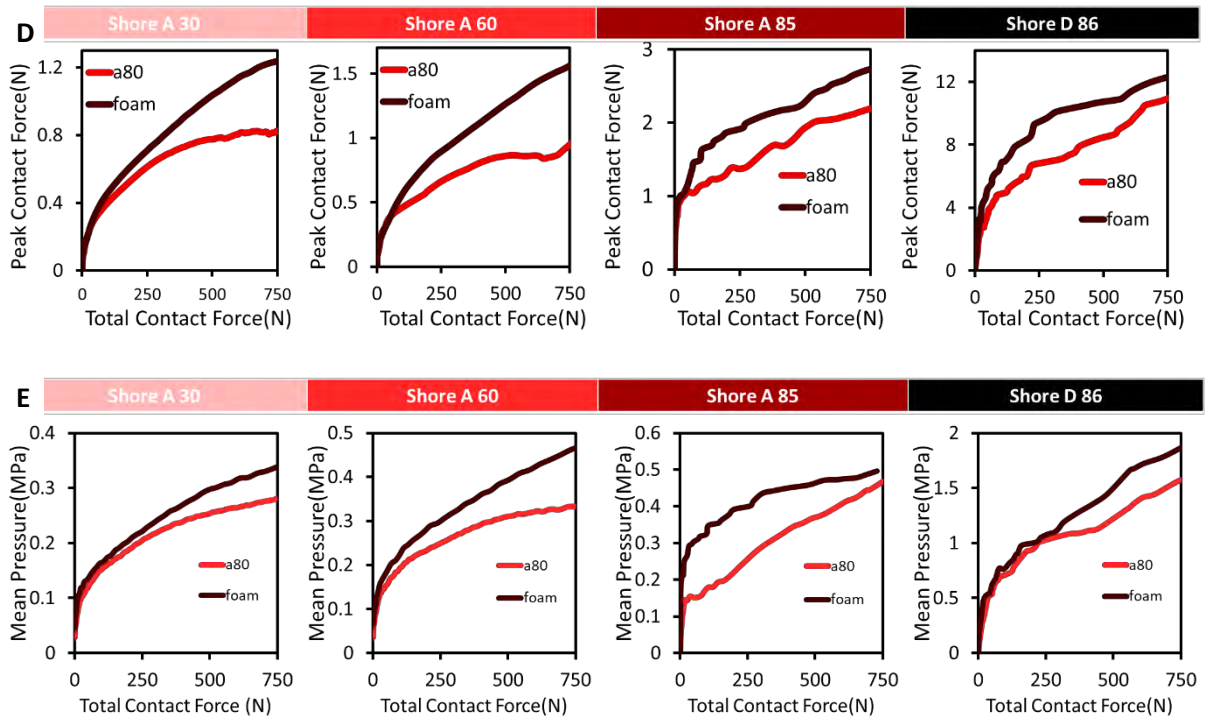

Figure 6. 8. Comparison of **(A)** peak contact force and **(B)** mean pressure of heel pads with auxetic and non-auxetic structures with hemispheres of different degrees of hardness; **(C)** contact area and **(D)** peak contact force, and **(E)** mean pressure of heel pad with auxetic structure and PU foam heel pad with hemispheres of different degrees of hardness.

6.3.4 Wear trial result

To further observe the performance of the heel pads, a laboratory wear trial was carried out to compare the dynamic changes in the plantar contact pressure between the proposed and PU foam heel pads as shown in **Figure 6.9 A**, the peak pressure of auxetic 80° is considerably lower than that of the PU foam heel pad by 19.17%. The wear trial result confirms that the heel pad with an auxetic structure has a better pressure relief performance than the traditional heel pad (see **Figure 6.9 B**), hence reducing the risk of heel ulcers.

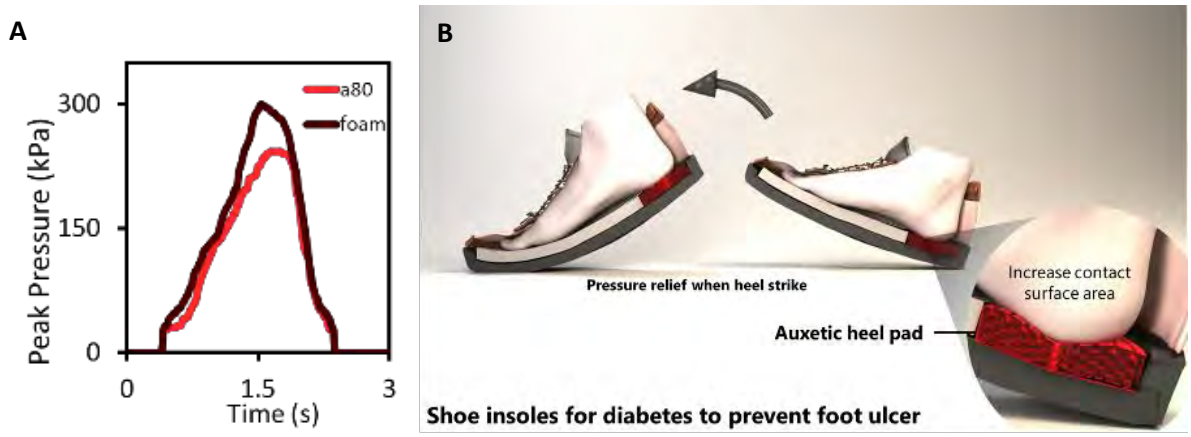

Figure 6. 9. (A) Peak plantar heel pressure: heel pads with auxetic structure vs. PU foam heel pad, and **(B)** Illustration of plantar heel contact during wear trial.

6.4 Summary

A novel heel pad with an auxetic structure by using SLA printing technology was proposed to reduce the pressure on the heel of the plantar during walking. Since stiffness of the plantar soft tissues in diabetics is different from non-diabetics, hemisphere with different degrees of hardness is used to simulate the different deformation of the soft tissues. Due to the complex internal structure of the heel pads, FE modelling is used to further understand the deformation and the change in the internal cell structure under pressure. According to the mechanical characterization, the FE modelling shows a similar result as that obtained experimentally by using different heel pads and hemisphere. The results of the FEM show that auxetic 80° has the lowest peak contact force and mean pressure compared to the other heel pads. Upon compression, the heel pad material tends to move toward the centre, which can increase the foot-heel pad contact area and reduce the peak contact force. It is expected that this

new approach is not limited to heel pads for the diabetic foot, but also various personal protective gear for optimal cushioning and protection from impact forces.

Chapter 7 Conclusions and Suggestions for Future Research

7.1 Conclusions

Diabetes mellitus (DM) is one of the most common life-long health conditions found worldwide. Patients usually suffer from neuropathy which affects their foot sensitivity and daily life. Due to the poor sensitivity of the feet, DM patients may frequently injure their feet, but the healing of the wound can be very slow due to the insulin resistance of the body. To improve the quality of life of DM patients, this study aims to improve diabetic insoles which are the most common footwear device that protects the plantar of the foot from high impact and pressure and provides a larger contact area to the plantar of the foot. To begin with, a literature review is conducted to understand the background information for the further development of diabetic insole designs according to previous studies and they are reviewed in Chapter 2. This has led to the 4 objectives in this study. The first objective is to find the changes in the geometry of the foot during walking and the contact interface between the skin of the foot and footwear. The second objective is to understand the mechanical properties of the insole materials that affect the plantar pressure. The third objective is to analyse the contact mechanics of the heel strike posture and formulate biomechanical models. Finally, the last objective is to propose a new insole material structure and undertake laboratory wear trials. Details of the objectives are provided in Section 1.3 of Chapter 1. Based on the research objectives, the results of this study are summarised as follows:

1) In Chapter 3, the effects of different insole materials on the plantar pressure and gait performance of diabetic patients are investigated. The mechanical properties of 3 types of traditional insole materials are examined: EVA (Lunalastik®), PE foam (PeLite®),

and PU foam (Poron®). It is found that the PU foam has the lowest Young's modulus and hardness as well as the highest energy absorption amongst all of the insoles. A total of twenty DM male subjects have participated in a walking and standing trial with three different insoles and a bare foot condition. The plantar pressure during walking and standing is measured by using a Pedar® insole sensor. Amongst the 3 insole materials, PU foam has the highest density, lowest compression strain and best energy absorption performance because the material tends to readily absorb energy and reduce the plantar pressure. As compared to the barefoot condition, the use of PU foam insoles significantly reduces the mean peak plantar pressure during both standing (15%) and walking (19.8%). The laboratory wear trials show that the PU foam has the best offloading performance in comparison to the other two types of insole materials studied. As for the insole design, it is very important to divide the insole into different regions. It is important to reduce the contact pressure by improving the material properties or structure.

2) The changes in the geometry of the foot during walking has been explored in Chapter 4. These changes are very difficult to scan with a traditional handheld 3D scanner since the plantar of the foot is always in contact with the ground. By using the newly developed technology, that is, a 4D scanning system, the changes in the geometry of the foot including the plantar can be scanned. Totally there are fourteen mal DM subjects are recruited and they participate in a 3D scanning experiment with three different walking speeds. The 3D scanned data provide the information to analyse the foot measurements during slow, normal, and fast walking speeds as well as the foot for five different stances during walking - first heel contact, first metatarsal head contact, first toe contact, heel take off and metatarsal head take off. Based on the statistical

analysis, the foot measurements show no significant differences related to the different walking speeds. The changes in walking speed in this study (±10%) might be too subtle to cause any significant foot deformation. However, 12 of the 13 foot measured dimensions have a significant difference related to the stance during walking. The results show the least deformation in the length of the foot amongst all of the foot measurements. This suggests that the length dimension should not be the only measurement for selecting an insole or footwear. The width and the angular changes should also be considered to ensure that the footwear offers adequate protection for the foot and enough space for the toes to move. The deformation ratio can be used to provide a better understanding of the foot deformation to advance the design and development of diabetic insoles when these insoles are worn for daily activities. The insole design should provide an enough area for the toes to move, and a 3D shape that fit the shape of the plantar.

3) With reference to the planter pressure distribution and the mechanical properties of the insole materials, the addition of an internal structure is recommended for the insole to further improve the performance and prevent very high contact pressure and shear stresses. The shear stress is the lateral stress that is applied to the foot and contributes up to 30% of the vertical loading on the foot. In Chapter 5, a new internal structure of the insole material is proposed and investigated. A braced frame structure is usually used to prevent excessive lateral loading under the influence of lateral loads by using diagonal steel members or shear cores in building constructions. The XBF, MXBF and SQ designs are used with two traditional types of materials: PU and PE foams. An FEM is used to simulate the standing position of a male subject. A non-weight foot model is obtained from a healthy male subject through scanning and the bone model is inserted

into the foot model. A force of 350 N is applied to simulate the foot during standing. The result shows that the XBF can reduce the most shear stress and contact pressure as well as increase the contact area the most as compared to the other tested insoles. The XBF shows a 21% reduction in shear stress, 64% increase in contact area and a 55% reduction in contact peak force. It is likely that the beam of the XBF is the key element for these improvements. The X-shaped beams of the XBF structure can be readily compressed, thus conforming to the curvature of the foot with increased contact area. The findings of this study provide useful information and insights to manufacturers to better understand insole structures, thus prescribing suitable insoles for diabetic patients so that they receive optimal foot protection from ulcers.

4) As discussed in Chapter 3, the plantar pressure of the rearfoot is very high during walking, especially in the heel strike position. In this chapter, a novel heel pad with an auxetic structure by using stereolithography (SLA), which is a printing technology, to reduce the pressure on the heel of the plantar during walking is proposed. Three different internal angles are tested: 60^{o}, 80^{o} and 90^{o}. Auxetic honeycomb structures are fabricated in a circular shape. Also, 3D printed hemispheres with 4 different degrees of hardness are used to simulate the different levels of heel hardness. Due to the complex internal structure of the heel pads, FE modelling is used to further understand the deformation and the changes in the internal cell structure under pressure. It is found that by using hemispheres with different degrees of hardness, the auxetic structure with an angle of 80^{o} has the highest contact area, and lowest peak contact force and mean pressure compared to the other heel pads. The contact area can increase more than 15%, and peak contact force and mean pressure are reduced by more than 23% and 11%, respectively through comparisons with other heel pads. It is believed that the inner

elastic rods bend more than the outer elastic rods, which causes the tilting of the bridging beam. Hence, the heel pad can more easily accommodate the curved surface and has a higher contact area with the hemisphere. After that, a healthy male subject is recruited for the wear trial. It is found that the peak pressure is reduced by 19.17% compared with the traditional PU foam heel pad. Auxetic heel pad can help to increase the contact area and reduce the contact pressure. Upon compression, the heel pad material tends to move toward the centre, which can increase the foot-heel pad contact area and reduce the peak contact force. It is expected that this new approach is not limited to heel pads for the diabetic foot, but also various personal protective gear for optimal cushioning and protection from impact forces.

7.2 Limitations

Some of the limitations of the theory and generalization of knowledge are listed below.

1) The sample size is very small. Only 20 subjects are recruited for the investigation on pressure distribution during walking and 14 subjects for the investigation on changes in the geometry of the foot during walking. One of the main reasons for the small sample is due to the selection criteria. Subjects who have wounds or foot deformities are excluded since they may be at risk of developing foot ulcerations. Moreover, due to the COVID-19 pandemic at the time of this study, some of the subjects withdrew from the study because the interaction may increase their risk of infection. The small sample might not reflect the total targeted population. Therefore, it is recommended that increasing the number of subjects is essential to obtain statistical power in future related studies.

2) The braced frame structure insole in Chapter 5 was a virtual design. The designed insole was not able to develop in real world. The effect of the insole can only present virtually. Apart from that, this experiment only focusses on the standing posture. However, the pressure add to the insole during walking is totally different from standing. The effect of the braced frame structure insole can be further discovered.

3) The auxetic internal structure design in Chapter 6 can be further studied. Only the auxetic re-entrant honeycomb structure has been developed. As this is a new application of a heel pad with an auxetic structure, therefore, a simple auxetic structure is used. There are other auxetic structures that can provide a greater auxetic effect; for example, double arrowheads and lozenge grids. Apart from the selection of the auxetic structure, the wall thickness, and the size of the auxetic structure can be further discussed. It is recommended that more parameters like the length of the re-entrant should be studied.

4) In this study, the heel strike posture is simulated since the contact area of the heel is very small but very high in contact pressure. Furthermore, the posture presents a very high risk of foot injury. However, other postures like the heel-off posture have not been examined. As the locomotion of the human foot is a highly complex motion, more foot stances should be studied.

7.3 Suggestions for Future Research

Future studies on advancing diabetic insoles can investigate different points of view to provide better features. The ideas and viewpoints are discussed below accordingly.

1) To optimise the heel pad with an auxetic structure, the formability of the shape, and related mathematical models of different types of auxetic structures can be analysed to further increase the contact area. Different materials such as thermoplastic polyurethane (TPU) can be examined as the insole material to evaluate their mechanical properties, which directly affect the contact area and pressure of the sole of the foot. Also, TPU has excellent tensile strength and high elongation at break, which is very suitable for insole development.

2) The diabetic insole design can use more active ingredients. For example, an antivirus coating can be added on the insole so that the in-shoe environment can be sterilised and cleaned. Chemical compounds like ammonia plus nitrogen are usually used as a long-lasting protective coating. They can remain on a material for days to maintain a clean in-shoe environment. As a result, this method can actively reduce the risk of diabetic foot ulceration as foot fungus can be minimised.

3) More complex and high load-bearing stances can be simulated for designing diabetic insoles. During a gait cycle, the body weight shifts from the heel to the forefoot. For example, during the heel off stance, the pressure at the forefoot is very high and that is one of the areas with a high risk of ulceration. New structures like those that are reconfigurable can be used for the insole to reduce the contact pressure at the forefoot.

Appendices

The HONG KONG
POLYTECHNIC UNIVERSITY

參與研究項目同意書

研究主題: 人體工程的鞋履項目 (糖尿病者)

研究員: 易潔倫博士

研究目的: 利用人工智能系統學習和研究糖尿病患者的足部形態和狀況，以改善糖尿病患者穿著的鞋履設計和舒適度。

第一階段: 個人足部及平衡力健康評估

參加者需填寫個人健康和鞋履問卷，另外物理治療師會為參加者的足部作基本檢查，包括量度雙腳尺碼，腳形及皮膚檢查，腳部觸感評估，以及平衡力與跌倒風險評估。

腳部三維立體掃描

參加者亦會進行足部三維立體掃描，以收集足部尺碼和形狀作數據分析。參加者需要站立以及躺著讓研究人員掃描不同姿勢和壓力下的足部形狀。

第二階段: 鞋履試穿

在第一階段中的20-24名參加者將會被邀請進行第二階段測試。期間，參加者須試穿一些鞋履或鞋墊進行坐 (15分鐘) 和步行(20分鐘)測試，以研究參加者腳部在不同鞋履或鞋墊中的溫度和濕度，從而改善糖尿病患者穿著的鞋履設計和舒適度。

1. 本人確定已詳細閱讀並了解於_____/____/____提供之資料單張，並已有足夠時間發問問題。

2. 本人明白是次參與全是自願性質，本人有權隨時退出而不必提出任何理由，而本人法律權利不會有改變。

3. 通過簽訂書面同意書，本人授權臨床研究倫理委員會和監管機構直接核查本人的研究數據。

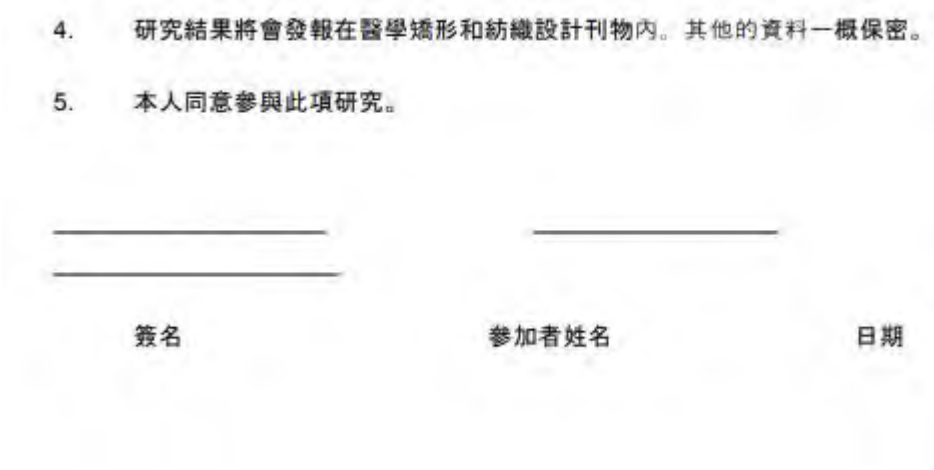
4. 研究結果將會發報在醫學矯形和紡織設計刊物內。其他的資料一概保密。

5. 本人同意參與此項研究。

_____ _____

_____

簽名 參加者姓名 日期

Figure S 1 Chinese version of participant consent form

References

[1] Y. Zou, J. Lan, Y. Zhong, S. Yang, H. Zhang, and G. Xie, "Association of remnant cholesterol with nonalcoholic fatty liver disease: a general population-based study," *Lipids in Health and Disease,* Article vol. 20, no. 1, 2021, Art no. 139, doi: 10.1186/s12944-021-01573-y.

[2] T. Li, Z. Wang, W. Lu, Q. Zhang, and D. Li, "Electronic health records based reinforcement learning for treatment optimizing," *Information Systems,* Article vol. 104, 2022, Art no. 101878, doi: 10.1016/j.is.2021.101878.

[3] D. Acharya and D. K. Das, "An efficient nonlinear explicit model predictive control to regulate blood glucose in type-1 diabetic patient under parametric uncertainties," *Biomedical Signal Processing and Control,* Article vol. 71, 2022, Art no. 103166, doi: 10.1016/j.bspc.2021.103166.

[4] E. K. Hameed, L. T. Al-Ameri, H. S. Hasan, and Z. H. Abdulqahar, "The cut-off values of triglycerides - Glucose index for metabolic syndrome associated with type 2 diabetes mellitus," *Baghdad Science Journal,* Article vol. 19, no. 2, pp. 340-346, 2022, doi: 10.21123/BSJ.2022.19.2.0340.

[5] R. Nimer, G. Kamel, M. A. Obeidat, and L. A. Dahabiyeh, "Investigating the molecular structure of plasma in type 2 diabetes mellitus and diabetic nephropathy by synchrotron Fourier-transform infrared microspectroscopy," *Spectrochimica Acta - Part A: Molecular and Biomolecular Spectroscopy,* Article vol. 264, 2022, Art no. 120259, doi: 10.1016/j.saa.2021.120259.

[6] J. J. Sánchez-Hidalgo *et al.*, "Urine transferrin as an early endothelial dysfunction marker in type 2 diabetic patients without nephropathy: a case control study," *Diabetology and Metabolic Syndrome,* Article vol. 13, no. 1, 2021, Art no. 128, doi: 10.1186/s13098-021-00745-1.

[7] D. W. Cooke and L. Plotnick, "Type 1 diabetes mellitus in pediatrics," *Pediatrics in Review,* Article vol. 29, no. 11, pp. 374-385, 2008, doi: 10.1542/pir.29-11-374.

[8] K. McDermott, M. Fang, A. J. M. Boulton, E. Selvin, and C. W. Hicks, "Etiology, Epidemiology, and Disparities in the Burden of Diabetic Foot Ulcers," *Diabetes Care,* Review vol. 46, no. 1, pp. 209-211, 2023, doi: 10.2337/dci22-0043.

[9] C. Agyemang, E. L. van der Linden, and L. Bennet, "Type 2 diabetes burden among migrants in Europe: unravelling the causal pathways," *Diabetologia,* Review vol. 64, no. 12, pp. 2665-2675, 2021, doi: 10.1007/s00125-021-05586-1.

[10] E. Li, X. Long, S. Liao, D. Pang, Q. Li, and Y. Zou, "Effect of mulberry galacto-oligosaccharide isolated from mulberry on glucose metabolism and gut microbiota in a type 2 diabetic mice," *Journal of Functional Foods,* Article vol. 87, 2021, Art no. 104836, doi: 10.1016/j.jff.2021.104836.

[11] S. Pai and W. R. Ledoux, "The compressive mechanical properties of diabetic and non-diabetic plantar soft tissue," *Journal of Biomechanics,* vol. 43, no. 9, pp. 1754-1760, 2010, doi: 10.1016/j.jbiomech.2010.02.021.

[12] R. Vardasca and D. Martinho. *Towards an Effective Decision Support System for Diabetic Foot Ulcers Diagnostic and Treatment Assessment, Lecture Notes in Networks and Systems*, vol. 216, pp. 307-321, 2022.

[13] D. X. E. Lim *et al.*, "Extracellular matrix and cellular senescence in venous leg ulcers," *Scientific Reports,* Article vol. 11, no. 1, 2021, Art no. 20168, doi: 10.1038/s41598-021-99643-9.

[14] M. Jongebloed-Westra *et al.*, "Using motivational interviewing combined with digital shoe-fitting to improve adherence to wearing orthopedic shoes in people with diabetes

at risk of foot ulceration: study protocol for a cluster-randomized controlled trial," *Trials,* Article vol. 22, no. 1, 2021, Art no. 750, doi: 10.1186/s13063-021-05680-0.

[15] E. Jafarzadeh, R. Soheilifard, and A. Ehsani-Seresht, "Design optimization procedure for an orthopedic insole having a continuously variable stiffness/shape to reduce the plantar pressure in the foot of a diabetic patient," *Medical Engineering and Physics,* Article vol. 98, pp. 44-49, 2021, doi: 10.1016/j.medengphy.2021.10.008.

[16] S. Ahmed, A. Barwick, P. Butterworth, and S. Nancarrow, "Footwear and insole design features that reduce neuropathic plantar forefoot ulcer risk in people with diabetes: a systematic literature review," *Journal of Foot and Ankle Research,* vol. 13, no. 1, 2020, doi: 10.1186/s13047-020-00400-4.

[17] J. J. Van Netten *et al.*, "Diabetic Foot Australia guideline on footwear for people with diabetes," *Journal of Foot and Ankle Research,* vol. 11, no. 1, 2018, doi: 10.1186/s13047-017-0244-z.

[18] L. Brady, S. Pai, J. M. Iaquinto, Y. N. Wang, and W. R. Ledoux, "The compressive, shear, biochemical, and histological characteristics of diabetic and non-diabetic plantar skin are minimally different," *Journal of Biomechanics,* Article vol. 129, 2021, Art no. 110797, doi: 10.1016/j.jbiomech.2021.110797.

[19] Z. Jia *et al.*, "Proteomics changes after negative pressure wound therapy in diabetic foot ulcers," *Molecular Medicine Reports,* Article vol. 24, no. 6, 2021, Art no. 834, doi: 10.3892/mmr.2021.12474.

[20] Y. Terabe, N. Kaneko, K. Nakabayashi, A. Matsui, and H. Ando, "Long-term efficient management of diabetic foot ulcer using simultaneous foot ulcer closure and surgical off-loading," *JPRAS Open,* Article vol. 30, pp. 1-5, 2021, doi: 10.1016/j.jpra.2021.04.012.

[21] W. Hanna, D. Friesen, C. Bombardier, D. Gladman, and A. Hanna, "Pathologic features of diabetic thick skin," *Journal of the American Academy of Dermatology,* Article vol. 16, no. 3, pp. 546-553, 1987, doi: 10.1016/S0190-9622(87)70072-3.

[22] M. A. Vuori *et al.*, "Diabetes status-related differences in risk factors and mediators of heart failure in the general population: results from the MORGAM/BiomarCaRE consortium," *Cardiovascular Diabetology,* Article vol. 20, no. 1, 2021, Art no. 195, doi: 10.1186/s12933-021-01378-4.

[23] R. Waaijman, M. L. J. Arts, R. Haspels, T. E. Busch-Westbroek, F. Nollet, and S. A. Bus, "Pressure-reduction and preservation in custom-made footwear of patients with diabetes and a history of plantar ulceration," *Diabetic Medicine,* Article vol. 29, no. 12, pp. 1542-1549, 2012, doi: 10.1111/j.1464-5491.2012.03700.x.

[24] S. Xiong, R. S. Goonetilleke, J. Zhao, W. Li, and C. P. Witana, "Foot deformations under different load-bearing conditions and their relationships to stature and body weight," *Anthropological Science,* Article vol. 117, no. 2, pp. 77-88, 2009, doi: 10.1537/ase.070915.

[25] M. M. Tran and M. N. Haley, "Does exercise improve healing of diabetic foot ulcers? A systematic review," *Journal of Foot and Ankle Research,* Review vol. 14, no. 1, 2021, Art no. 19, doi: 10.1186/s13047-021-00456-w.

[26] J. Singbo, M. Locketz, and I. L. Ross, "Challenge of coexisting type 2 diabetes mellitus and insulinoma: a case report," *Journal of Medical Case Reports,* Article vol. 15, no. 1, 2021, Art no. 479, doi: 10.1186/s13256-021-03047-2.

[27] W. A. Marston, J. Hanft, P. Norwood, and R. Pollak, "The efficacy and safety of Dermagraft in improving the healing of chronic diabetic foot ulcers: Results of a prospective randomized trial," *Diabetes Care,* Article vol. 26, no. 6, pp. 1701-1705, 2003, doi: 10.2337/diacare.26.6.1701.

[28] R. Ahluwalia, N. Maffulli, J. L. Lázaro-Martínez, K. Kirketerp-Møller, and I. Reichert, "Diabetic foot off loading and ulcer remission: Exploring surgical off-loading," *Surgeon,* Review vol. 19, no. 6, pp. e526-e535, 2021, doi: 10.1016/j.surge.2021.01.005.
[29] J. Tak-Man Cheung, M. Zhang, and K. N. An, "Effects of plantar fascia stiffness on the biomechanical responses of the ankle-foot complex," *Clinical Biomechanics,* Article vol. 19, no. 8, pp. 839-846, 2004, doi: 10.1016/j.clinbiomech.2004.06.002.
[30] Y. Gao *et al.*, "Effects of novel diabetic therapeutic footwear on preventing ulcer recurrence in patients with a history of diabetic foot ulceration: study protocol for an open-label, randomized, controlled trial," *Trials,* Article vol. 22, no. 1, 2021, Art no. 151, doi: 10.1186/s13063-021-05098-8.
[31] R. Ravanbod, N. Eslami, and M. N. Ashtiani, "Immediate effects of footwear with vibration applied to the swing phase of the gait cycle on dynamic balance in patients with diabetic peripheral neuropathy," *Journal of Biomechanics,* Article vol. 128, 2021, Art no. 110710, doi: 10.1016/j.jbiomech.2021.110710.
[32] S. W. Mansour, M. M. Hasan, H. E. Salah, T. El-Deep, S. Hussein, and N. F. El-Malkey, "Effect of irisin on metabolic and platelet functions in type 2 diabetic rats: role of soluble receptor of advanced glycation end products (sRAGE)," *Beni-Suef University Journal of Basic and Applied Sciences,* Article vol. 10, no. 1, 2021, Art no. 62, doi: 10.1186/s43088-021-00148-1.
[33] A. Tuttolomondo *et al.*, "Assessment of heart rate variability (HRV) in subjects with type 2 diabetes mellitus with and without diabetic foot: correlations with endothelial dysfunction indices and markers of adipo-inflammatory dysfunction," *Cardiovascular Diabetology,* Article vol. 20, no. 1, 2021, Art no. 142, doi: 10.1186/s12933-021-01337-z.
[34] T. Q. Bui *et al.*, "Epidermal growth factor is effective in the treatment of diabetic foot ulcers: Meta-analysis and systematic review," *International Journal of Environmental Research and Public Health,* Review vol. 16, no. 14, 2019, Art no. 2584, doi: 10.3390/ijerph16142584.
[35] H. P. Mai, N. T. Trinh, V. B. Long, N. T. Binh, D. Q. Nguyen, and H. X. Duong, "The High D-Glucose Concentration Reduces the Ability of Wound Healing in Vitro of Human Adipose Tissue-Derived Mesenchymal Stem Cells," in *IFMBE Proceedings*, 2022, vol. 85, pp. 581-590, doi: 10.1007/978-3-030-75506-5_49. [Online]. Available: https://www.scopus.com/inward/record.uri?eid=2-s2.0-85115048014&doi=10.1007%2f978-3-030-75506-5_49&partnerID=40&md5=bec0030357beb1639c3589ce969e93e7
[36] Y. Jiang, Z. Xu, and X. Fu, "Healing diabetic foot ulcers step by step," *International Journal of Lower Extremity Wounds,* Article vol. 11, no. 4, pp. 307-310, 2012, doi: 10.1177/1534734612463700.
[37] Q. Li *et al.*, "Injectable and self-healing chitosan-based hydrogel with MOF-loaded α-lipoic acid promotes diabetic wound healing," *Materials Science and Engineering C,* Article vol. 131, 2021, Art no. 112519, doi: 10.1016/j.msec.2021.112519.
[38] X. Zhi, W. Wang, B. Xu, and J. Zhou, "Effectiveness of pressure-relieving shoes/insoles on lowering the plantar pressure of diabetic foot: A meta-analysis," *Leather and Footwear Journal,* Article vol. 20, no. 4, pp. 361-374, 2020, doi: 10.24264/lfj.20.4.3.
[39] Z. Q. Feng *et al.*, "Time in range, especially overnight time in range, is associated with sudomotor dysfunction in patients with type 1 diabetes," *Diabetology and Metabolic Syndrome,* Article vol. 13, no. 1, 2021, Art no. 119, doi: 10.1186/s13098-021-00739-z.
[40] Y. Duan, W. Ren, L. Xu, W. Ye, Y. K. Jan, and F. Pu, "The effects of different accumulated pressure-time integral stimuli on plantar blood flow in people with

diabetes mellitus," *BMC Musculoskeletal Disorders,* Article vol. 22, no. 1, 2021, Art no. 554, doi: 10.1186/s12891-021-04437-9.
[41] H. Lin *et al.*, "Impact of diabetes mellitus developing after kidney transplantation on patient mortality and graft survival: a meta-analysis of adjusted data," *Diabetology and Metabolic Syndrome,* Review vol. 13, no. 1, 2021, Art no. 126, doi: 10.1186/s13098-021-00742-4.
[42] L. Li *et al.*, "New risk score model for identifying individuals at risk for diabetes in southwest China," *Preventive Medicine Reports,* Article vol. 24, 2021, Art no. 101618, doi: 10.1016/j.pmedr.2021.101618.
[43] T. A. Jeckson, Y. P. Neo, S. P. Sisinthy, J. B. Foo, H. Choudhury, and B. Gorain, "Formulation and characterisation of deferoxamine nanofiber as potential wound dressing for the treatment of diabetic foot ulcer," *Journal of Drug Delivery Science and Technology,* Article vol. 66, 2021, Art no. 102751, doi: 10.1016/j.jddst.2021.102751.
[44] Y. Hu *et al.*, "Cryogenic 3D printed hydrogel scaffolds loading exosomes accelerate diabetic wound healing," *Chemical Engineering Journal,* Article vol. 426, 2021, Art no. 130634, doi: 10.1016/j.cej.2021.130634.
[45] C. K. Hsu *et al.*, "Renal function trajectories in hepatitis C infection: differences between renal healthy and chronic kidney disease individuals," *Scientific Reports,* Article vol. 11, no. 1, 2021, Art no. 17197, doi: 10.1038/s41598-021-96782-x.
[46] G. Jarl, J. J. van Netten, P. A. Lazzarini, R. T. Crews, B. Najafi, and M. J. Mueller, "Should weight-bearing activity be reduced during healing of plantar diabetic foot ulcers, even when using appropriate offloading devices?," *Diabetes Research and Clinical Practice,* Review vol. 175, 2021, Art no. 108733, doi: 10.1016/j.diabres.2021.108733.
[47] S. Chen *et al.*, "Impact of glycemic control on the association of endothelial dysfunction and coronary artery disease in patients with type 2 diabetes mellitus," *Cardiovascular Diabetology,* Article vol. 20, no. 1, 2021, Art no. 64, doi: 10.1186/s12933-021-01257-y.
[48] J. S. Kim, S. Lee, J. Y. Kim, E. J. Seo, J. B. Chae, and D. Y. Kim, "Visual/anatomical outcome of diabetic macular edema patients lost to follow-up for more than 1 year," *Scientific Reports,* Article vol. 11, no. 1, 2021, Art no. 18353, doi: 10.1038/s41598-021-97644-2.
[49] A. Shetty, L. Madhu, and M. Kodali, "Promise of metformin for preventing age-related cognitive dysfunction," *Neural Regeneration Research,* vol. 17, no. 3, p. 503, 2022, doi: 10.4103/1673-5374.320971.
[50] K. Raju, G. W. Taylor, P. Tahir, and S. Hyde, "Association of tooth loss with morbidity and mortality by diabetes status in older adults: a systematic review," *BMC Endocrine Disorders,* Article vol. 21, no. 1, 2021, Art no. 205, doi: 10.1186/s12902-021-00830-6.
[51] P. C. Aldana and A. Khachemoune, "Diabetic Foot Ulcers: Appraising Standard of Care and Reviewing New Trends in Management," *American Journal of Clinical Dermatology,* Review vol. 21, no. 2, pp. 255-264, 2020, doi: 10.1007/s40257-019-00495-x.
[52] S. Poonguzhali and R. Chakravarthi, "Design of an intelligent foot insole using dynamic sensor network for prevention of diabetic foot ulceration-telemedicine application," *Journal of Advanced Research in Dynamical and Control Systems,* Article vol. 12, no. 4, pp. 369-378, 2020, doi: 10.5373/JARDCS/V12I4/20201451.
[53] "A new drug for diabetic foot ulcer launched in Taiwan, aims at gobal markets by 2030." https://ibmi.taiwan-healthcare.org/en/news_detail.php?REFDOCTYPID=&REFDOCID=0qvqzoph51soexmk (accessed.

[54] L. Sun *et al.*, "Integrated lipidomics, transcriptomics and network pharmacology analysis to reveal the mechanisms of Danggui Buxue Decoction in the treatment of diabetic nephropathy in type 2 diabetes mellitus," *Journal of Ethnopharmacology,* Article vol. 283, 2022, Art no. 114699, doi: 10.1016/j.jep.2021.114699.

[55] P. Venkat and M. Chopp, "Exosome treatment for stroke with diabetic comorbidity," *Neural Regeneration Research,* Review vol. 17, no. 2, pp. 315-317, 2022, doi: 10.4103/1673-5374.319190.

[56] Z. Junli, W. Xiaojun, W. Haijiao, and L. Chun, "A network meta-analysis of the efficacy of new medical dressings for diabetic foot ulcers," *Chinese Journal of Tissue Engineering Research,* Article vol. 26, no. 16, pp. 2682-2689, 2022, Art no. 2095-4344(2022)16-02682-08, doi: 10.12307/2022.258.

[57] Y. Zhang, J. Luo, Q. Zhang, and T. Deng, "Growth factors, as biological macromolecules in bioactivity enhancing of electrospun wound dressings for diabetic wound healing: A review," *International Journal of Biological Macromolecules,* Review vol. 193, pp. 205-218, 2021, doi: 10.1016/j.ijbiomac.2021.09.210.

[58] Z. Xinyu *et al.*, "Mechanism of exercise improving bone metabolism in type 2 diabetics mellitus based on "muscle-bone" crosstalk," *Chinese Journal of Tissue Engineering Research,* Article vol. 26, no. 2, pp. 301-308, 2022, Art no. 2095-4344(2022)02-00301-08, doi: 10.12307/2022.047.

[59] A. Perrier *et al.*, "Smart Diabetic Socks: Embedded device for diabetic foot prevention," *IRBM,* Article vol. 35, no. 2, pp. 72-76, 2014, doi: 10.1016/j.irbm.2014.02.004.

[60] Z. Zhao *et al.*, "3D printing of complex origami assemblages for reconfigurable structures," *Soft Matter,* vol. 14, no. 39, pp. 8051-8059, 2018, doi: 10.1039/c8sm01341a.

[61] J. H. Park, I. C. Choi, T. C. Hong, J. W. Kang, and J. W. Park, "Reconstruction of the weight-bearing heel with nonsensate reverse sural artery flaps," *Injury,* Article vol. 52, no. 7, pp. 1993-1998, 2021, doi: 10.1016/j.injury.2021.04.007.

[62] J. Boateng and O. Catanzano, "Advanced Therapeutic Dressings for Effective Wound Healing - A Review," *Journal of Pharmaceutical Sciences,* Review vol. 104, no. 11, pp. 3653-3680, 2015, doi: 10.1002/jps.24610.

[63] R. Collings, J. Freeman, J. M. Latour, S. Glasser, and J. Paton, "Footwear and insole design features to prevent foot ulceration in people with diabetes: a systematic review protocol," *JBI database of systematic reviews and implementation reports,* Review vol. 15, no. 7, pp. 1824-1834, 2017, doi: 10.11124/JBISRIR-2016-003291.

[64] D. J. Janisse, "Prescription insoles and footwear," *Clinics in Podiatric Medicine and Surgery,* Review vol. 12, no. 1, pp. 41-61, 1995. [Online]. Available: https://www.scopus.com/inward/record.uri?eid=2-s2.0-0028861812&partnerID=40&md5=30364720f322da63eff4328add93923c.

[65] S. K. Paul, E. Rajkumar, and T. Mendis, "Micro Cellular Rubber (MCR) - a boon for leprosy affected patients with anesthetic feet in preventing secondary impairments," *Journal of Foot and Ankle Research,* vol. 7, no. S1, p. A92, 2014, doi: 10.1186/1757-1146-7-s1-a92.

[66] J. W. Brodsky, F. E. Pollo, D. Cheleuitte, and B. S. Baum, "Physical properties, durability, and energy-dissipation function of dual-density orthotic materials used in insoles for diabetic patients," *Foot and Ankle International,* Article vol. 28, no. 8, pp. 880-889, 2007, doi: 10.3113/FAI.2007.0880.

[67] J. G. Foto and J. A. Birke, "Evaluation of multidensity orthotic materials used in footwear for patients with diabetes," *Foot and Ankle International,* Article vol. 19, no. 12, pp. 836-841, 1998, doi: 10.1177/107110079801901208.

[68] A. Healy, D. N. Dunning, and N. Chockalingam, "Materials used for footwear orthoses: A review," *Footwear Science,* Review vol. 2, no. 2, pp. 93-110, 2010, doi: 10.1080/19424280.2010.486045.

[69] O. Mohamed, K. Cerny, L. Rojek, K. Herbert, R. Turner, and S. Waistell, "The effects of plastazote® and aliplast®/plastazote® orthoses on plantar pressures in elderly persons with diabetic neuropathy," *Journal of Prosthetics and Orthotics,* Article vol. 16, no. 2, pp. 55-63, 2004, doi: 10.1097/00008526-200404000-00005.

[70] J. W. K. Tong and E. Y. K. Ng, "Preliminary investigation on the reduction of plantar loading pressure with different insole materials (SRP - Slow Recovery Poron®, P - Poron®, PPF - Poron®+Plastazote, firm and PPS - Poron®+Plastazote, soft)," *Foot,* Article vol. 20, no. 1, pp. 1-6, 2010, doi: 10.1016/j.foot.2009.12.004.

[71] K. Mohammedi *et al.*, "History of lower-limb complications and risk of cancer death in people with type 2 diabetes," *Cardiovascular Diabetology,* Article vol. 20, no. 1, 2021, Art no. 3, doi: 10.1186/s12933-020-01198-y.

[72] J. Paton, S. Abey, P. Hendy, J. Williams, R. Collings, and L. Callaghan, "Behaviour change approaches for individuals with diabetes to improve foot self-management: a scoping review," *Journal of Foot and Ankle Research,* Review vol. 14, no. 1, 2021, Art no. 1, doi: 10.1186/s13047-020-00440-w.

[73] Z. Ma *et al.*, "Design and 3D printing of adjustable modulus porous structures for customized diabetic foot insoles," *International Journal of Lightweight Materials and Manufacture,* Article vol. 2, no. 1, pp. 57-63, 2019, doi: 10.1016/j.ijlmm.2018.10.003.

[74] D. G. Armstrong, A. J. M. Boulton, and S. A. Bus, "Diabetic foot ulcers and their recurrence," *New England Journal of Medicine,* Review vol. 376, no. 24, pp. 2367-2375, 2017, doi: 10.1056/NEJMra1615439.

[75] A. Hazzaa Walaa Eldin and K. Mattes, "Influence of foot strike pattern and local fatigue of plantar flexors and dorsiflexors on plantar pressure during running," *Deutsche Zeitschrift fur Sportmedizin,* Article vol. 69, no. 1, pp. 19-25, 2018, doi: 10.5960/dzsm.2017.314.

[76] H. Nagano and R. K. Begg, "Shoe-insole technology for injury prevention in walking," *Sensors (Switzerland),* Review vol. 18, no. 5, 2018, Art no. 1468, doi: 10.3390/s18051468.

[77] D. R. Bonanno, K. B. Landorf, and H. B. Menz, "Pressure-relieving properties of various shoe inserts in older people with plantar heel pain," *Gait and Posture,* Article vol. 33, no. 3, pp. 385-389, 2011, doi: 10.1016/j.gaitpost.2010.12.009.

[78] J. M. A. Melvin, S. Preece, C. J. Nester, and D. Howard, "An investigation into plantar pressure measurement protocols for footwear research," *Gait and Posture,* Article vol. 40, no. 4, pp. 682-687, 2014, doi: 10.1016/j.gaitpost.2014.07.026.

[79] B. C. Chang, D. H. Liu, J. L. Chang, S. H. Lee, and J. Y. Wang, "Plantar pressure analysis of accommodative insole in older people with metatarsalgia," *Gait and Posture,* Article vol. 39, no. 1, pp. 449-454, 2014, doi: 10.1016/j.gaitpost.2013.08.027.

[80] J. Han, D. Wang, Z. Li, and F. Shi, "Deep self-organizing map neural networks for plantar pressure image segmentation employing marr-hildreth features," *International Journal of Ambient Computing and Intelligence,* Article vol. 12, no. 4, pp. 1-21, 2021, doi: 10.4018/IJACI.2021100101.

[81] D. G. Cronkwright, M. J. Spink, K. B. Landorf, and H. B. Menz, "Evaluation of the pressure-redistributing properties of prefabricated foot orthoses in older people after at least 12 months of wear," *Gait and Posture,* Article vol. 34, no. 4, pp. 553-557, 2011, doi: 10.1016/j.gaitpost.2011.07.016.

[82] P. Jones, M. J. Davies, K. Khunti, D. T. P. Fong, and D. Webb, "In-shoe pressure thresholds for people with diabetes and neuropathy at risk of ulceration: A systematic

review," *Journal of Diabetes and its Complications,* Review vol. 35, no. 3, 2021, Art no. 107815, doi: 10.1016/j.jdiacomp.2020.107815.
[83] W. B. A. De Stegge, M. C. Schut, A. Abu-Hanna, J. G. Van Baal, J. J. Van Netten, and S. A. Bus, "Development of a prediction model for foot ulcer recurrence in people with diabetes using easy-to-obtain clinical variables," *BMJ Open Diabetes Research and Care,* Article vol. 9, no. 1, 2021, Art no. e002257, doi: 10.1136/bmjdrc-2021-002257.
[84] L. Cao *et al.*, "Diabetic plantar pressure analysis using image fusion," *Multimedia Tools and Applications,* Article vol. 79, no. 15-16, pp. 11213-11236, 2020, doi: 10.1007/s11042-018-6269-x.
[85] Q. Chen *et al.*, "Identification of circulating sphingosine kinase-related metabolites for prediction of type 2 diabetes," *Journal of Translational Medicine,* Article vol. 19, no. 1, 2021, Art no. 393, doi: 10.1186/s12967-021-03066-z.
[86] S. K. Bhullar *et al.*, "Design and fabrication of auxetic PCL nanofiber membranes for biomedical applications," *Materials Science and Engineering C,* Article vol. 81, pp. 334-340, 2017, doi: 10.1016/j.msec.2017.08.022.
[87] M. B. R. Chattopadhyay, "Prediction of pressure due to elastic fabric tube following energy principle," *Journal of Textile Engineering & Fashion Technology,* vol. 2, no. 5, p. 00075, 2017.
[88] J. T. M. Cheung, M. Zhang, A. K. L. Leung, and Y. B. Fan, "Three-dimensional finite element analysis of the foot during standing - A material sensitivity study," *Journal of Biomechanics,* Article vol. 38, no. 5, pp. 1045-1054, 2005, doi: 10.1016/j.jbiomech.2004.05.035.
[89] P. E. Chatzistergos, R. Naemi, A. Healy, P. Gerth, and N. Chockalingam, "Subject Specific Optimisation of the Stiffness of Footwear Material for Maximum Plantar Pressure Reduction," *Annals of Biomedical Engineering,* Article vol. 45, no. 8, pp. 1929-1940, 2017, doi: 10.1007/s10439-017-1826-4.
[90] M. J. Ghazali, X. Ren, A. Rajabi, W. F. H. W. Zamri, and N. M. Mustafah, "Finite element analysis of cushioned diabetic footwear using ethylene vinyl acetate polymer," *Polymers,* Article vol. 13, no. 14, 2021, Art no. 2261, doi: 10.3390/polym13142261.
[91] G. Lu and B. Fei, "Medical hyperspectral imaging: A review," *Journal of Biomedical Optics,* Article vol. 19, no. 1, 2014, Art no. 010901, doi: 10.1117/1.JBO.19.1.010901.
[92] P. Zhang, J. Lu, Y. Jing, S. Tang, D. Zhu, and Y. Bi, "Global epidemiology of diabetic foot ulceration: a systematic review and meta-analysis," *Annals of Medicine,* vol. 49, no. 2, pp. 106-116, 2017, doi: 10.1080/07853890.2016.1231932.
[93] H. Shaulian, A. Gefen, D. Solomonow-Avnon, and A. Wolf, "Finite element-based method for determining an optimal offloading design for treating and preventing heel ulcers," *Computers in Biology and Medicine,* Article vol. 131, 2021, Art no. 104261, doi: 10.1016/j.compbiomed.2021.104261.
[94] Y. Wang, Z. Li, D. W.-C. Wong, C.-K. Cheng, and M. Zhang, "Finite element analysis of biomechanical effects of total ankle arthroplasty on the foot," *Journal of Orthopaedic Translation,* vol. 12, pp. 55-65, 2018, doi: 10.1016/j.jot.2017.12.003.
[95] V. H. Chuter, M. J. Spink, M. David, S. Lanting, and A. Searle, "Clinical foot measurements as a proxy for plantar pressure testing in people with diabetes," *Journal of Foot and Ankle Research,* Article vol. 14, no. 1, 2021, Art no. 56, doi: 10.1186/s13047-021-00494-4.
[96] D. L. Bader and P. R. Worsley, "Technologies to monitor the health of loaded skin tissues," *BioMedical Engineering Online,* Review vol. 17, no. 1, 2018, Art no. 40, doi: 10.1186/s12938-018-0470-z.

[97] M. Hahn *et al.*, "3D imaging of human organs with micrometer resolution - applied to the endocrine pancreas," *Communications Biology,* Article vol. 4, no. 1, 2021, Art no. 1063, doi: 10.1038/s42003-021-02589-x.
[98] Y. Liu, Q. Yu, X. Luo, L. Yang, and Y. Cui, "Continuous monitoring of diabetes with an integrated microneedle biosensing device through 3D printing," *Microsystems and Nanoengineering,* Article vol. 7, no. 1, 2021, Art no. 75, doi: 10.1038/s41378-021-00302-w.
[99] E. Borrelli *et al.*, "Volume rendered 3D OCTA assessment of macular ischemia in patients with type 1 diabetes and without diabetic retinopathy," *Scientific Reports,* Article vol. 11, no. 1, 2021, Art no. 19793, doi: 10.1038/s41598-021-99297-7.
[100] S. Telfer and J. Woodburn, "The use of 3D surface scanning for the measurement and assessment of the human foot," *Journal of Foot and Ankle Research,* Review vol. 3, no. 1, 2010, Art no. 19, doi: 10.1186/1757-1146-3-19.
[101] S. M. Mitu, N. A. Rahman, A. M. Taib, A. B. Ramli, and D. Z. A. Hasbollah, "The evolution of spectral analysis of surface wave method – A review," *Journal of Mines, Metals and Fuels,* Review vol. 69, no. 8, pp. 140-150, 2021. [Online]. Available: https://www.scopus.com/inward/record.uri?eid=2-s2.0-85114990793&partnerID=40&md5=bf632bd417db97d4bae9c3e9589493d7.
[102] O. C. Zienkiewicz and R. L. Taylor, *The Finite Element Method Set* (The Finite Element Method Set). 2005.
[103] M. J. Turner, Clough, R. W., Martin H. C. and Topp, L. J., "Stiffness and Deflection Analysis of Complex Structures " *Journal of the Aeronautical Sciences,* vol. 23 no. 9, pp. 805-823, 1956
[104] I. Ergatoudis, Irons, B. M., and Zienkiewicz, O. C., "Curved, isoparametric,"quadrilateral" elements for finite element analysis.," *International Journal of Solids and Structures,* vol. 4, no. 1, pp. 31-42., 1968.
[105] P. E. Chatzistergos and N. Chockalingam, "An in vivo model for overloading-induced soft tissue injury," *Scientific Reports,* vol. 12, no. 1, 2022, Art no. 6047, doi: 10.1038/s41598-022-10011-7.
[106] M. S. H. Leung, K. L. Yick, Y. Sun, L. Chow, and S. P. Ng, "3D printed auxetic heel pads for patients with diabetic mellitus," *Computers in Biology and Medicine,* vol. 146, 2022, Art no. 105582, doi: 10.1016/j.compbiomed.2022.105582.
[107] F. Mo, Y. Li, J. Li, S. Zhou, and Z. Yang, "A three-dimensional finite element foot-ankle model and its personalisation methods analysis," *International Journal of Mechanical Sciences,* Article vol. 219, 2022, Art no. 107108, doi: 10.1016/j.ijmecsci.2022.107108.
[108] N. Ahanchian, C. J. Nester, D. Howard, L. Ren, and D. Parker, "Estimating the material properties of heel pad sub-layers using inverse Finite Element Analysis," *Medical Engineering and Physics,* Article vol. 40, pp. 11-19, 2017, doi: 10.1016/j.medengphy.2016.11.003.
[109] Q. Zhang, T. Chon, Y. Zhang, J. S. Baker, and Y. Gu, "Finite element analysis of the lumbar spine in adolescent idiopathic scoliosis subjected to different loads," *Computers in Biology and Medicine,* Article vol. 136, 2021, Art no. 104745, doi: 10.1016/j.compbiomed.2021.104745.
[110] S. Li, Y. Zhang, Y. Gu, and J. Ren, "Stress distribution of metatarsals during forefoot strike versus rearfoot strike: A finite element study," *Computers in Biology and Medicine,* Article vol. 91, pp. 38-46, 2017, doi: 10.1016/j.compbiomed.2017.09.018.
[111] C. Mastromauro *et al.*, "Peculiar characteristics of new-onset Type 1 Diabetes during COVID-19 pandemic," *Italian Journal of Pediatrics,* Article vol. 48, no. 1, 2022, Art no. 26, doi: 10.1186/s13052-022-01223-8.

[112] F. Çınar and G. Ekinci, "Investigation of the effect of comorbidity on mortality in patients with covid-19: A systematic review and meta-analysis," *Biointerface Research in Applied Chemistry,* Article vol. 12, no. 4, pp. 5579-5590, 2022, doi: 10.33263/BRIAC124.55795590.

[113] A. B. Irez, E. Bayraktar, and I. Miskioglu, "Fracture toughness analysis of epoxy-recycled rubber-based composite reinforced with graphene nanoplatelets for structural applications in automotive and aeronautics," *Polymers,* Article vol. 12, no. 2, 2020, Art no. 448, doi: 10.3390/polym12020448.

[114] F. A. O. Fernandes, R. J. Alves De Sousa, R. Willinger, and C. Deck, "Finite element analysis of helmeted impacts and head injury evaluation with a commercial road helmet," in *2013 IRCOBI Conference Proceedings - International Research Council on the Biomechanics of Injury*, 2013, pp. 431-442. [Online]. Available: https://www.scopus.com/inward/record.uri?eid=2-s2.0-84896602190&partnerID=40&md5=3ad3e420256cb8beb3faa8674e87eb87. [Online]. Available: https://www.scopus.com/inward/record.uri?eid=2-s2.0-84896602190&partnerID=40&md5=3ad3e420256cb8beb3faa8674e87eb87

[115] M. Zhang, J. T. M. Cheung, and Y. Li, "Computational modeling the foot-insole interface," *Studies in Computational Intelligence,* Article vol. 55, pp. 311-321, 2007, doi: 10.1007/978-3-540-70658-8_21.

[116] P. Franciosa, S. Gerbino, A. Lanzotti, and L. Silvestri, "Improving comfort of shoe sole through experiments based on CAD-FEM modeling," *Medical Engineering and Physics,* Article vol. 35, no. 1, pp. 36-46, 2013, doi: 10.1016/j.medengphy.2012.03.007.

[117] M. Curryer and E. D. Lemaire, "Effectiveness of various materials in reducing plantar shear forces: A pilot study," *Journal of the American Podiatric Medical Association,* vol. 90, no. 7, pp. 346-353, 2000, doi: 10.7547/87507315-90-7-346.

[118] W. T. Lo, D. P. Wong, K. L. Yick, S. P. Ng, and J. Yip, "Effects of custom-made textile insoles on plantar pressure distribution and lower limb EMG activity during turning," *Journal of Foot and Ankle Research,* vol. 9, no. 1, 2016, Art no. 22, doi: 10.1186/s13047-016-0154-5.

[119] F. Nilsen, M. Molund, E. M. Lium, and K. H. Hvaal, "Material Selection for Diabetic Custom Insoles: A Systematic Review of Insole Materials and Their Properties," *Journal of Prosthetics and Orthotics,* vol. 34, no. 3, pp. E131-E143, 2022, doi: 10.1097/JPO.0000000000000403.

[120] R. Montuori, E. Nastri, V. Piluso, and P. Todisco, "Performance-based rules for the simplified assessment of steel CBFs," *Journal of Constructional Steel Research,* Article vol. 191, 2022, Art no. 107167, doi: 10.1016/j.jcsr.2022.107167.

[121] R. Ullah, M. Vafaei, S. C Alih, and A. Waheed, "A review of buckling-restrained braced frames for seismic protection of structures," *Physics and Chemistry of the Earth,* vol. 128, 2022, Art no. 103203, doi: 10.1016/j.pce.2022.103203.

[122] R. Sabelli, S. Mahin, and C. Chang, "Seismic demands on steel braced frame buildings with buckling-restrained braces," *Engineering Structures,* vol. 25, no. 5, pp. 655-666, 2003, doi: 10.1016/S0141-0296(02)00175-X.

[123] D. A. Skolnik and J. W. Wallace, "Critical assessment of interstory drift measurements," *Journal of Structural Engineering,* vol. 136, no. 12, pp. 1574-1584, 2010, doi: 10.1061/(ASCE)ST.1943-541X.0000255.

[124] L. Wang *et al.*, "An Inductive Force Sensor for In-Shoe Plantar Normal and Shear Load Measurement," *IEEE Sensors Journal,* vol. 20, no. 22, pp. 13318-13331, 2020, Art no. 9130766, doi: 10.1109/JSEN.2020.3006316.

[125] T. Y. Yang, H. Sheikh, and L. Tobber, "Influence of the brace configurations on the seismic performance of steel concentrically braced frames," *Frontiers in Built Environment,* vol. 5, 2019, Art no. 27, doi: 10.3389/fbuil.2019.00027.
[126] T.-C. Lim, *Auxetic materials and structures*. Singapore: Springer, 2015.
[127] H. Hu, M. Zhang, and Y. Liu, "Auxetic fibre–reinforced composites," in *Auxetic Textiles*, 2019, pp. 285-335.
[128] V. Carneiro, J. Meireles, and H. Puga, "Auxetic materials—A review," *Materials Science-Poland,* vol. 31, no. 4, pp. 561-571, 2013.
[129] H. Hu, M. Zhang, and Y. Liu, "Introduction," in *Auxetic Textiles*, 2019, pp. 1-17.
[130] D. T. Ho, S. D. Park, S. Y. Kwon, K. Park, and S. Y. Kim, "Negative Poisson's ratios in metal nanoplates," *Nature Communications,* Article vol. 5, 2014, Art no. 3255, doi: 10.1038/ncomms4255.
[131] V. L. Coenen and K. L. Alderson, "Mechanisms of failure in the static indentation resistance of auxetic carbon fibre laminates," *Physica Status Solidi (B) Basic Research,* Article vol. 248, no. 1, pp. 66-72, 2011, doi: 10.1002/pssb.201083977.
[132] K. L. Alderson, R. S. Webber, A. P. Kettle, and K. E. Evans, "Novel fabrication route for auxetic polyethylene. Part 1. Processing and microstructure," *Polymer Engineering and Science,* Article vol. 45, no. 4, pp. 568-578, 2005, doi: 10.1002/pen.20311.
[133] F. Scarpa, J. A. Giacomin, A. Bezazi, and W. A. Bullough, "Dynamic behavior and damping capacity of auxetic foam pads," in *Proceedings of SPIE - The International Society for Optical Engineering*, 2006, vol. 6169, doi: 10.1117/12.658453. [Online]. Available: https://www.scopus.com/inward/record.uri?eid=2-s2.0-33745816709&doi=10.1117%2f12.658453&partnerID=40&md5=e8853aaef54e011d96b59c16ae5cb7fc
[134] J. M. Burnfield, C. D. Few, O. S. Mohamed, and J. Perry, "The influence of walking speed and footwear on plantar pressures in older adults," *Clinical Biomechanics,* Article vol. 19, no. 1, pp. 78-84, 2004, doi: 10.1016/j.clinbiomech.2003.09.007.
[135] M. J. Simmonds, C. E. Lee, B. R. Etnyre, and G. S. Morris, "The influence of pain distribution on walking velocity and horizontal ground reaction forces in patients with low back pain," *Pain Research and Treatment,* Article vol. 2012, 2012, Art no. 214980, doi: 10.1155/2012/214980.
[136] V. L. Houston, G. Luo, C. P. Mason, M. Mussman, M. Garbarini, and A. C. Beattie, "Changes in male foot shape and size with weightbearing," *Journal of the American Podiatric Medical Association,* Article vol. 96, no. 4, pp. 330-343, 2006, doi: 10.7547/0960330.
[137] B. Y. S. Tsung, M. Zhang, Y. B. Fan, and D. A. Boone, "Quantitative comparison of plantar foot shapes under different weight-bearing conditions," *Journal of Rehabilitation Research and Development,* Article vol. 40, no. 6, pp. 517-526, 2003, doi: 10.1682/JRRD.2003.11.0517.
[138] B. Novak, J. Možina, and M. Jezeršek, "3D laser measurements of bare and shod feet during walking," *Gait and Posture,* Article vol. 40, no. 1, pp. 87-93, 2014, doi: 10.1016/j.gaitpost.2014.02.015.
[139] J. X. Wen *et al.*, "Trunk balance, head posture and plantar pressure in adolescent idiopathic scoliosis," *Frontiers in Pediatrics,* Article vol. 10, 2022, Art no. 979816, doi: 10.3389/fped.2022.979816.
[140] L. Zhang, K. L. Yick, P. L. Li, J. Yip, and S. P. Ng, "Foot deformation analysis with different load-bearing conditions to enhance diabetic footwear designs," *PLoS ONE,* Article vol. 17, no. 3 March, 2022, Art no. e0264233, doi: 10.1371/journal.pone.0264233.

[141] H. B. Menz and D. R. Bonanno, "Footwear comfort: a systematic search and narrative synthesis of the literature," *Journal of Foot and Ankle Research,* Review vol. 14, no. 1, 2021, Art no. 63, doi: 10.1186/s13047-021-00500-9.
[142] J. J. van Netten *et al.*, "Diabetic Foot Australia guideline on footwear for people with diabetes," *Journal of Foot and Ankle Research,* Article vol. 11, no. 1, 2018, Art no. 2, doi: 10.1186/s13047-017-0244-z.
[143] A. Gefen, M. Megido-Ravid, Y. Itzchak, and M. Arcan, "Biomechanical analysis of the three-dimensional foot structure during gait: A basic tool for clinical applications," *Journal of Biomechanical Engineering,* Article vol. 122, no. 6, pp. 630-639, 2000, doi: 10.1115/1.1318904.
[144] R. W. Ogden, "LARGE DEFORMATION ISOTROPIC ELASTICITY - ON THE CORRELATION OF THEORY AND EXPERIMENT FOR INCOMPRESSIBLE RUBBERLIKE SOLIDS," *Rubber Chemistry and Technology,* Article vol. 46, no. 2, pp. 398-416, 1973, doi: 10.5254/1.3542910.
[145] T. Yamaguchi, K. Shibata, H. Wada, H. Kakehi, and K. Hokkirigawa, "Effect of foot–floor friction on the external moment about the body center of mass during shuffling gait: a pilot study," *Scientific Reports,* Article vol. 11, no. 1, 2021, Art no. 12133, doi: 10.1038/s41598-021-91683-5.
[146] Y. Duan, W. Ren, L. Xu, W. Ye, Y.-K. Jan, and F. Pu, "The effects of different accumulated pressure-time integral stimuli on plantar blood flow in people with diabetes mellitus," *BMC Musculoskeletal Disorders,* vol. 22, no. 1, 2021, doi: 10.1186/s12891-021-04437-9.
[147] F. Davani, M. Alishahi, M. Sabzi, M. Khorram, A. Arastehfar, and K. Zomorodian, "Dual drug delivery of vancomycin and imipenem/cilastatin by coaxial nanofibers for treatment of diabetic foot ulcer infections," *Materials Science and Engineering C,* Article vol. 123, 2021, Art no. 111975, doi: 10.1016/j.msec.2021.111975.
[148] A. Peker *et al.*, "Additive manufacturing and biomechanical validation of a patient-specific diabetic insole," *Polymers for Advanced Technologies,* vol. 31, no. 5, pp. 988-996, 2020, doi: 10.1002/pat.4832.
[149] A. Saidou, O. Gauron, A. Busson, and P. Paultre, "High-order finite element model of bridge rubber bearings for the prediction of buckling and shear failure," *Engineering Structures,* Article vol. 240, 2021, Art no. 112314, doi: 10.1016/j.engstruct.2021.112314.